

CHAPTER 3 – INTERMEDIATE DIAPHRAGM STUDY

TABLE OF CONTENTS

| | |
|---|----|
| 1—EXECUTIVE SUMMARY | 1 |
| 2—INTRODUCTION | 4 |
| 2.1—Background | 4 |
| 2.2—Scope of Work..... | 5 |
| 2.2.1—Task 1: Literature Review..... | 5 |
| 2.2.2—Task 2: Sensitivity Study | 6 |
| 2.2.3—Task 3: Parametric Study | 6 |
| 2.2.4—Task 4: Development of Design Recommendations..... | 6 |
| 3—LITERATURE REVIEW | 7 |
| 3.1—Effect of Intermediate Diaphragms on Vehicular Live Load Distribution..... | 7 |
| 3.2—Effect of Intermediate Diaphragm on Skewed Bridges..... | 14 |
| 3.3—Effect of Intermediate on Curved Bridges | 15 |
| 3.4—Published Policies and Standard Details of State Departments of Transportation..... | 15 |
| 3.5—Summary and Conclusions of Literature Review..... | 23 |
| 4—SENSITIVITY STUDY | 24 |
| 4.1—Objective | 24 |
| 4.2—Numerical Modeling Technique..... | 24 |
| 4.2.1—Details of Modeling Techniques..... | 24 |
| 4.2.1.1—Grillage Model..... | 24 |
| 4.2.1.2—Planar Model | 24 |
| 4.2.1.3—Solid Model | 25 |
| 4.2.2—Comparison of Modeling Techniques for Straight Bridges | 25 |
| 4.2.2.1—Details of models..... | 25 |
| 4.2.2.2—Comparison of Results..... | 27 |
| 4.2.3—Comparison of Modeling Techniques for Skew Bridges..... | 28 |
| 4.2.3.1—Details of Models..... | 28 |
| 4.2.3.2—Comparison of Results..... | 29 |
| 4.2.4—Comparison of Modeling Technique for Curved Bridges..... | 29 |
| 4.2.4.1—Details of Models..... | 29 |
| 4.2.4.2—Comparison of Results..... | 31 |
| 4.2.5—Summary of Selected Modeling Techniques | 31 |
| 4.3—Effect of Wind Loading..... | 32 |

| | |
|--|----|
| 4.3.1—General..... | 32 |
| 4.3.2—Wind Pressure on Structures (WS) | 32 |
| 4.3.3—Wind Pressure on Vehicles (WL) | 33 |
| 4.3.4—Wind Load Combinations and Load Factors | 34 |
| 4.4—Modeling of Elastomeric Bearings..... | 34 |
| 4.4.1—Elastomeric Bearings Stiffness | 34 |
| 4.4.2—Modeling of Bearing Pads | 37 |
| 4.5—Summary and Conclusions..... | 39 |
| 5—PARAMETRIC STUDY | 40 |
| 5.1—Methodology | 40 |
| 5.1.1—General..... | 40 |
| 5.1.2—Parameters..... | 40 |
| 5.1.3—Live Load Cases..... | 43 |
| 5.1.3.1—General | 43 |
| 5.1.3.2—BT-78 Girder Bridges..... | 43 |
| 5.1.3.3—LG-25 Girder Bridges..... | 44 |
| 5.1.3.4—Quad Beam Bridges..... | 46 |
| 5.2—Evaluation Criteria: Live load Moment Envelope..... | 47 |
| 5.3—Effect of Connection Rigidity | 49 |
| 5.3.1—General..... | 49 |
| 5.3.2—BT-78 Girder Bridges | 52 |
| 5.3.3—LG-25 Girder Bridges | 53 |
| 5.3.4—Quad Beam Bridges | 54 |
| 5.4—Effect of Girder Spacing and Span Length | 55 |
| 5.4.1—Combined Effect of Girder Spacing and Span Length..... | 55 |
| 5.4.1.1—BT-78 Girder Bridges..... | 55 |
| 5.4.1.2—LG-25 Girder Bridges..... | 57 |
| 5.4.1.3—Quad Beam Bridges..... | 59 |
| 5.4.2—Effect of Span Length | 61 |
| 5.4.3—Effect of Girder Spacing | 62 |
| 5.5—Effect of Skew Angle | 64 |
| 5.5.1—General..... | 64 |
| 5.5.2—BT-78 Girder Bridges | 65 |
| 5.5.3—LG-25 Girder Bridges | 66 |
| 5.5.4—Quad Beam Bridges | 68 |
| 5.6—Effect of Curvature and Cross-Slope..... | 70 |

| | |
|--|-----|
| 5.6.1—General | 70 |
| 5.6.2—BT-78 Girder Bridges | 75 |
| 5.6.3—LG-25 Girder Bridges | 78 |
| 5.6.4—Quad Beam Bridges | 81 |
| 5.7—Summary and Conclusions | 84 |
| 6—DESIGN RECOMMENDATIONS | 85 |
| 7—REFERENCES | 86 |
| 8—APPENDIX: LIVE LOAD MOMENT OF PARAMETRIC STUDY BRIDGE MODELS | 88 |
| 8.1—Effect of Connection Rigidity | 88 |
| 8.1.1—BT-78 Girder Bridges | 88 |
| 8.1.2—LG-25 Girder Bridges | 89 |
| 8.1.3—Quad Beam Bridges | 90 |
| 8.2—girder spacing and span length | 91 |
| 8.2.1—Combined Effect of Girder Spacing and Span Length..... | 91 |
| 8.2.1.1—BT-78 Girder Bridges | 91 |
| 8.2.1.2—LG-25 Girder Bridges..... | 92 |
| 8.2.1.3—Quad Beam Bridges..... | 94 |
| 8.2.2—Effect of Span Length | 95 |
| 8.2.3—Effect of Girder Spacing | 98 |
| 8.3—Effect of Skew Angle | 101 |
| 8.3.1—BT-78 Girder Bridges | 101 |
| 8.3.2—LG-25 Girder Bridges | 102 |
| 8.3.3—Quad Beam Bridges | 104 |
| 8.4—Effect of Curvature and Cross Slope | 105 |
| 8.4.1—BT-78 Girder Bridges | 105 |
| 8.4.2—LG-25 Girder Bridges | 108 |
| 8.4.3—Quad Beam Bridges | 111 |

LIST OF FIGURES

Figure 3-1: The load-distribution test applies transverse post-tensioning forces at five diaphragms (Grace et al., 2010) 12

Figure 3-2: Deflection of bridge model while loading beam B-4 at different levels of transverse post-tensioning force (Grace et al., 2010) 13

Figure 3-3: Deflection of bridge model while loading beam B-2 at different levels of transverse post-tensioning force (Grace et al., 2010). 13

Figure 3-4: DOTs published policies schematic on intermediate diaphragms 16

Figure 4-1: Cross-section of straight bridge 25

Figure 4-2: Design of straight BT-78 girder bridge (SmartBridge) 26

Figure 4-3: Grillage models of straight bridge 26

Figure 4-4: Planar model of straight bridge..... 27

Figure 4-5: Solid model of straight bridge 27

Figure 4-6: Framing Plan of Skew Bridge (30° skew angle) 28

Figure 4-7: Grillage models of skew bridge..... 28

Figure 4-8: Planar model of skew bridge 28

Figure 4-9: Solid model of skew bridge 29

Figure 4-10: Cross-Section of curved bridge 30

Figure 4-11: Framing plan of curved bridge 30

Figure 4-12: Planar model of curved bridge..... 30

Figure 4-13: Solid model of curved bridge 31

Figure 4-14: Application of wind pressure on structure (WS) 33

Figure 4-15: Application of wind pressure on vehicles (WL)..... 34

Figure 4-16: Stress-Strain Curves of elastomeric bearings in compression (C14.7.6.3.3-1) 36

Figure 4-17: Modeling of bearings using one spring with three translational and two rotational stiffness..... 37

Figure 4-18: Modeling of bearings using three springs with translational stiffness only..... 38

Figure 4-19: Live load BMD of girders for bearings two modeling approaches 38

Figure 5-1: Live load case of BT-78 exterior girder (G1)..... 43

Figure 5-2: Live load cases of BT-78 interior girder (G2) 44

Figure 5-3: Live load cases of LG-25 exterior girder (G1) 45

Figure 5-4: Live load cases of LG-25 interior girder (G2)..... 46

Figure 5-5: Live load case of Quad exterior beam (G1)..... 47

Figure 5-6: Live load case of Quad interior beam (G2) 47

Figure 5-7: Moment envelope of a representative BT-78 girder bridge with ID 48

Figure 5-8: Moment envelope of a representative BT-78 girder bridge without ID 48

Figure 5-9: Moment envelope of BT-78 girder bridge with and without ID..... 49

Figure 5-10: Typical connection between ID and girder using coil insert 50

Figure 5-11: Moment envelope of BT-78 girder bridges with partial-moment connection 51

Figure 5-12: Cross-section of BT-78 girder bridge with different connection rigidities..... 52

Figure 5-13: Moment envelopes of BT-78 girder bridges with different connection rigidities 53

Figure 5-14: LG-25 girder bridge with different connection rigidities 53

Figure 5-15: Moment envelopes of LG-25 girder bridges with different connection rigidities 54

Figure 5-16: Quad beam bridges with different connection rigidities..... 54

Figure 5-17: Moment envelopes of Quad beam bridges with different connection rigidities 55

Figure 5-18: Cross-sections of BT-78 girder bridges with variable girder spacing and span length ... 56

Figure 5-19: Moment difference of BT-78 girder bridges with variable girder spacing and span length 57

Figure 5-20: Cross-sections of LG-25 girder bridges with variable girder spacing and span length ... 58

Figure 5-21: Moment difference of LG-25 girder bridges with variable girder spacing and span length 59

Figure 5-22: Cross-sections of Quad beam bridges with variable girder spacing and span length..... 60

Figure 5-23: Moment difference of Quad beam bridges with different girder spacing and span length 61

Figure 5-24: Cross-section of BT-78 girder bridges with constant girder spacing and variable span length..... 62

Figure 5-25: Moment difference of BT-78 girder bridges with constant girder spacing and variable span length..... 62

Figure 5-26: Cross-section of BT-78 girder bridges with variable girder spacing and constant span length..... 63

Figure 5-27: Moment difference of BT-78 girder bridges with variable girder spacing and constant span length..... 64

Figure 5-28: Details of skew BT-78 girder bridges..... 65

Figure 5-29: Moment difference of skew BT-78 girder bridges 66

Figure 5-30: Details of skew LG-25 girder bridges 67

Figure 5-31: Moment difference of skew LG-25 girder bridges 68

Figure 5-32: Details of skew Quad beam bridges 69

Figure 5-33: Moment difference of skew Quad beam bridges 70

Figure 5-34: Framing plans of curved BT-78 girder bridges with different radii of curvature 72

Figure 5-35: Framing plans of curved LG-25 girder bridges with different radii of curvature..... 73

Figure 5-36: Framing plans of curved Quad beam bridges with different radii of curvature..... 74

Figure 5-37: Moment difference of curved BT-78 girder bridges with different radii of curvature 76

Figure 5-38: Moment difference vs. cross-slope for curved BT-78 girder bridges..... 77

Figure 5-39: Moment difference of curved LG-25 girder bridges with different radii of curvature.... 79

Figure 5-40: Moment difference vs. cross-slope for curved LG-25 girder bridges..... 80

Figure 5-41: Moment difference of curved Quad beam bridges with different radii of curvature..... 82

Figure 5-42: Moment difference vs. cross-slope for curved Quad beam bridges..... 83

Figure 8-1: BT-78 girder bridge – ID with full moment connection..... 88

Figure 8-2: BT-78 girder bridge – ID with pinned connection..... 88

Figure 8-3: LG-25 girder bridge – ID with full moment connection..... 89

Figure 8-4: LG-25 girder bridge – ID with pinned connection 89

Figure 8-5: Quad beam bridge – ID with full moment connection 90

Figure 8-6: Quad beam bridge – ID with pinned connection 90

Figure 8-7: BT-78 girder bridge – 12 ft. girder spacing and 130 ft. span length..... 91

Figure 8-8: BT-78 girder bridge – 9 ft. girder spacing and 146 ft. span length..... 91

Figure 8-9: BT-78 girder bridge – 7.2 ft. girder spacing and 156 ft. span length..... 92

Figure 8-10: LG-25 girder bridge – 9 ft. girder spacing and 44 ft. span length 92

Figure 8-11: LG-25 girder bridge – 7.2 ft. girder spacing and 47 ft. span length 93

Figure 8-12: LG-25 girder bridge – 6 ft. girder spacing and 50 ft. span length 93

Figure 8-13: Quad beam bridge – 5 ft. spacing and 40 ft. span..... 94

Figure 8-14: Quad beam bridge – 4.4 ft. spacing and 40 ft. span..... 94

Figure 8-15: Quad beam bridge – 3.5 ft. spacing and 40 ft. span..... 95

Figure 8-16: BT-78 girder bridge – 12 ft. girder spacing and 145 ft. span length..... 95

Figure 8-17: BT-78 girder bridge – 12 ft. girder spacing and 130 ft. span length..... 96

Figure 8-18: BT-78 girder bridge – 12 ft. girder spacing and 115 ft. span length..... 96

Figure 8-19: BT-78 girder bridge – 12 ft. girder spacing and 100 ft. span length..... 97

Figure 8-20: BT-78 girder bridge – 12 ft. girder spacing and 85 ft. span length..... 97

Figure 8-21: BT-78 girder bridge – 12 ft. girder spacing and 70 ft. span length..... 98

Figure 8-22: BT-78 girder bridge – 12 ft. girder spacing and 130 ft. span length..... 98

Figure 8-23: BT-78 girder bridge – 10 ft. girder spacing and 130 ft. span length..... 99

Figure 8-24: BT-78 girder bridge – 9 ft. girder spacing and 130 ft. span length..... 99

Figure 8-25: BT-78 girder bridge – 7.2 ft. girder spacing and 130 ft. span length..... 100

Figure 8-26: BT-78 girder bridge – 6 ft. girder spacing and 130 ft. span length..... 100

Figure 8-27: BT-78 girder bridge – 08 skew angle 101

Figure 8-28: BT-78 girder bridge – 308 skew angle 101

Figure 8-29: BT-78 girder bridge – 608 skew angle 102

Figure 8-30: LG-25 girder bridge — 08 skew angle 102

Figure 8-31: LG-25 girder bridge — 308 skew angle 103

Figure 8-32: LG-25 girder bridge — 608 skew angle 103

Figure 8-33: Quad beam bridge — 08 skew angle 104

Figure 8-34: Quad beam bridge — 308 skew angle 104

Figure 8-35: Quad beam bridge — 608 skew angle 105

Figure 8-36: BT-78 girder bridge — 1200 ft. radius of curvature and 8% cross slope 105

Figure 8-37: BT-78 girder bridge — 1200 ft. radius of curvature and 10% cross slope 106

Figure 8-38: BT-78 girder bridge — 1400 ft. radius of curvature and 8% cross slope 106

Figure 8-39: BT-78 girder bridge — 1400 ft. radius of curvature and 10% cross slope 107

Figure 8-40: BT-78 girder bridge — 2100 ft. radius of curvature and 8% cross slope 107

Figure 8-41: BT-78 girder bridge — 2100 ft. radius of curvature and 10% cross slope 108

Figure 8-42: LG-25 girder bridge — 500 ft. radius of curvature and 8% cross slope 108

Figure 8-43: LG-25 girder bridge — 500 ft. radius of curvature and 10% cross slope 109

Figure 8-44: LG-25 girder bridge — 800 ft. radius of curvature and 8% cross slope 109

Figure 8-45: LG-25 girder bridge — 800 ft. radius of curvature and 10% cross slope 110

Figure 8-46: LG-25 girder bridge — 1000 ft. radius of curvature and 8% cross slope 110

Figure 8-47: LG-25 girder bridge — 1000 ft. radius of curvature and 10% cross slope 111

Figure 8-48: Quad beam bridge — 500 ft. radius of curvature and 8% cross slope 111

Figure 8-49: Quad beam bridge — 500 ft. radius of curvature and 10% cross slope 112

Figure 8-50: Quad beam bridge — 800 ft. radius of curvature and 8% cross slope 112

Figure 8-51: Quad beam bridge — 800 ft. radius of curvature and 10% cross slope 113

Figure 8-52: Quad beam bridge — 1000 ft. radius of curvature and 8% cross slope 113

Figure 8-53: Quad beam bridge — 1000 ft. radius of curvature and 10% cross slope 114

LIST OF TABLES

Table 2-1: LADOTD BDEM Policy for Intermediate Diaphragms (Dated 11/17/2014) 5

Table 3-1: Expressions of Rd Value for different cases 11

Table 3-2: Values of SK, St, and PL for different bridge configurations 11

Table 3-3: Values of C in Rd expression 11

Table 3-4: Effect of intermediate diaphragms on vertical live load distribution 14

Table 3-5: DOTs published policies on intermediate diaphragms 17

Table 4-1: Results of different modeling techniques of straight bridges 27

| | |
|---|----|
| Table 4-2: Results of different modeling techniques of skew bridges | 29 |
| Table 4-3: Results of different modeling techniques of curved bridges..... | 31 |
| Table 4-4: Base Pressures, PB Corresponding to VB = 100 mph | 32 |
| Table 4-5: Values of V0 and Z0 for various surface conditions..... | 32 |
| Table 4-6: Factored flexure moments at mid-span (kip-ft.) | 34 |
| Table 5-1: Matrix of parametric study..... | 40 |
| Table 5-2: Live load moments of BT-78 interior girder (G2) | 44 |
| Table 5-3: Live load moments of LG-25 interior girder (G2)..... | 46 |
| Table 5-4: Bridges models investigated for the effect of partial-moment connection rigidity (12 models)..... | 50 |
| Table 5-5: Bridges models investigated for the effect of connection rigidity (9 models)..... | 51 |
| Table 5-6: BT-78 girder bridge models with variable girder spacing and span length (6 models)..... | 55 |
| Table 5-7: LG-25 girder bridge models with variable girder spacing and span length (6 models)..... | 57 |
| Table 5-8: Quad beam bridge models with variable girder spacing and span length (6 models)..... | 60 |
| Table 5-9: BT-78 girder bridge models with constant girder spacing and variable span length (12 models)..... | 61 |
| Table 5-10: BT-78 girder bridge models with variable girder spacing and constant span length (10 models)..... | 63 |
| Table 5-11: Skew bridge models (36 models)..... | 64 |
| Table 5-12: Curved bridge models (36 models)..... | 70 |
| Table 5-13: Framing plans details of curved bridges | 71 |

1–EXECUTIVE SUMMARY

The use of intermediate diaphragms (ID) in I-shaped precast concrete girder bridges has been a controversial subject. It has been always believed that ID contribute to the distribution of the gravity live loads among the main girders. However, many studies and research have shown that live load distribution is essentially independent of the type and location of ID. In addition, ID helps resist impacts caused by lateral loads, mainly due to collision of over-height vehicles for bridge overpasses. However, concerns have been raised about ID being damage-limiting or damage-spreading members and in many cases collision resulted in damaging multiple girders instead of limiting the damage to the fascia girder. Further, research has showed that the flexural rigidity of the connection between ID and the precast concrete girders determines to a great extent the effectiveness of ID.

The current ID policy (dated 11/17/2014) given in *D5.13.2.2* is shown in Table 2-1. This policy requires one (1) ID at mid-span to be used for spans supported by BT-78 girder, LG-25 girder, and Quad beam under normal loading conditions (Case 1), and for spans on curve (Case 3). In addition, the new LADOTD BDEM requires ID to be full-height (extend from bottom of deck to the top of bottom flange) with a minimum width of eight (8) inches.

The scope of this study was to evaluate the effectiveness of ID in Cases 1 and 3 of the current policy given in LADOTD BDEM and provide recommendations to refine the policy, if required. Accordingly, the study evaluated the impact of inclusion/elimination of ID in BT-78 girder, LG-25 girder, and Quad beam bridges with different configurations utilizing Finite Element Analysis. The project constituted four (4) tasks as follows:

Task 1 – Literature Review

The available literature was summarized along with the findings and conclusions of those studies. The literature review also included surveying the web sites of the 50 States Department of Transportation to determine their current practices regarding the use of ID in precast concrete bridges as well as their Standard Details.

Task 2 – Sensitivity Study

The objective of the sensitivity study was i) determine appropriate modeling technique for straight, skew, and curved bridges, ii) investigate the effect of wind forces under normal loading conditions on bridge design, and iii) best approach to represent the bearings pads in the numerical model.

Three (3) different modeling techniques using Finite Element Analysis were deployed to determine the most appropriate technique for straight, skew, and curved bridges. The three (3) investigated modeling techniques are Grillage Model (2-D using beam elements only), Planar Model (3-D using beam and plate elements), and Solid Model (3-D using solid elements).

The effect of wind pressure on structures (WS) and wind pressure on vehicles (WL) on the design of bridges under normal loading conditions was also investigated utilizing a straight bridge and grillage modeling technique.

The modeling of bearing pads was investigated using two (2) different approaches. In the first approach, the bearing pad was represented using one linear spring with three (3) translational and two (2) rotational stiffness. In the second approach, the bearing pad was represented using three (3) linear springs, each spring with three (3) translational stiffness only. In the second approach, the rotational stiffness of the bearing pad is implicitly considered due to the use of three (3) springs. For both approaches the vertical translational movement was considered as compression only, thus the bearing pad cannot resist tension.

Based on the observations and the findings of the sensitivity study, the following conclusion were drawn:

- Grillage modeling technique (2-D using beam elements only) is appropriate for straight bridges.

- Planar modeling technique (3-D using beam and plate elements) is better for skewed and curved bridges.
- Wind load forces and wind load combinations does not govern the design of bridges under normal loading conditions.
- Bearing pad can best modeled utilizing three (3) linear springs with translational (horizontal and vertical) stiffness only.

Task 3 – Parametric Study

A parametric study was conducted using Finite Element Analysis. The validated numerical modeling techniques (grillage model or planar model) were used to investigate the effect of different parameters that are believed to affect the contribution of ID to BT-78 girder, LG-25 girder, and Quad beam bridges.

The three types of bridges were investigated for different geometric configurations including straight, skew, and curved bridges. The study also investigated the effect of the rigidity of the connection between ID and the girder assuming full moment and pinned connections.

To evaluate the role of the ID, each bridge was analyzed for two conditions, with and without ID. Moment envelopes were developed for each case and the moment difference due to removal of ID was determined for the exterior and interior girders of the bridge. The moment difference served as the basis for the evaluation of the role of ID. The effect of the investigated parameters on the moment difference was realized for each case. Based on the findings of the parametric study, the following conclusion could be drawn:

- Removal of ID results in increasing the mid-span moment of the interior girder and decreasing the mid-span moment of the exterior girder.
- The rigidity of the connection between ID and the girder impacts their role. ID with pinned connection showed to be less effective in comparison with ID with full moment connection.
- For BT-78, LG-25, and Quad beam bridges, contribution of ID to mid-span moment is insignificant when using pinned connection.
- Effectiveness of ID decreases with increasing span length and/or decreasing girder spacing.
- Skew bridge with skew angle less than 30° behaves like straight bridges. ID had virtually no effect on the mid-span moment of the exterior or interior girders when the skew angle was increased from 30° to 60°.
- For spans on curve with curved deck and straight (chorded) girders, the curvature of the deck has minimal effect on the mid-span moment of exterior and interior girders due to the removal of ID. In addition, cross-slope has absolutely no effect on the girders due the removal of ID.

Task 4 – Design Recommendations

The results of the parametric study showed that removal of ID has insignificant effect on the live load moment at mid-span under normal loading conditions for BT-78 girder, LG-25 girder, and Quad beam bridges. Therefore, it is recommended to remove ID from straight, skew and curved (curved deck on straight (chorded) girders) of BT-78 girder, LG-25 girder, and Quad beams bridges. The intermediate diaphragm policy given in *D5.13.2.2* can be revised as follows:

| Case | Requirement for Intermediate Diaphragms (ID) |
|---|---|
| All spans unless otherwise specified as follows: | ID is not required. |
| <u>Case 1</u> : Spans over roadways, railroads, navigational channels, and water body with anticipated marine traffic under normal loading condition except for <u>Cases 2</u> and <u>3</u> | One ID shall be provided at center of span. |
| <u>Case 2</u> : Spans on curve with curved girders only | Requirement of ID shall be determined for the design condition. Minimum one ID shall be provided. |
| <u>Case 3</u> : Spans subject to wave force, extreme high wind conditions, other anticipated lateral forces, or other unusual loading conditions | Requirement of ID shall be determined for the design condition. Minimum one ID shall be provided. |

2—INTRODUCTION

2.1—Background

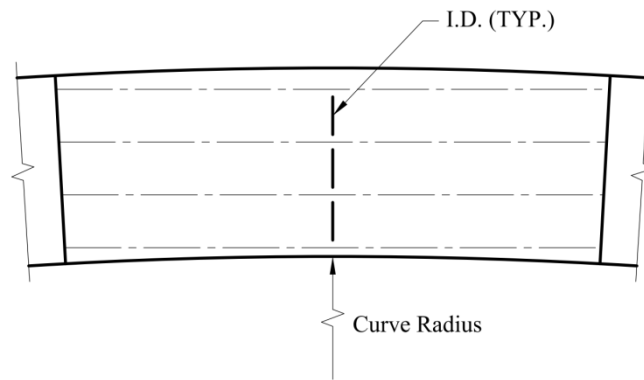
The use of intermediate diaphragms in I-shaped precast concrete girder bridges has been a controversial subject. It has been always believed that intermediate diaphragms contribute to the distribution of the gravity live loads among the main girders. However, many studies and research have shown that live load distribution is essentially independent of the type and location of intermediate diaphragm. In addition, intermediate diaphragm helps resist impacts caused by lateral loads, mainly due to collision of over-height vehicles for bridge overpasses. However, concerns have been raised about intermediate diaphragms being damage-limiting or damage-spreading members and in many cases collision resulted in damaging multiple girders instead of limiting the damage to the fascia girder. Further, research has showed that the flexural rigidity of the connection between the intermediate diaphragm and the precast concrete girders determines to a great extent the effectiveness of intermediate diaphragm.

The Seventh Edition of AASHTO LRFD Bridge Design Specification (AASHTO 2014) does not give clear guidelines on the use of intermediate diaphragms. Article 5.13.2.2 of previous editions of AASHTO Specification stated that intermediate diaphragms may be omitted where tests or structural analysis show them to be unnecessary. However, this statement was removed starting from the Sixth Edition (AASHTO 2012). This is mainly due to the technical debate about the role of intermediate diaphragms in bridges in general, and I-shaped precast concrete girder bridge in particular. Based on studies and practice, many State Departments of Transportation (DOTs) have eliminated intermediate diaphragms from their design of new I-shaped precast concrete girder bridges, while other DOTs still require them. The Annual State Bridge Engineers' Survey of 2013 by AASHTO Subcommittee on Bridges & Structures shows that 27 states out of 46 provide intermediate diaphragms for all their precast prestressed I-girder bridges, while 18 states do not. These 18 states have different cases where they provide intermediate diaphragms for their precast prestressed I-girder bridges. Furthermore, the survey shows that 32 states out of 46 have standard details for intermediate diaphragms, while 14 states do not.

The previous, Fourth English Edition, Version 1.4 of LADOTD Bridge Design Manual shows in Chapter 5, that for prestressed girders, one intermediate diaphragm is required for spans more than 50 ft. and less than 100 ft., and two intermediate diaphragms are required for spans more than 100 ft. In addition, the diaphragm details given in the same chapter of the manual shows that intermediate diaphragms are connected to the webs of the girders only (partial-height) and are not connected to the bridge deck, similar to end diaphragms. The new LADOTD Bridge Design and Evaluation Manual (BDEM) refined the intermediate diaphragm policy as given in Part II, Vol. 1, Chapter 5, Section 5.13.2.2 and shown below. In addition, the new LADOTD BDEM requires intermediate diaphragms to be full-height (extend from bottom of deck to the top of bottom flange) with a minimum width of 8 inches.

Table 2-1: LADOTD BDEM Policy for Intermediate Diaphragms (Dated 11/17/2014)

| Case | Requirement for Intermediate Diaphragms (ID) |
|--|---|
| All spans unless otherwise specified as follows: | ID is not required. |
| <u>Case 1:</u> Spans supported by BT-78, LG-25, and Quad Beam under normal loading condition except for Cases 3 and 4 | One ID shall be provided at center of span. |
| <u>Case 2:</u> Spans over roadways, railroads, navigational channels, and water body with anticipated marine traffic under normal loading condition except for Cases 3 and 4 | One ID shall be provided at center of span. |
| <u>Case 3:</u> Spans on curve | One ID shall be provided at the center of the span along the radius line. (See Diagram Below.) |
| <u>Case 4:</u> Spans subject to wave force, extreme high wind conditions, other anticipated lateral forces, or other unusual loading conditions | Requirement of ID shall be determined for the design condition. Minimum one ID shall be provided. |



2.2—Scope of Work

The scope of this study is to evaluate the effectiveness of intermediate diaphragms in Cases 1 and 3 of the current policy given in the new LADOTD BDEM (see table above) and provide recommendations to refine the policy, if required. Accordingly, the study evaluated the impact of inclusion/elimination of intermediate diaphragm in BT-78, LG-25, and Quad concrete girder bridges with different configurations utilizing Finite Element Analysis. The study constituted four (4) tasks as follows:

2.2.1—Task 1: Literature Review

Several studies and research have been carried out addressing the effects of intermediate diaphragms on prestressed concrete girder bridges. The available literature was summarized along with the findings and conclusions of those studies. The literature review also included surveying the web sites of the 50 States Department of Transportation to determine their current practices of other regarding the use of intermediate diaphragms in precast concrete bridges as well as their Standard Details.

2.2.2—Task 2: Sensitivity Study

The sensitivity study comprises numerical modeling using the Finite Element (FE) method using commercially-available software(s). The sensitivity study aims at optimizing the numerical model to be used for the parametric study (task 3). The optimization will include i) idealization of superstructure (e.g. planar model, grillage analogy, and three-dimensional model), ii) type of numerical element (e.g. beam element, shell element, solid element, etc.), iii) mesh size, and iv) computational time and effort.

2.2.3—Task 3: Parametric Study

The parametric study included parameters believed to influence the behavior of intermediate diaphragms. The parameters investigated in this study are as follows:

- Girders spacing
- Cross-section of main girders (rigidity of girders)
- Rigidity of connection between the intermediate diaphragm and girders
- Skew angle
- Curvature of the bridge
- Cross-slope

2.2.4—Task 4: Development of Design Recommendations

In light of the findings of the sensitivity and parametric studies, as well as the reported literature, recommended design guidelines were developed. Upon approval of the recommended design guidelines, the BDEM policy for intermediate diaphragm will be updated to reflect these recommendations.

3—LITERATURE REVIEW

3.1—Effect of Intermediate Diaphragms on Vehicular Live Load Distribution

The live load distribution factors were first introduced to the American Association of State Highway and Transportation Officials (AASHTO) Standard Specifications in 1931. The distribution factors consider the transverse effects of the vehicular loads on girders. After computing the maximum live load moment caused by a truck or lane of traffic, the value of the moment is multiplied by the live load distribution factor to obtain the design live load moment (Dupaquier, 2014).

While some researchers emphasize the importance of intermediate diaphragms in improving the distribution of vehicular live loads between girders, others claim that their role is insignificant. However, AASHTO LRFD Bridge Design Specifications (AASHTO LRFD BDS) introduced new equations for the live load distribution factors. These equations take into account the girder stiffness, girder spacing, span length, skew angle, and slab stiffness. The live load distribution factors introduced by the AASHTO LRFD BDS, however, do not take the effects of intermediate diaphragms into account.

The 1996 AASHTO Standard Specifications for Highway Bridges (AASHTO SSHB) load distribution factors were based on the empirical equations developed by Newmark (1938). The live load distribution factors in the AASHTO SSHB were developed for interior beams of simply supported spans. These formulas were developed for straight, non-skewed bridges and were dependent on one variable, which is the spacing between the main girders. The distribution factors were in the form of S/D , where S is the spacing between the girders, and D is a constant related to the bridge type. These formulas have proven accurate for certain geometries of bridges, but their accuracy decreased swiftly with the change of the bridge geometry. In other words, these equations tend to be conservative in the case of long span bridges, but exceptionally unsafe when used in bridges with small girder spacing and short spans. Moreover, the above equations do not account for important factors such as geometric dimensions, skew angle, position of girder, and material properties (Sotelino et al., 2004).

The NCHRP project 12-26 (1993) investigated the live load distribution formulas in the AASHTO SSHB. The study was performed in two phases. The first phase of the project concentrated on beam-and-slab and box girder bridges, while the second phase the concentration was slab, multibox, and spread box beam bridges. The NCHRP project 12-26 (1993) utilized three (3) levels of analysis. The first level involved the use of simplified equations to estimate the live load distribution. The second level used grillage analysis, influence surfaces, and graphical methods to compute the live load distribution factors. The third level, which was proven to be the most accurate one, involved modeling of the superstructure using a refined Finite Element Analysis (Sotelino et al., 2004). The equations developed for the first level of analysis are based on the standard AASHTO HS trucks. However, levels 2 and 3 can be used for truck outside the AASHTO family of trucks. NCHRP project No. 12-26 deployed the detailed Finite Element and grillage analyses to develop the simplified live load distribution equations by performing a parametric study. These formulas accounted for important parameters such as span length, slab thickness, girder inertia, and girder spacing. These equations were adopted by the AASHTO LRFD BDS (1998). The project studied 5 different types of bridges, beam and slab, box girder, slab, multi-box beam and spread box beam, and calculated the mean and standard deviation values using the database from the actual bridges. Then they created a hypothetical bridge that consists of all the average values (average bridge). They changed the values of the bridge parameters on at the time in order to create variations from the average bridge. A large variation of values was covered by choosing a maximum and minimum range of each parameter that is the database standard deviation above and below the mean value of the particular parameter, and in most cases at least twice the standard deviation. The project made certain assumptions in order to derive a formula in a systematic way. The first assumption is that the effect of each parameter can be modeled by an exponential function of the form ax^b , where x is the value of the given parameter, and a and b are coefficients to be determined based on the variation of x . The second assumption is that the effects of each parameter are independent from the other parameters, this allows every parameter to be

investigated separately. The final distribution factor is modeled by an exponential formula of the form: $g = (a)(S^{b1})(L^{b2})(t^{b3})(...)$ where g is the wheel load distribution factor; S , L , and t are parameters included in the formula; a is the scale factor; and $b1$, $b2$, and $b3$ are determined from the variation of S , L , and t , respectively. For instance, in two cases where all bridge parameters are the same except for S , then:

$$g^1 = (a)(S_1^{b1})(L^{b2})(t^{b3})(...)$$

$$g^2 = (a)(S_2^{b1})(L^{b2})(t^{b3})(...)$$

therefore:

$$\frac{g_1}{g_2} = \left(\frac{S_1}{S_2}\right)^{b1}$$

or:

$$b_1 = \frac{\ln\left(\frac{g_1}{g_2}\right)}{\ln\left(\frac{S_1}{S_2}\right)}$$

However, if one examines n different values of S and successive pairs are used to establish the value of $b1$, $n-1$ values for $b1$ can be acquired. Based on the obtained values of $b1$, an exponential curve can be used to model the variation of the distribution factor with S accurately. Therefore, the mean of $n-1$ values of $b1$ is used as the best match. After establishing all of the power factors (i.e., $b1$, $b2$, $b3$, etc.), the value of the scale factor, a can be obtained from the average bridge as follows:

$$a = \frac{g_0}{(S_0^{b1})(L_0^{b2})(t_0^{b3})(...)}$$

The NCHRP project 12-26 employed the above procedure to develop new formulas as needed during the entire course of the study. However, in some cases where the effect of a parameter could not be modeled by an exponential function, the required accuracy was achieved by a slightly different procedure. Nevertheless, in most of the cases the above procedure worked very well, and the developed formulas demonstrate high quality.

The NCHRP Project 12-62 team collected data for over 1500 bridges from different sources. The study investigated the effect of vehicle loading position, skew angle, intermediate diaphragms, and supports on the live load distribution for bridges with precast concrete and steel I beams. The investigated skew angles were 0°, 30°, and 60°. The precast concrete I-beam bridges were modeled with and without intermediate diaphragms installed at quarter points along the span. It was concluded that intermediate diaphragms and end diaphragms decreased the distribution factors of controlling moments in both interior and exterior girders. It was noted that in some of the studies cases, the decrease in the moment distribution factors due to the presence of intermediate diaphragms was noteworthy. In addition, it was pointed out that intermediate diaphragms and end diaphragms increased the distribution factors of shear. The increase in shear distribution factors caused by intermediate diaphragms is related to the stiffness of the diaphragm. However, for the most practical intermediate diaphragms locations, this increase was insignificant (Pucket, 2006).

The Pennsylvania Department of Highways, the U. S. Bureau of Public Roads, and the Reinforced Concrete Research Council sponsored an experimental research by Lin and VanHorn (1968) to evaluate the role of the intermediate diaphragms in distributing the live vehicular loads between adjacent girders. Beam-deck bridge constructed with prestressed concrete spread box girders were tested. The bridge was tested twice, first with intermediate diaphragms, and then after removal of the intermediate diaphragms. It was reported that when several lanes of the bridge were loaded simultaneously, the intermediate

diaphragms did not affect the distribution of the vehicular load. However, when they loaded the bridge with only one truck, they noted a slight decrease in the distribution of the truck load and deflections for girders directly under the truck loads. Lin and VanHorn (1968) concluded that the intermediate diaphragms slightly improved the live load distribution for box girders for single lane loading.

Sengupta and Breen (1973) performed a comprehensive study to assess the influence of the reinforced concrete diaphragms in slab bridges and precast prestressed concrete I girder bridges. The study concluded that intermediate diaphragms have a major contribution in distributing the vertical live loads evenly between the adjacent girders. In addition, the presence of intermediate diaphragms decreased the maximum bending moment slightly. This decrease varied between 5-8% when AASHTO standard trucks were applied. Moreover, the study suggested that it is more efficient to increase the strength in girders which, in turn, will reduce the flexural stresses in the girders, rather than depending on the intermediate diaphragms to decrease the flexural stresses by distributing the loads between the adjacent girders. However, since the 1969 AASHTO specifications have already conservatively neglected the effects of intermediate diaphragms, these design change suggestions were unnecessary (Dupaquier, 2014).

Abendroth et al. (1995) tested two full-scale simply-supported, precast concrete girder bridge models, of which one of the tested bridges was with eight intermediate diaphragms and the other was without any diaphragms. The study included analytical modeling of the tested bridges using Finite Element Analysis (FEA) assuming both pinned and fixed-end conditions. The study concluded that the vehicular load distribution is independent of the location and type of the intermediate diaphragms. Furtherer the study concluded that vertical load distribution is dependent on the girder-end restrains.

Barr et al. (2001) studied the distribution of vertical live loads in three-span prestressed concrete girder bridges. They built a Finite Element (FE) model and verified their model against the response of one bridge, measured during a static live-load test. the study also investigated 24 different cases to assess the processes for calculating the vertical live load distribution factors obtained from three bridge design codes. In addition, they employed the FE models to study the effects of the following variables: lifts, end diaphragms, intermediate diaphragms, skew angle, continuity, and loading type. They pointed out that the Finite Element distribution factors were within 6% of the code values when the geometries considered are similar to those of the American Association of State Highway and Transportation Officials Load and Resistance Factor Design Specifications. On the other hand, the geometries of the tested bridges yielded in 28% discrepancy (Barr et al., 2001).

In addition, the study noted that while end diaphragms, lifts, loading type, and skew angle reduced the distribution factors considerably, intermediate diaphragms and continuity demonstrated minor effect. They also stated that the use of distribution factors that have been calculated based on finite element model rather than the code equations would reduce the concrete release strength by 6.9 MPa (1,000 psi) or would increase the live load by 39% (Barr et al., 2001).

After noticing that the AASHTO LRFD (1998) did not include edge stiffening elements, barrier railings and sidewalks, and intermediate diaphragms in the live load distribution factors, Eamon and Nowak (2002) investigated the effects of intermediate diaphragms and edge stiffening elements on the ultimate capacity and live load distribution factors. Eamon and Nowak (2002) performed a detailed Finite Element analysis and compared it to the AASHTO LRFD specifications. Eamon and Nowak (2002) concluded that the combined effect of including the intermediate diaphragms, barrier railings and sidewalks, and stiffening elements in the analysis reduced the live load distribution factors between 10-40% in the elastic range, and 5-20% in the inelastic range. In addition, they reported an increase in the ultimate capacity between 110-220%. However, when only intermediate diaphragms were installed, they reduce the maximum girder moment by up to 13% (4% on average).

A study on the effects of intermediate diaphragms in enhancing the performance of prestressed AASHTO type bridge girder performance was carried out by Green et al. (2004). The study investigated the following parameters: presence of intermediate diaphragms, temperature change, bridge skew angle, and an increase in bearing stiffness due to cold temperature or aging. Green et al. (2004) built a Finite

Element model to simulate the behavior of a bridge superstructure constructed with Florida Bulb Tee 78 girders. They concluded that the presence of intermediate diaphragms causes a 19%, 11%, and 6% reduction in maximum deflections for straight, 15-30° skew, and 60° skew bridges respectively.

Cai and Shahawy (2004) used the testing results of six existing precast concrete bridges to evaluate the analytical methods. The study included Finite Element analysis and compared values of the strains, load distribution factors, and ratings obtained by the Finite Element analysis to those obtained by the experimental data and the AASHTO LRFD specifications. The study pointed out that the significant difference between the experimental tests and the analytical models is due to the effects of various field factors such as a high bearing stiffness, slab stiffening, and parapet stiffening. They classified the existing bridges as field bridges pointing out that they are different from the idealized calculation models. Therefore, they developed a refined Finite Element model to investigate the effects of the field factors. Cai and Shahawy (2004) concluded that these field factors have a minor effect on the live load distribution factors; however, they have a major effect on the maximum strain.

Cai (2005) presented a new set of equations for computing the live load distribution factors to substitute the AASHTO LRFD equations. In addition, Cai (2005) developed an equation to measure the effect of intermediate diaphragms on live load distribution. They estimated the Preliminary coefficients of the above equations from fitting a curve either with the developed Finite Element model or with the AASHTO LRFD formulas. The study suggested adding a modification factor (R_D) to account for the effects of intermediate diaphragms on moment load distribution. The presented equations are as follows:

$$LFD = C_1 + \frac{S}{C_2} + C_3 \left(\frac{S}{L} \right)^{0.75} \left(\frac{K_g}{12L t_s^3} \right)^{0.25} = C_1 + \frac{S}{C_2} + C_3 R$$

$$R = \left(\frac{S}{L} \right)^{0.75} \left(\frac{K_g}{12L t_s^3} \right)^{0.25}$$

$$R_D = 1 - C_{T1} \frac{R_{sk}}{R} \left(\frac{I_T}{I_T + 12L t_s^3} \right)^{C_{T2}}$$

where LFD = load distribution factor, S = girder spacing, L = span length, Kg = longitudinal stiffness parameter, ts = slab thickness, RD = intermediate diaphragm modification factor, Rsk reduction factor of skew angle effect per LRFD codes (AASHTO 1998); CT1 and CT2 = coefficients to be determined; and IT =intermediate diaphragm stiffness at the bridge section considered that is calculated as (or evaluated alternatively to find the actual stiffness). In addition, the constant C_1 reflects the fact that the LDF is nonzero even when the girder spacing S approaches zero, as evidenced by many studies and also reflected in the current LRFD codes (AASHTO 1998), the C_2 term reflects the linear relationship of the LDF versus girder spacing, which results from the simple beam action and is consistent with the traditional “S-over” term. and the C_3 term represents the effect of relative longitudinal stiffness and transverse stiffness on load distributions.

Cai and Avent (2008) performed a study for the Louisiana Transportation Research Center to investigate the need of reinforced concrete intermediate diaphragms in precast concrete girder bridges, evaluate their effectiveness, and find a steel alternative that can possibly replace the concrete intermediate diaphragms. They obtained the information about the intermediate diaphragm applications in the State of Louisiana through reviewing the Louisiana Department of Transportation and Development (LADOTD) Bridge Design Manual (BDM) and a feedback survey. They selected a few bridges for inspection using the LADOTD state bridge database and direct meetings with engineers. They performed their research on simply supported and continuous bridges, and skewed and non-skewed. In addition, they developed a finite element model to evaluate the influence of the intermediate diaphragms on the live load distribution factors. The following parameters were investigated: span length, skew angle, girder spacing, girder stiffness, and diaphragm stiffness. As a result of their study, Cai and Avent (2008) suggested a reduction

factor (Table 3-1, Table 3-2, and Table 3-3) to be applied to the live load distribution factors that are given in the AASHTO LRFD BDS. This reduction factor is to account for the effects of the intermediate diaphragms in distributing the live load. Also, they indicated that steel diaphragms could possibly replace the reinforced concrete diaphragms in precast concrete girder bridges.

Table 3-1: Expressions of Rd Value for different cases

| No. of diaphragms | Interior or exterior | Equation for Rd |
|-------------------|----------------------|----------------------------------|
| 1 | Interior | $[(0.132 L + 4.85) + C] S_t S_k$ |
| 2 | | $(-0.112 L + 25.81) C S_t S_k$ |
| 1 | Exterior | $(0.132 L - 15.81 - C) P_L S_k$ |
| 2 | | $(0.147 L - 19.05 - C) P_L S_k$ |

Table 3-2: Values of SK, St, and PL for different bridge configurations

| No. of Diaphragms | θ° | Interior Girder | | Exterior Girder | |
|-------------------|------------------------|------------------------|---------------------------------|-------------------|---|
| | | S_k | S_t | S_k | P_L |
| 1 | $\theta \leq 30^\circ$ | $1 - 0.015\theta$ | $0.0264X^{0.8062}$ | $1 - 0.01\theta$ | $0.45 + 0.55d$ ($0 \leq d \leq 3ft$) |
| | $\theta > 30^\circ$ | $0.775 - 0.0075\theta$ | | 0.7 | |
| 2 | $\theta \leq 30^\circ$ | $1 - 0.0167\theta$ | $0.0264X^{0.5358}$ (Type IV) | $1 - 0.013\theta$ | $0.45 + 0.55d$ ($0 \leq d \leq 3ft$) |
| | $\theta > 30^\circ$ | $0.725 - 0.0075\theta$ | $0.0264X^{0.2641}$ (Type BT) | 0.6 | |

Table 3-3: Values of C in Rd expression

| Girder Type | Interior | | Exterior | |
|-------------|-------------------|-------|-------------------|-------|
| | No. of Diaphragms | | No. of Diaphragms | |
| | 1 | 2 | 1 | 2 |
| II | 0 | ----- | 0 | ----- |
| III | 2 | ----- | 3 | ----- |
| IV | 3.5 | 1 | 5 | 0 |
| BT | ----- | 1.98 | ----- | 4 |

where R_d = influence in load distribution due to diaphragm, L = length of girder (ft.), C = constant, S_t = stiffness influence factor, P_L = correction factor for taking into account position of lateral loading system, S_k = skew influence factor, d = distance between center of exterior girder to wheel line closest to edge, S_t = stiffness reduction factor, θ = skew angle (degrees), and X = (possible diaphragm stiffness contributing to load distribution/absolute diaphragm stiffness)*100.

Li and Ma (2010) developed a Finite Element model and calibrated their model against field tests. The calibrated model was used to perform a parametric study on the influence of intermediate diaphragms on the flexural strain in girders, deflections, and live load factors in longitudinal joints. The parametric study, investigated the number of intermediate diaphragms, diaphragm type (steel or concrete), and cross-sectional area of steel diaphragms. They noted that the location of the intermediate diaphragm has a minor effect on the flexural strain, girder deflection, and live load factors in longitudinal joints.

Grace et al. (2010) investigated the use of transverse un-bonded post-tensioning strands to control the longitudinal cracks in the deck slab of box-beam bridges. They used Carbon-Fiber-Reinforced-Polymer (CFRP) strands. The advantages of CFRP strands in comparison with steel strands are larger longitudinal axial strength, less thermal expansion, less density, and noncorrosive nature (ACI 440.1R-03, 2003). They performed an extensive experimental study on a half-scale, 30-degree-skew, precast, prestressed concrete

side-by-side box-beam bridge model. performed strain and load-distribution tests to investigate the efficiency of transverse post-tensioning forces and the number of intermediate diaphragms. They performed the load distribution tests by applying a single point load of 15 kip at the mid-span of each box girder for various levels of transverse post-tensioning forces. Linear-motion transducers installed at the mid-span of each box girder were used to measure the corresponding deflections as shown in Figure 3-1.

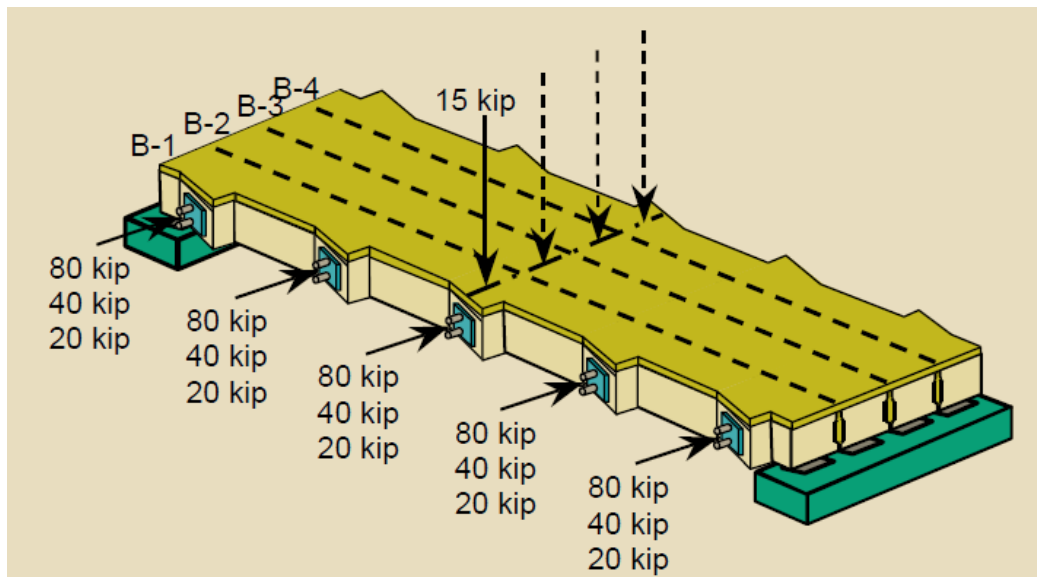


Figure 3-1: The load-distribution test applies transverse post-tensioning forces at five diaphragms (Grace et al., 2010)

They noted that the largest deflection occurred in the loaded beam and as the distance from the loaded beam increased the deflection decreased. In addition, the study reported a decrease in the differences in the above deflections with the increase of the level of post-tensioning forces. For instance, when the transverse post-tensioning forces were applied at all 5 diaphragms, and the load was applied at beam B-4 in the cracked phase, the difference in deflection between beams B-1 and B-4 were 0.22 in., 0.05 in., 0.04 in., and 0.03 in. corresponding to the transverse post-tensioning forces of 0 kip, 20 kip, 40 kip, and 80 kip respectively. Similarly, in the repaired phase, the differences in recorded deflections were 0.17 in., 0.05 in., 0.05 in., and 0.03 in. corresponding to the transverse post-tensioning forces of 0 kip, 20 kip, 40 kip, and 80 kip respectively. Furthermore, they noted that the deflections of the loaded exterior beams were higher than the deflection in the loaded interior beams regardless of the level of the bridge model phase or the transverse post-tensioning force level. For instance, in the cracked phase, and when the exterior beam B-4 was loaded, the deflections recorded between beams B-1 and B-4 were 0.42 in., 0.34 in., 0.33 in., and 0.30 in. corresponding to the transverse post-tensioning forces of 0 kip, 20 kip, 40 kip, and 80 kip applied to five diaphragms, respectively. Whereas the deflections recorded between beams B-1 and B-4 when the interior beam B-2 was loaded were 0.36 in., 0.32 in., 0.31 in., and 0.29 in. (9.14 mm, 8.13 mm, 7.87 mm, and 7.37 mm) for the same transverse post-tensioning forces order mentioned above as shown in Figure 3-2 and Figure 3-3. This undoubtedly indicates that the increase in the transverse post-tensioning forces extensively improves load distribution among the adjacent beams.

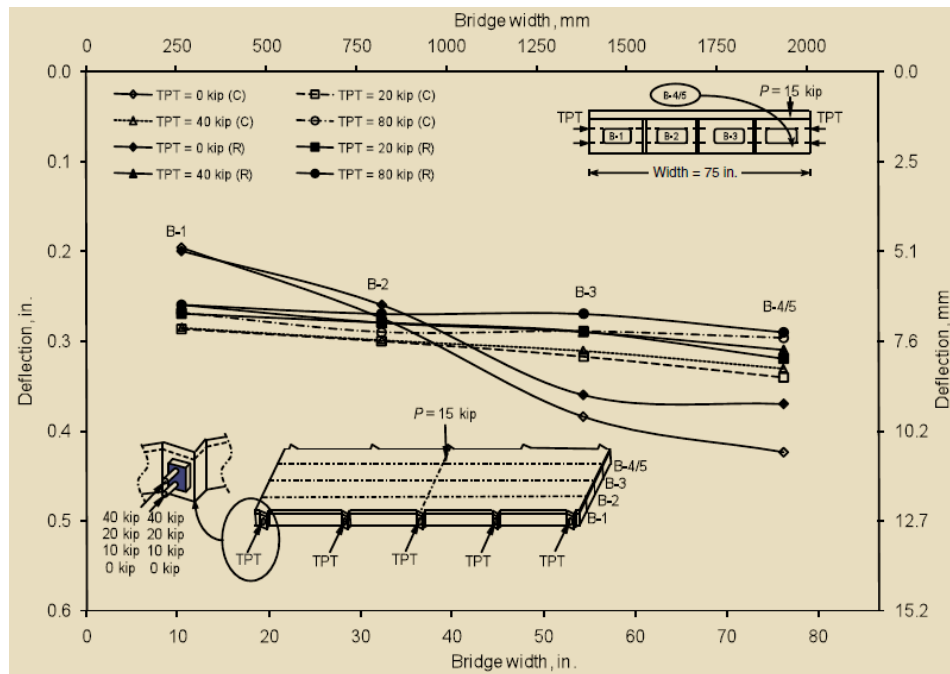


Figure 3-2: Deflection of bridge model while loading beam B-4 at different levels of transverse post-tensioning force (Grace et al., 2010)

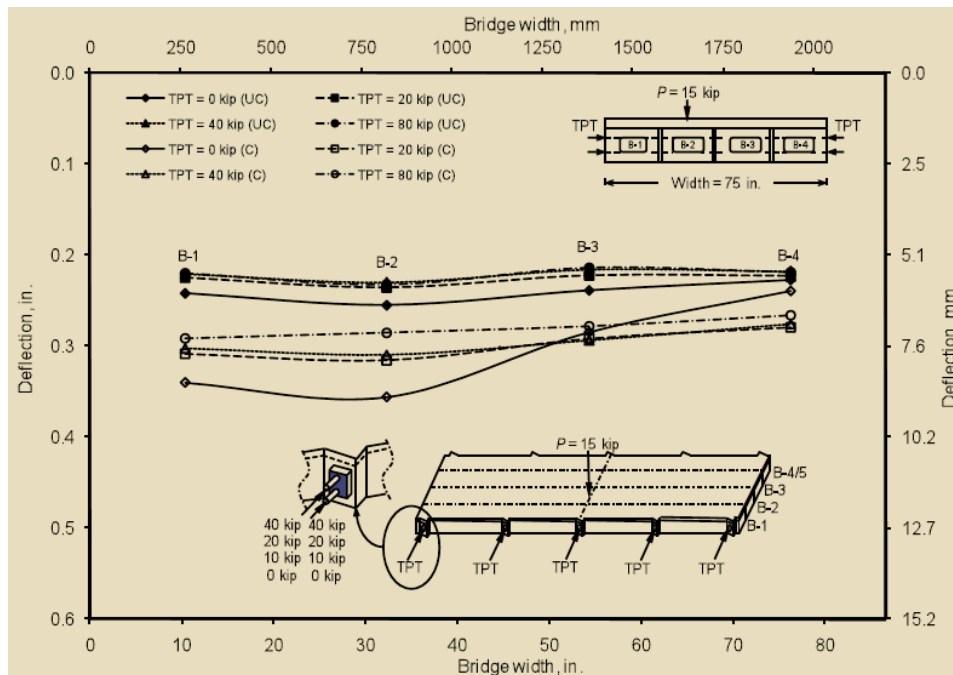


Figure 3-3: Deflection of bridge model while loading beam B-2 at different levels of transverse post-tensioning force (Grace et al., 2010).

Note: C = cracked deck slab; R = damaged beam replacement; P = load; TPT = transverse post-tensioning

Table 3-4 shows the findings of other researches regarding the effectiveness of the intermediate diaphragms in improving the load distribution factors of the live vehicular load.

Table 3-4: Effect of intermediate diaphragms on vertical live load distribution

| Intermediate Diaphragms | Improve vertical load distribution |
|---------------------------|------------------------------------|
| Lin and VanHorn (1968) | Slightly |
| Sengupta and Breen (1973) | Yes |
| Abendroth et al. (1995) | Yes |
| Barr et al. (2001) | Slightly |
| Green et al. (2004) | Modestly |
| Cai and Shahawy (2004) | Slightly |

3.2—Effect of Intermediate Diaphragm on Skewed Bridges

In bridges with skew angle, installation of intermediate diaphragms is time consuming, cumbersome, and costly. In addition, there is a variety of possible geometric configurations. For instance, the intermediate diaphragms could be parallel to the bent cap, perpendicular to the girder line, or perpendicular to the girder line with discontinuity after each girder to insure a constant distance from the support. The latter is primarily used in Louisiana. However, for small skew angles, the configuration of the intermediate diaphragms has a minimal effect because the spacing between the positions of intermediate diaphragms for different configurations is small (2008). In all of the above cases, the effectiveness of the presence of intermediate diaphragms is questionable.

Kostem and deCastro (1977) studied the effect of intermediate diaphragms on precast concrete I-beam bridges. The developed finite element model was verified against two field tested bridges. They concluded that only 20-30% of the concrete intermediate diaphragm stiffness contributes to the load distribution. Moreover, they highlighted that this contribution is minor when all the lanes are loaded. In addition, they concluded that the distribution of loads at mid-span was not affected by the increase in the number of diaphragms. They suggested that above conclusions can be applied to bridges with a skew angle up to 30°. They also recommended that in the case of large skew angles and vehicle overload, a further investigation is required before eliminating the intermediate diaphragms.

Griffin (1997) conducted a research on two precast concrete I-girder bridges with a 50° skew angle. One of the two bridges was constructed with concrete intermediate diaphragms. The bridges were along the coal haul route system of Southeastern Kentucky. The aim of the study was to investigate the effect of intermediate diaphragms on the vehicular live load distribution. Griffin (1997) noted that bridges along coal haul routes, which have similar design to the two investigated bridges, have experienced excessive concrete spalling at the interface between the bottom flange of the prestressed concrete girder and the intermediate diaphragm. Griffin (1997) reported that the intermediate diaphragms were amplifying the rate of damage and deterioration rather than distributing the traffic loads and reducing the moment. They performed experimental static and dynamic field testing on both bridges, and used the test data to calibrate the Finite Element Models. Griffin (1997) employed the Finite Element Models to investigate the cause of the concrete spalling at the interface between the bottom flange of the precast concrete girder and the intermediate diaphragm, and to study the effect of intermediate diaphragm on the load distribution. They did not report any significant advantage in structural response in bridges with intermediate diaphragms. Despite the large difference, percent-wise, in response between the two bridges, Griffin (1997) suggested that the stresses and displacements of bridges without intermediate diaphragms would still be within the American Concrete Institute (ACI) and the AASHTO limits. As large skewed bridges are loaded, the girders tend to separate which, in turn, creates large stress concentrations at the interface between the bottom flange of the girder and the intermediate diaphragm. This is the primary reason for the concrete spalling at the interface region. They recommended installing steel diaphragms instead of concrete diaphragms.

Barr et al. (2001) investigated the effect of intermediate diaphragms on live load distribution in a three-span prestressed continuous concrete girder bridge with a skew angle of 40° and span lengths of 80

ft., 137 ft., and 80 ft. Barr et al. (2001) built a FEM to assess the AASHTO live load distribution equations. They concluded that the addition of intermediate diaphragms has a minimal effect on the live load distribution in both interior and exterior girders. They concluded that for interior girders, the intermediate diaphragms reduced the distribution factor by about 2% regardless of the skew angle. For exterior girders and when the skew angle is relatively small ($<30^\circ$) the distribution factor was reduced up to 2%; however, this reduction increased with the increase of the skew angle to reach 5% for a 60° skew angle. They concluded that the effect of intermediate diaphragms on the distribution factors is minor regardless of the skew angle. This conclusion by the authors agrees with the findings of others (Sithichaikasem and Gamble, 1972; and Stanton and Mattock, 1986).

Cai et al. (2002) developed a Finite Element Model and compared the results to the field measurements of six prestressed concrete bridges in Florida. They suggested that in order for the intermediate diaphragms to have a significant effect on the live load distribution, a full moment connection shall be ensured between the intermediate diaphragms and the girders where the intermediate diaphragm stiffness is about 10% of the girder. They also concluded that in the absence of intermediate diaphragms, the increase in the skew angle is associated with a decrease in the load distribution factor as recommended in the AASHTO LRFD 2004. On the other hand, in the presence of full stiffness intermediate diaphragms, the increase in the skew angle causes an increase in the load distribution factor.

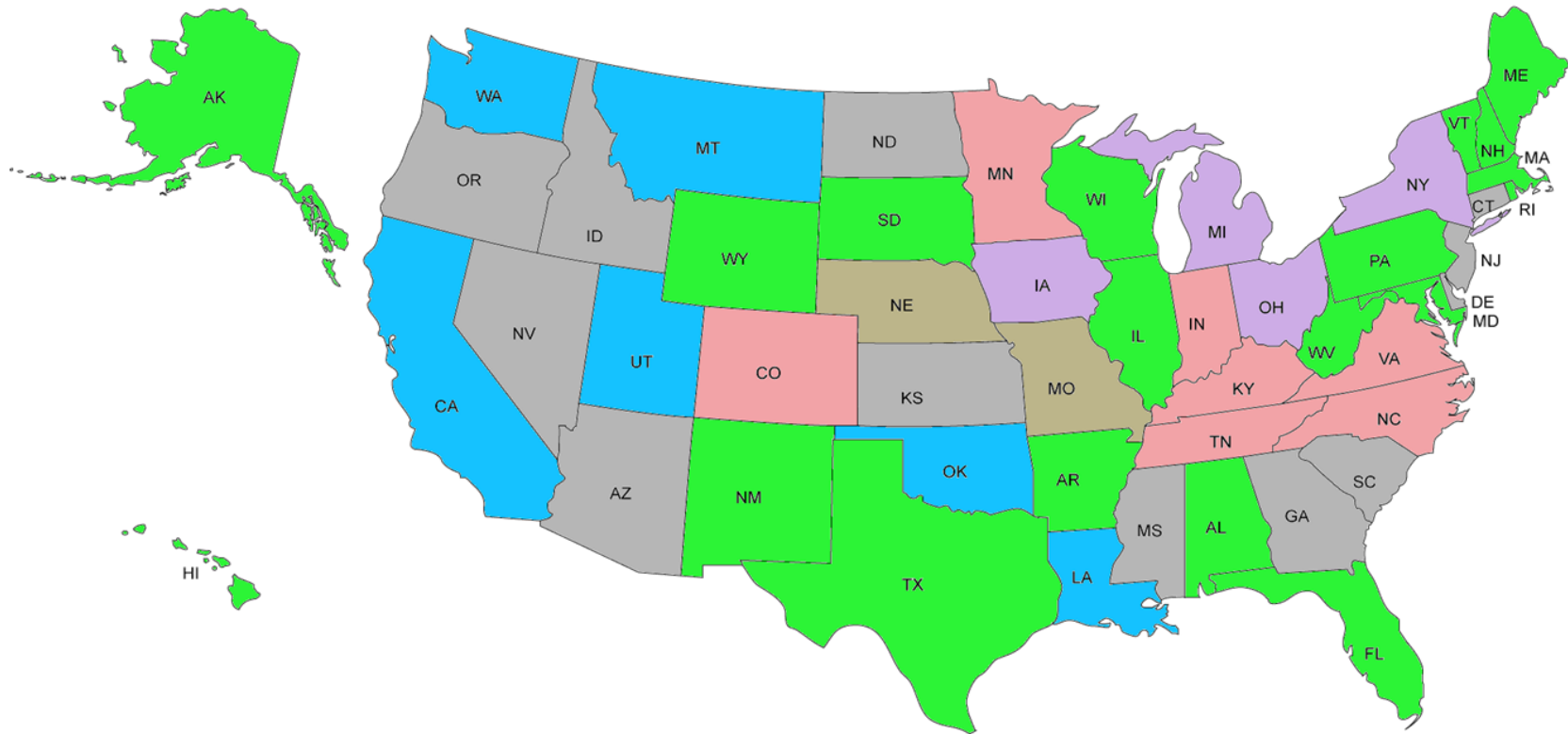
Green et al. (2004) carried out a study to investigate the effect of intermediate diaphragms in enhancing precast bridge girder performance. In addition to the contribution of the intermediate diaphragms, they studied the effect of skew angle, temperature change, and an increase in bearing stiffness due to cold temperature or aging. They developed a Finite Element Model to simulate a bridge with Florida Bulb Tee 78. Green et al. (2004) performed a parametric study to evaluate the effect of the above variables and assessed the effectiveness of the intermediate diaphragms by comparing the maximum deflections. The deflections were measured at the midspan of the critical girder. Their model was loaded with HL93 truck as recommended by the AASHTO LRFD. They concluded that the presence of intermediate diaphragms reduces the deflection by 19% for straight bridges, 11% for bridges with $15-30^\circ$ skew angle, and 6% for bridges with 60° skew angle.

3.3—Effect of Intermediate on Curved Bridges

AASHTO LRFD Bridge Design Specifications in Article 5.13.2.2 suggests that intermediate diaphragms may be used in between beams in curved bridges in order to provide torsional resistance and support at points of discontinuity or at right angle points of discontinuity or at angle points in girders. In addition, AASHTO LRFD Bridge Design Specifications in Article C5.13.2.2 states that the need and required spacing for diaphragms in curved bridges is dependent on the radius of curvature and the proportions of the webs and flanges. However, it was found that the intermediate diaphragms' contribution to the global behavior of concrete box girder bridges is very minimal.

3.4—Published Policies and Standard Details of State Departments of Transportation

Each state's Department of Transportation was investigated as to their current policy and procedure of the use of intermediate diaphragms (ID). This was accomplished by surveying each state's websites for published materials relating to the use of ID. The results were that 31 states have either a policy or a standard drawing listed on their website. The other 19 states do not have any reference to ID listed on their website. Texas specifically states that internal diaphragms are not required. In addition, Florida does require ID, although their website does not make this specific claim. Of the 31 states with some mention of ID, 14 have a policy and no standard drawing, and 17 have a standard drawing but may or may not have a policy. Figure 3-4 has a schematic of each state's policy on ID. Table 3-5 gives specific information for each state's policy and/or standard detail information.



| Standard Policy | No Policy* | Policy Defined <u>NO</u> Standard Detail | | Standard Details May Have a Policy | | |
|-----------------|------------|--|----------|------------------------------------|----------|----------------------|
| | | Concrete ID | Steel ID | Concrete ID | Steel ID | Steel OR Concrete ID |
| 31 | 19 | 12 | 2 | 6 | 7 | 4 |

* Texas and Florida: ID are not required

Figure 3-4: DOTs published policies schematic on intermediate diaphragms

Table 3-5: DOTs published policies on intermediate diaphragms

| State | | ID Policy Definition | | ID size, shape, material defined by either Standard Detail or Policy | Standard Detail |
|-------|-------------|--|--------|--|--|
| | | Span | Skewed | | |
| AL | Alabama | ID shall be used only as required by calculation" | | Null | Null |
| AK | Alaska | Null | | Null | Null |
| AZ | Arizona | span < 40', not required 40' > span, @ mid-span | | CIP concrete 9" thick | Null |
| AR | Arkansas | Null | | Null | Null |
| CA | California | span > 40', required ID @ max. moment Memo to Designers Recommends: • 80' < span < 120 one ID • span > 120' use two or three ID | | Memo to Designers Recommends: Skew $\leq 20^{\circ}$, either normal or skewed ID Skew $>20^{\circ}$, ID normal to girder | CIP Concrete 8" thick, placed 1'-9" from bottom of deck to bottom of girder |
| CO | Colorado | When required, placed normally or radially to girders | | Null | w16x26 galvanized steel, bolted to the girder on top flange and web |
| CT | Connecticut | ID Requirements: • span $\leq 80'$, one at mid-span • 80' \leq span, at 3rd points | | ID Requirements • span $\leq 30^{\circ}$, ID placed inline along skew • 30 $^{\circ}$ < skew, ID normal & staggered to girder | CIP and monolithic with the concrete deck. Steel ID are prohibited. ID must be poured and cured prior to pouring the deck. |
| DE | Delaware | Minimum one ID @ mid-span | | ID are normal to beams | ID must be poured and cured prior to pouring the deck. |
| FL | Florida | Null | | Null | Null |

| | | | | | |
|----|----------|---|---|---|------|
| GA | Georgia | span > 40', place ID @ mid-span | Placed normal to girders; placed so line through girder-mid-points crosses ID @ mid-bay | Steel diaphragms (w/ concrete girders) are not preferred | Null |
| HI | Hawaii | Null | Null | Null | Null |
| ID | Idaho | span < 40', not required 40' < span < 80', @ mid-span 80' < span < 120', @ third points span > 120', @ quarter points | Skew > 20°, ID normal to girder and staggered | CIP Concrete 10" thick min., Placed from bottom of deck to top of bottom flange of girder | Null |
| IL | Illinois | Null | Null | Null | Null |
| IN | Indiana | Provide ID for I-beam or bulb-tee: spans < 80', not required 80' < span < 120', @ mid-span span > 120', @ third points | Null | Steel Channel bolted to web | Yes |
| IA | Iowa | <u>Beams A-D, similar to AASHTO beams</u> spans above roadways use CIP concrete spans above waterway or railways use either steel or CIP concrete one ID at mid-span <u>Beams BTB-BTE, similar to Bulb Tee beams (steel diaphragms only)</u> spans ≤ 120 one at mid-span spans > 120' @ 20' of each side of beam centerline | For Beams BTB-BTE skews < 7.5° ID skewed skews > 7.5° ID normal to girder | Steel channel bolted to web OR CIP concrete 10" thick min placed from bottom of deck to top of bottom flange. | Yes |
| KA | Kansas | Use CIP intermediate diaphragms when the structure is heavily skewed or splayed | Null | Cast-in-place | Yes |
| KY | Kentucky | ID Requirements: • span < 40', not required • 40 < span < 80', one at mid-span • span > 80', at quarter points | Null | Steel cross frames OR steel channel bolted to web | Yes |

| | | | | | |
|----|---------------|---|------|--|------|
| LA | Louisiana | See scope of work for this project | Null | Null | Yes |
| ME | Maine | Null | Null | Null | Null |
| MD | Maryland | Null | Null | Null | Null |
| MS | Massachusetts | Null | Null | Null | Null |
| MC | Michigan | Null | Null | CIP concrete, steel channel, or steel cross frames bolted to web | Yes |
| MN | Minnesota | ID are not required for 14RB, 18RB, 22RB, and 27M beams. For all other beams: span < 45'-0" no ID 45'-0" < span < 90' 1 @ mid-span 90'-0" < span < 135' 2 @ third points 135'-0" < span < 180' 3 @ quarter points span > 180' 4 plus an additional diaphragm for each additional 45 ft. of span length greater than 180' | Null | Steel cross frame or channel bolted to web | Yes |
| MS | Mississippi | required by BDM, but removed with memorandum for spans less than 150' | Null | Null | Null |
| MO | Missouri | ID Requirements: Spans < 90' one ID spans > 90', two ID @ 50' max spacing | Null | Steel channels bolted to web | Null |
| MT | Montana | Mid-span for spans > 40' | Null | CIP Concrete 10" thick | Yes |
| NE | Nebraska | Only required on spans > 160 feet | Null | Design Manual says "ID should be paid under Steel | Null |

| | | | | Diaphragm" | |
|----|----------------|---|--|---|------|
| NV | Nevada | ID requirements: span \leq 40', not required span > 40', min. one at mid-span | ID Requirements skew \leq 20 ⁰ , ID placed inline along skew skew > 20 ⁰ , ID normal & staggered to girder | Full depth CIP concrete | Null |
| NH | New Hampshire | Null | Null | Null | Null |
| NJ | New Jersey | span \leq 80', one at mid-span span > 80', at third points | skew \leq 15 ⁰ , ID placed inline along skew skew > 15 ⁰ , ID normal & staggered | Null | Null |
| NM | New Mexico | Null | Null | Null | Null |
| NY | New York | ID requirements: span \leq 65', not required 65' < span \leq 100', at mid-span only 100' < span, at third points | Null | Steel cross frame or channel bolted to web OR 12" CIP concrete depth depends on beam | Yes |
| NC | North Carolina | ID Requirements: span < 40', not required span > 40', required (location(s) not specified) | skews between 70 and 110, ID shall be along the skew | Steel channel or cross-frame | Yes |
| ND | North Dakota | ID Requirements: span \leq 45', not required unless over a roadway or rail tracks 45 < span < 90', one at mid-span span > 90', at third points | Null | Steel IDs are prohibited | Null |
| OH | Ohio | ID Max spacing is 40' | ID always normal to beam skew \leq 10 ⁰ , ID placed in line skew > 10 ⁰ , ID staggered | <ul style="list-style-type: none"> • For beam depth < 60", cast-in-place concrete • For 60" \leq beam depth, either steel cross frames, channels or cast-in-place | Yes |

| | | | | | |
|----|----------------|--|---|---|------|
| | | | | concrete | |
| OK | Oklahoma | 1 or 2 ID per span, depending on beam type" | Null | CIP concrete 9" or 10" placed only at the web | Yes |
| OR | Oregon | IDs required only for bridges crossing major truck routes spans < 40, not required 40 < span ≤ 80', at mid-span only 80 < span < 120, at third points 120' < span, at quarter points For other bridges, recommend one at mid-span | 25° < skew, IDs normal and staggered to girder | CIP concrete | Null |
| PA | Pennsylvania | Null | Null | Null | Null |
| RI | Rhode Island | Null | Null | Null | Null |
| SC | South Carolina | Span > 40', required (location(s) not specified) | 20° ≤ skew, ID may be placed along skew 20° > skew, ID shall be place normal to girder | CIP concrete | Null |
| SD | South Dakota | Null | Null | Null | Null |
| TN | Tennessee | Null | Null | Steel cross frames or 12" CIP concrete placed from bottom of deck to top of bottom flange | Yes |
| TX | Texas | ID not required unless for erection stability of beam sizes stretched beyond their normal span limits. | Null | Null | Null |

| | | | | | |
|----|---------------|---|---|--|------|
| UT | Utah | span < 80', one at midpoint 80' < span < 120', at third-points 120' < span < 160', at quarter points span > 160', at 1/5 points | Null | Minimum 6" thick CIP concrete | Yes |
| VT | Vermont | Null | Null | Null | Null |
| VA | Virginia | ID Requirements: span < 40', not required 40' < span ≤ 80', required at mid-span span > 80', equally spaced with max spacing of 40' | 20° ≤ skew, IDs may be placed along skew 20° < skew, IDs shall be place normal to girder | Steel channel or cross frame | Yes |
| WA | Washington | CIP concrete intermediate diaphragms shall be provided for all prestressed girder bridges (except slabs) as shown below: span > 160'-0" at fifth points 120' < span length ≤ 160' at quarter points. 80' < span length ≤ 120 at third points. 40' < span length ≤ 80' at mid-span span ≤ 40', ID not required. | Null | CIP concrete 8" thick, placed from bottom of deck to an arbitrary distance on the web. | Yes |
| WV | West Virginia | Null | Null | Null | Null |
| WI | Wisconsin | Null | Null | Null | Null |
| WY | Wyoming | Null | Null | Null | Null |

3.5—Summary and Conclusions of Literature Review

Intermediate diaphragms are believed to improve the live load distribution between adjacent girders. However, most researchers agree that the presence of the intermediate diaphragms has a minimal effect on the live load distribution in precast concrete girder bridges. Moreover, the high cost of installing the intermediate diaphragms outweighs any slight improvements in the live load distribution. In other words, it is more efficient to increase the capacity of the girders rather than relying on the intermediate diaphragms to improve the vertical live load distribution. This can be attributed to the small stiffness of the intermediate diaphragms when compared to the stiffness of the concrete deck and girders. In addition, the weak connection between the concrete diaphragms and the precast girders allows deterioration at interface between the prestressed concrete girder and the intermediate diaphragm which defeats the purpose of installing the diaphragm. This weak connection will not be noticed by FEM models unless a pin connection is modeled. Most researchers model this connection between the intermediate diaphragm and main girders as a rigid connection, which never develop in reality, except in cast-in-place bridges with continuous reinforcement or by using transverse post-tensioning.

It can be noted from the literature review that the only researchers who reported a significant improvement in the load distributing are Grace et al. (2010). This is attributed to the use of five (5) diaphragms and transverse post-tensioning at each diaphragm. Moreover, they reported that the increase in transverse post-tensioning force significantly improves the load distribution among the adjacent beams. However, this conclusion cannot be extended to bridges with one (1) intermediate diaphragm at mid-span of girders having a weak connection between the diaphragm and the girders.

4—SENSITIVITY STUDY

4.1—Objective

The sensitivity study was carried out with the following objectives:

- Determine appropriate modeling technique for straight, skew, and curved bridges.
- Investigate the effect of wind forces under normal loading conditions on bridge design.
- Define the best approach to represent the bearings pads in the numerical model.

The findings of the sensitivity study were deployed in the parametric study.

4.2—Numerical Modeling Technique

4.2.1—Details of Modeling Techniques

Three different numerical modeling techniques using Finite Element Analysis were investigated, namely Grillage Model, Planar Model, and Solid Model.

4.2.1.1—Grillage Mode

Grillage model, which is two-dimensional (2-D) utilizes beam elements to model the main girders and the deck. Longitudinal beam elements represent the main girders with composite section to account for the composite action between the girders and the deck. Transverse beam elements represent the deck, and both end and intermediate diaphragms. In addition, construction staged analysis was deployed allowing composite section to be activated at the appropriate stage and live loads to be acting on the composite section of the main girders. Boundary conditions were represented by using nodal supports at the ends of the longitudinal beam elements assuming hinge and roller supports. The commercially-available software Midas Civil (2016) was used to develop the grillage models.

Beam element is defined by two (2) nodes with six (6) degrees of freedom (d.o.f.) at each node, three (3) rotational d.o.f and three (3) translational d.o.f. The formulation of the beam element is based on the "Timoshenko Beam Theory", which takes into account the stiffness effects of tension/compression, shear, bending and torsional deformations.

4.2.1.2—Planar Model

Planar model, which is three-dimensional (3-D) utilizes beam elements to model the main girders and plate elements to model the deck. In addition, transverse beam elements were used to model the end and intermediate diaphragms. The composite action between the girders and the deck is achieved by the interaction between the longitudinal beam elements and the plate elements. Similar to grillage model, construction staged analysis was deployed allowing plate elements, thus composite action to be activated at the appropriate stage. Accordingly, allowing live loads to be acting on the composite section of the main girders. Boundary conditions were represented by using nodal supports at the ends of the longitudinal beam elements assuming hinge and roller supports. The commercially-available software Midas Civil (2016) was used to develop the planar models.

The plate element is defined by three (3) or four (4) nodes that are placed in the same plane. The plate element accounts for in-plane tension/compression, in-plane/out-of-plane shear, and out-of-plane bending behaviors. The out-of-plane stiffness can be based on either thin plate theory (Kirchhoff element) or thick plate theory (Kirchhoff-Mindlin element). Plate element has five (5) degrees of freedom (d.o.f.) at each node, three (3) rotational d.o.f and two (2) translational d.o.f.

4.2.1.3—Solid Model

Solid elements (also known as brick elements) are used to create the 3-D solid model. A solid element is defined by four (4), six (6), or eight (8) nodes in a three-dimensional space. A solid element could be a tetrahedron, wedge, or hexahedron. Each node retains three (3) translation degrees of freedom.

The 8-node Hexahedron and 6-node wedge elements were used to model the girders, deck, and both end and intermediate diaphragms in the solid model. Boundary conditions were represented by using nodal supports at the edge of the solid beam elements assuming hinge and roller supports. The commercially-available software Midas FEA (2015) was used to develop the solid models.

4.2.2—Comparison of Modeling Techniques for Straight Bridges

4.2.2.1—Details of models

The straight bridge having the cross-section shown in Figure 4-1 was modeled using the three different modeling techniques. The bridge consisted of four (4), simply-supported, BT-78 girders spaced at 12 ft. and a span length of 130 ft. the bridge has a clear roadway of 40 ft. comprising two (2) travel lanes of 12 ft. width. The bridge has two (2) end diaphragms and one ID at mid-span. All diaphragms were full-height (extended from of bottom of deck to top of bottom flange) and were 8 in. wide, in accordance with Section 5.13.2.2 of LADOTD BDEM.

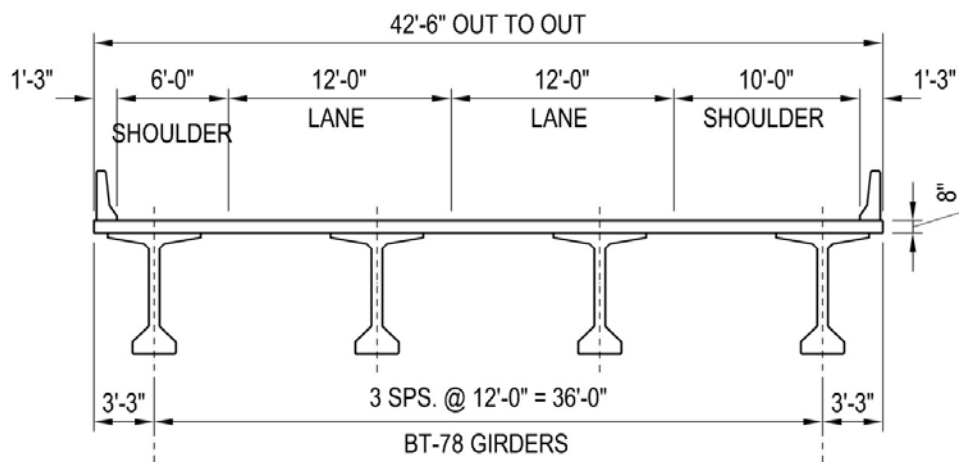


Figure 4-1: Cross-section of straight bridge

The bridge was designed using SmartBridge software to determine the number of required prestressing strands. As a result, each girder was designed to have 44 straight strands and 12 harped strands as shown in Figure 4-2. All prestressing strands are 0.6 in., Grade 270 ASTM A416 low-relaxation strands. The concrete compressive strengths of the girders and the deck were 8.5 and 4.0 ksi, respectively.

The design vehicular live load was LADV-11 according to BDEM. A magnification factor for the HL-93 of 1.30 was used to model the LADV-11, since the bridge is simply supported and the study is concerned with the mid-span positive moment only. Section 5.3 of this report gives full details and can be referred to for further explanations.

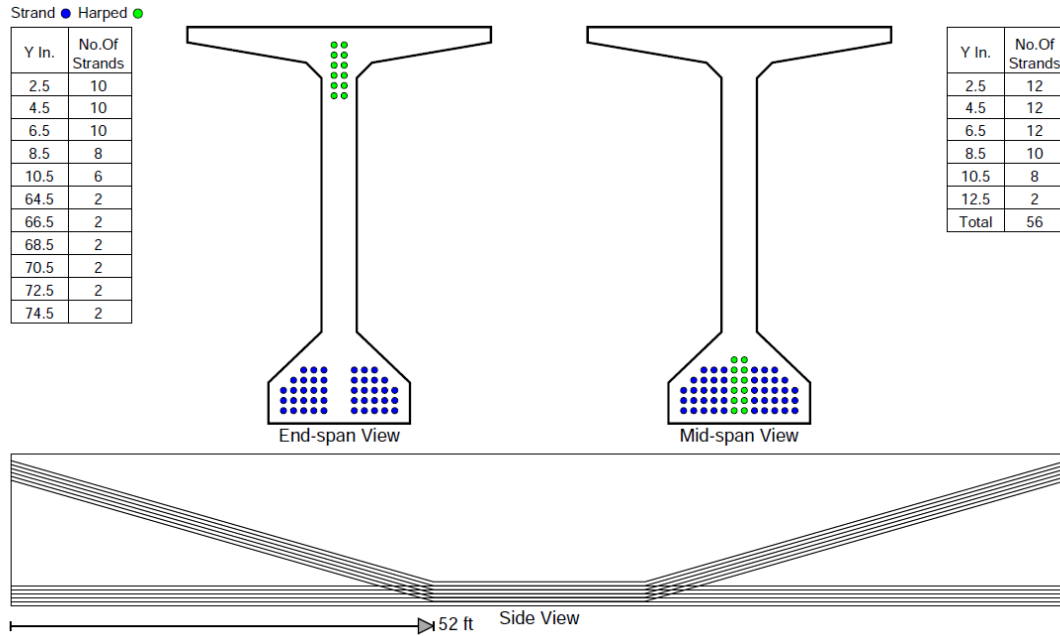


Figure 4-2: Design of straight BT-78 girder bridge (SmartBridge)

Two mesh sizes were investigated using the grillage model, where 5 ft. and 2.5 ft. longitudinal elements were used. The planar and solid models discretized the main girders using the 2.5 ft. elements only. Figure 4-3, Figure 4-4, and Figure 4-5 show the different view of the grillage, planar, and solid models of the straight bridge, respectively.

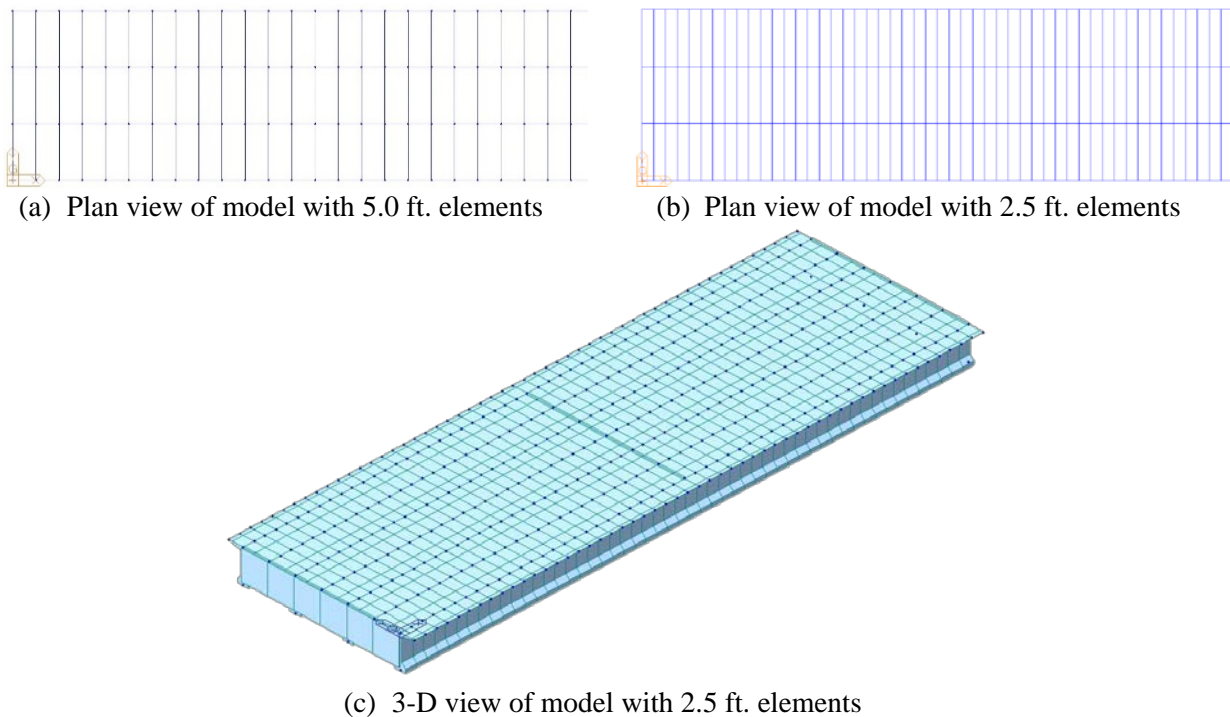


Figure 4-3: Grillage models of straight bridge

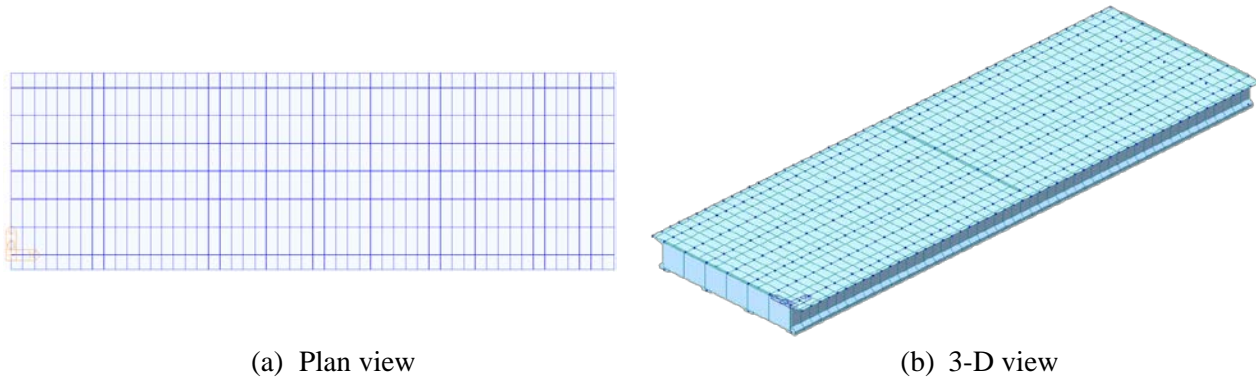


Figure 4-4: Planar model of straight bridge

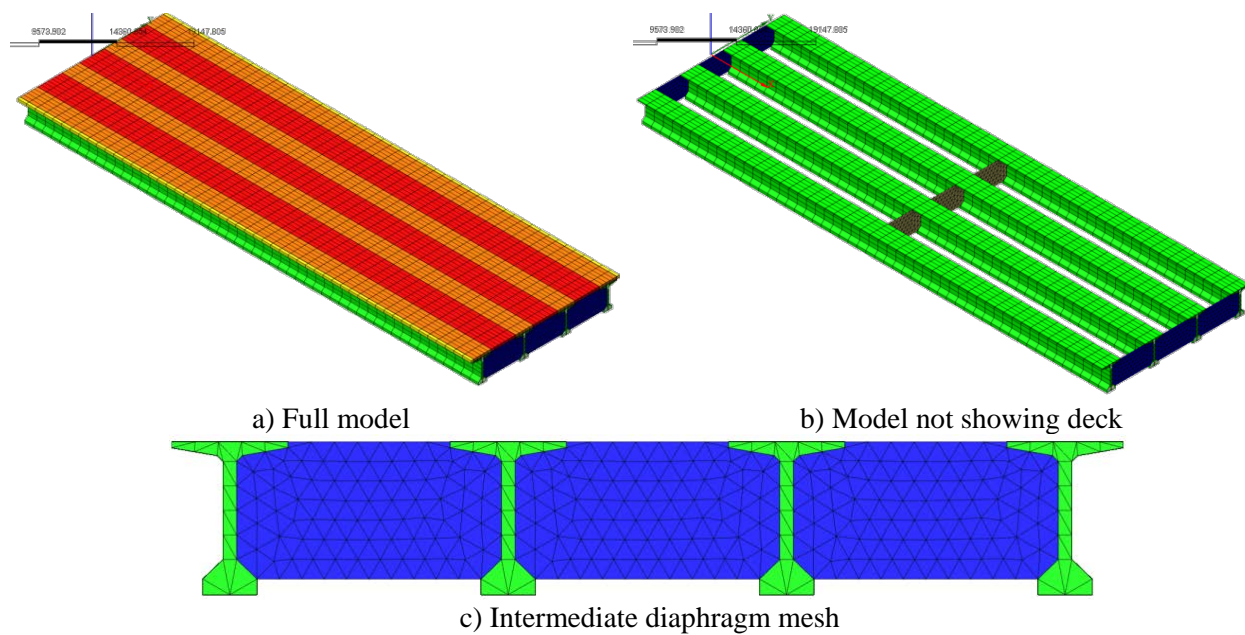


Figure 4-5: Solid model of straight bridge

4.2.2.2—Comparison of Results

In order to assess the accuracy of the three (3) different modeling techniques, the mid-span deformation and mid-span bottom fibers stress of the exterior and interior girders under the effect of live load (LADV-11), were compared as given in Table 4-1.

Table 4-1: Results of different modeling techniques of straight bridges

| Girder | Feature | Grillage | | Planar | Solid |
|----------|-------------------|----------|------|--------|-------|
| | | 5.0 | 2.5 | | |
| Exterior | Deformation (in.) | 1.24 | 1.20 | 1.19 | 1.17 |
| | Stress (ksi) | 1.63 | 1.60 | 1.37 | 1.39 |
| Interior | Deformation (in.) | 1.09 | 1.10 | 1.10 | 1.08 |
| | Stress (ksi) | 1.47 | 1.47 | 1.30 | 1.28 |

The solid model results were used as the basis for evaluating the grillage and planar models. It can be readily seen from Table 4-1 that both the grillage and planar models yield the same results of the solid

model. This confirms that for straight I-shaped girder bridges, both grillage and planar models accurately represent the bridge behavior and yield reliable results.

4.2.3—Comparison of Modeling Techniques for Skew Bridges

4.2.3.1—Details of Models

The same straight bridge with the cross-section shown in Figure 4-1 and the same girder design shown in Figure 4-2 was modeled with skewed ends of 30° as shown in Figure 4-6. The three different techniques were used to model the skew bridge under the effect of dead loads and vehicular live load (LADV-11).

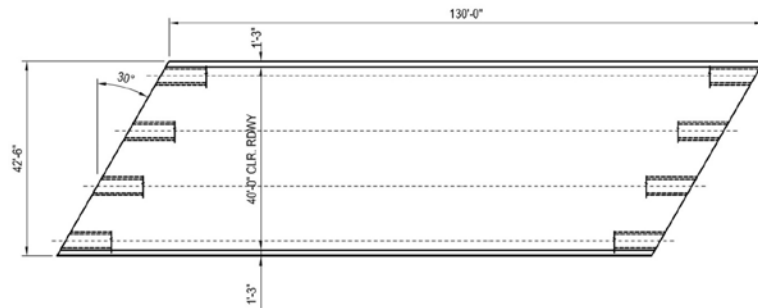
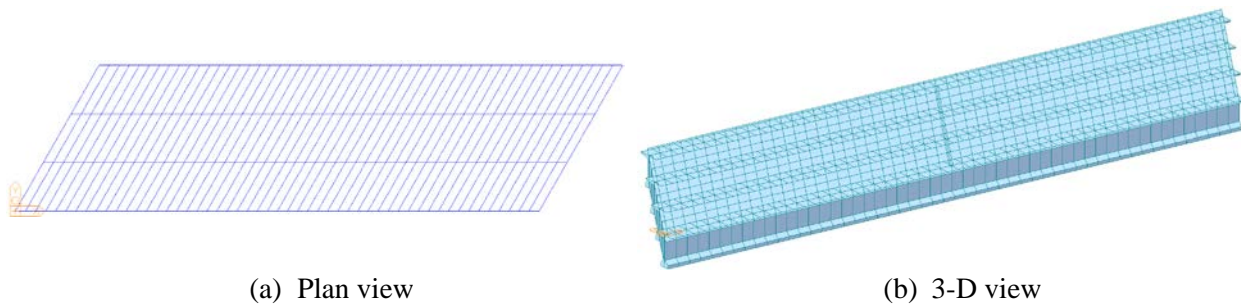


Figure 4-6: Framing Plan of Skew Bridge (30° skew angle)

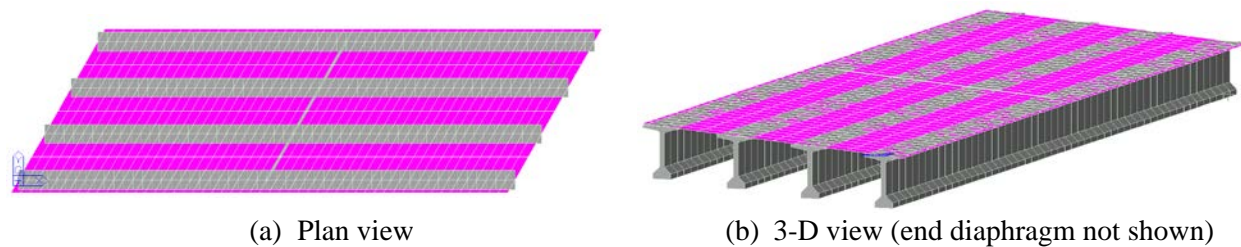
Mesh size with 2.5 ft. longitudinal elements were used for the three modeling techniques. In the grillage model the transverse beam elements were modeled parallel to the bridge, as shown in Figure 4-7. Similarly, the plate elements in the planar were parallel to the bridge end as shown in Figure 4-8. For the solid model, the girders were assumed to have square edges as shown in Figure 4-9.



(a) Plan view

(b) 3-D view

Figure 4-7: Grillage models of skew bridge



(a) Plan view

(b) 3-D view (end diaphragm not shown)

Figure 4-8: Planar model of skew bridge

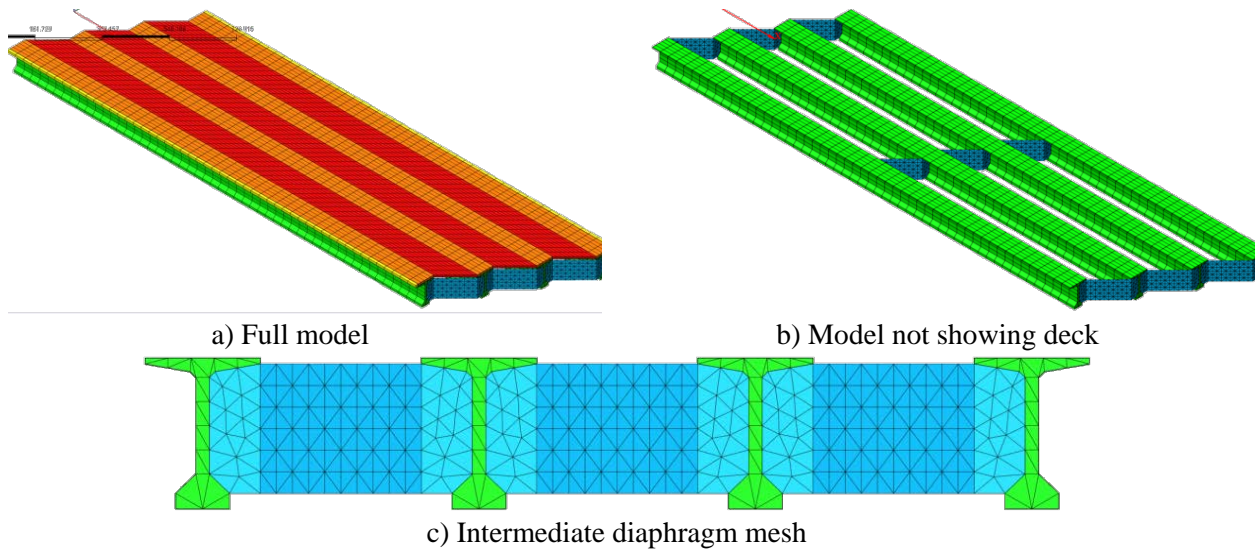


Figure 4-9: Solid model of skew bridge

4.2.3.2—Comparison of Results

In order to assess the accuracy of the three different modeling techniques, the mid-span deformation and mid-span bottom fibers stress of the exterior and interior girders under the effect of live load (LADV-11), were compared as given in Table 4-2.

Table 4-2: Results of different modeling techniques of skew bridges

| Girder | Feature | Grillage | Planar | Solid |
|----------|-------------------|----------|--------|-------|
| Exterior | Deformation (in.) | 0.86 | 0.82 | 1.11 |
| | Stress (ksi) | 1.20 | 1.03 | 1.25 |
| Interior | Deformation (in.) | 0.74 | 0.74 | 1.03 |
| | Stress (ksi) | 1.10 | 0.99 | 1.20 |

The solid model results were used as the basis for evaluating the grillage and planar models. It can be readily seen from Table 4-2 that both the grillage and planar models yield the same results of the solid model. This confirms that for skew I-shaped girder bridges, both grillage and planar models accurately represent the bridge behavior and yield reliable results.

4.2.4—Comparison of Modeling Technique for Curved Bridges

4.2.4.1—Details of Models

The curved bridge with the cross-section shown in Figure 4-10, which is similar to the straight and skew bridges was modeled using planar and solid models. The bridge has a radius of curvature of 2100 ft., arc offset from chord of 1'-9¹/₈", and cross-slope of 8%, as shown in Figure 4-11. Since the bridge has straight girders and curved deck, the grillage modelling technique is inappropriate. The planar and solid models discretized the main girders using elements that are approximately 2.5 ft. long.

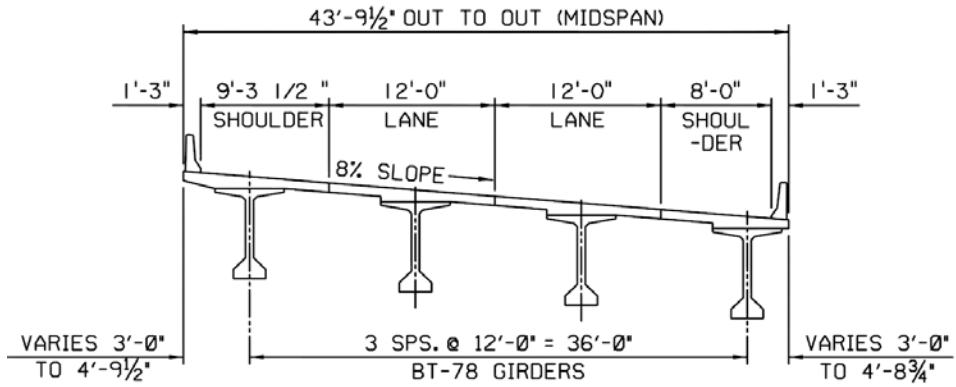


Figure 4-10: Cross-Section of curved bridge

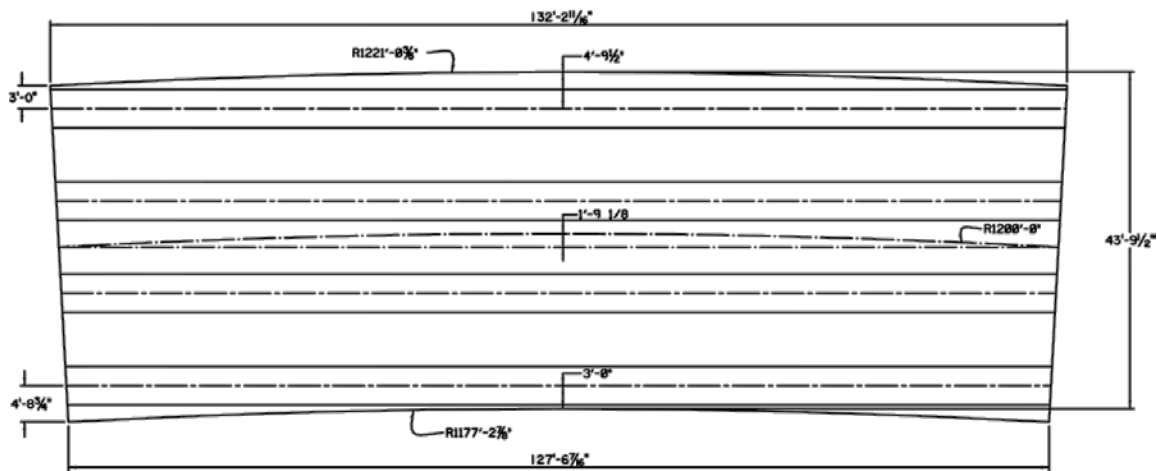
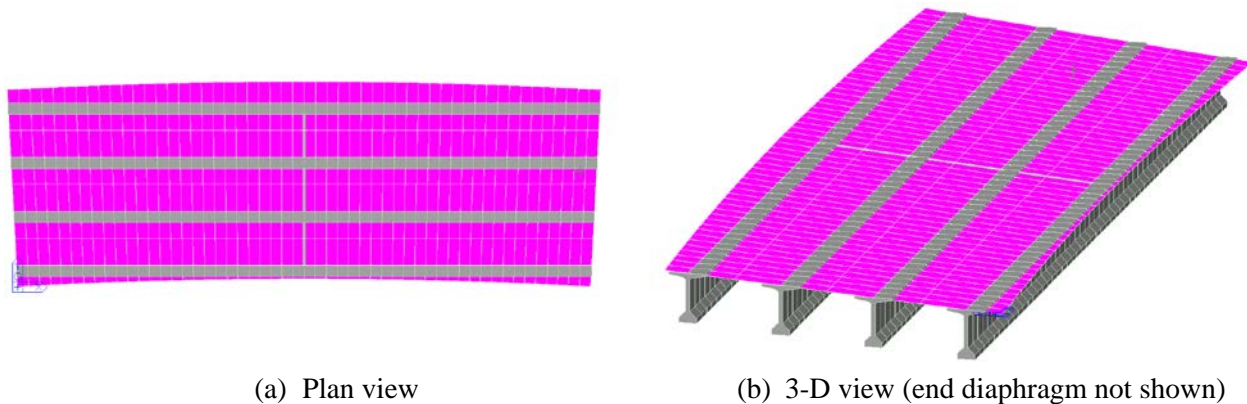


Figure 4-11: Framing plan of curved bridge

While main girders and diaphragms were modeled using beam elements, plate elements were used to model the deck as shown in Figure 4-12.



(a) Plan view

(b) 3-D view (end diaphragm not shown)

Figure 4-12: Planar model of curved bridge

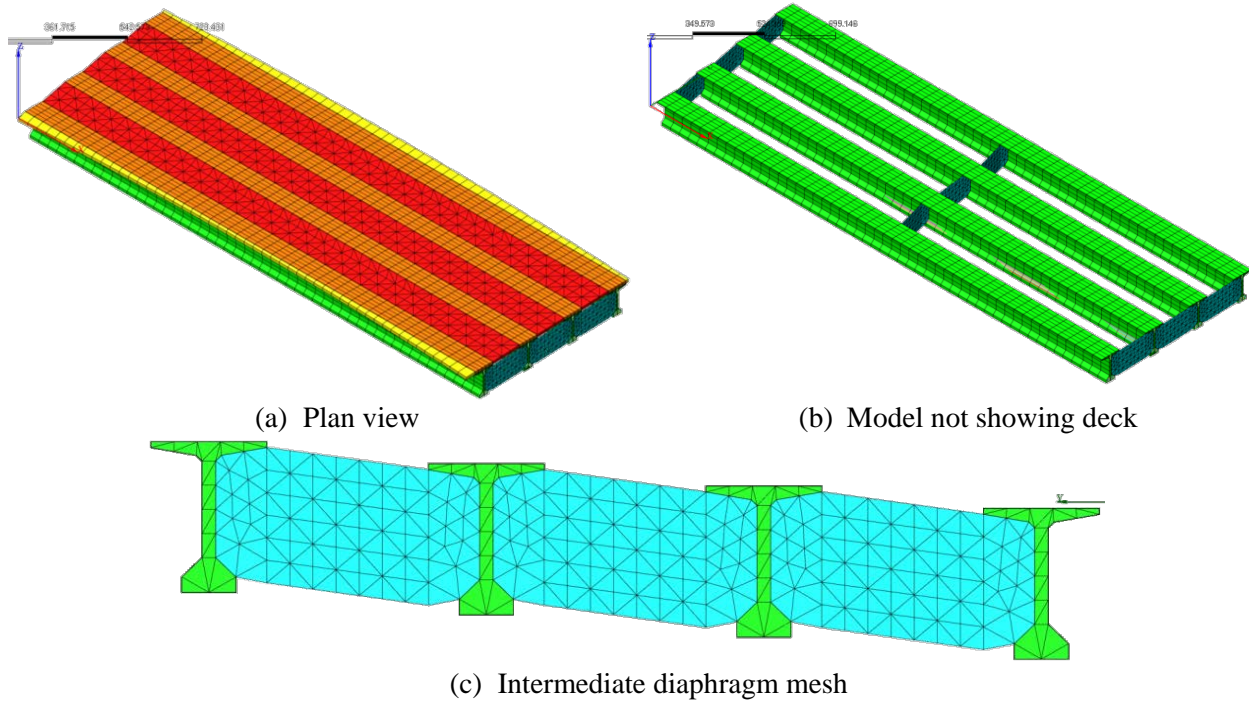


Figure 4-13: Solid model of curved bridge

4.2.4.2—Comparison of Results

In order to assess the accuracy of the three different modeling techniques, the mid-span deformation and mid-span bottom fibers stress of the exterior and interior girders under the effect of live load (LADV-11), were compared as given in Table 4-3.

Table 4-3: Results of different modeling techniques of curved bridges

| Girder | Feature | Planar | Solid |
|----------|-------------------|--------|-------|
| Exterior | Deformation (in.) | 1.27 | 1.23 |
| | Stress (ksi) | 1.61 | 1.58 |
| Interior | Deformation (in.) | 1.11 | 1.10 |
| | Stress (ksi) | 1.34 | 1.28 |

The solid model results were used as the basis for evaluating the grillage and planar models. It can be readily seen from Table 4-3 that the planar model yields the same results of the solid model. This confirms that for I-shaped girder bridges on curved spans with straight girders and curved deck, planar models accurately represent the bridge behavior and yield reliable results.

4.2.5 –Summary of Selected Modeling Techniques

Based on the comparisons of the results obtained from the three (3) different modeling techniques for the different bridge types, the following modeling techniques were selected for each bridge type:

- Straight bridges: grillage modeling
- Skew bridges: planar modeling
- Curved bridges: planar modeling

4.3—Effect of Wind Loading

4.3.1—General

According to AASHTO LRFD BDS, the wind pressure on structures (WS) as well as the wind pressure on vehicles (WL) must be investigated. The wind pressure is assumed to be caused by base design wind velocity, V_B , of 100 mph. Wind load is assumed to be uniformly distributed on areas that are exposed to wind. This area is to be taken as the sum of areas of all components, such as railing, floor system, and sound barrier, as seen in elevation taken perpendicular to the assumed wind direction. All the possible directions must be taken into account to determine the extreme force effect in the structure or in its components.

The effect of wind loading was investigated using the straight bridge with BT-78 girders defined in Section 4.2.2 of this report. For modeling purposes, the grillage modeling technique has been utilized based on the findings of Section 4.2 and summarized in Section 4.2.5 of this report.

4.3.2—Wind Pressure on Structures (WS)

AASHTO LRFD BDS recommends that the direction of the design wind shall be assumed to be horizontal, unless otherwise specified in Section 3.8.3. In the absence of more precise data, the design wind pressure (P_D) can be computed as follows according to AASHTO LRFD BDS equation 3.8.1.2.1-1:

$$P_D = P_B \left(\frac{V_{DZ}}{V_B} \right)^2 = P_B \frac{V_{DZ}^2}{10,000}$$

Where,

P_D = design wind pressure (ksf)

P_B = base wind pressure specified in AASHTO LRFD BDS Table 3.8.1.2.1-1 (Table 4-4) (ksf)

Table 4-4: Base Pressures, P_B Corresponding to $V_B = 100$ mph

| Superstructure Component | Windward (ksf) | Leeward (ksf) |
|------------------------------|----------------|---------------|
| Trusses, Columns, and Arches | 0.050 | 0.025 |
| Beams | 0.050 | NA |
| Large Flat Surfaces | 0.040 | NA |

V_B = base wind velocity equal to 100 mph at 30 ft. height

V_{DZ} = design wind velocity at design elevation, Z according to AASHTO LRFD BDS equation 3.8.1.1-1 (mph)

$$V_{DZ} = 2.5V_0 \left(\frac{V_{30}}{V_B} \right) \ln \left(\frac{Z}{Z_0} \right)$$

Z = height of structure at which wind loads are being calculated as measured from low ground, or from water level, > 30 ft.

V_0 = friction velocity, taken as specified in AASHTO LRFD BDS Table 3.8.1.1-1 (Table 4-5)

Z_0 = friction length of upstream fetch, taken as specified in AASHTO LRFD BDS Table 3.8.1.1-1 (Table 4-5)

Table 4-5: Values of V_0 and Z_0 for various surface conditions

| Condition | Open Country | Suburban | City |
|-------------|--------------|----------|-------|
| V_0 (mph) | 8.20 | 10.90 | 12.00 |
| Z_0 (ft.) | 0.23 | 3.28 | 8.20 |

In order to determine, and conservatively maximize the design wind velocity (VDZ), an open country surface condition was assumed, and the height of the structure was assumed to be 60 ft. Therefore,

$$V_{DZ} = 2.5 \times 8.20 \times \left(\frac{100}{100}\right) \ln\left(\frac{60}{0.23}\right)$$

$$V_{DZ} = 114.1 \text{ mph}$$

$$P_D = 0.05 \times \frac{114.1^2}{10,000}$$

$$P_D = 0.065 \text{ ksf (65 psf)}$$

The wind force on the structure (WS) was estimated by multiplying the design wind pressure (P_D) by the exposed area of the structure including the barrier. The height of the exposed area of the structure as shown in Figure 4-1 includes the girder (78 in.), haunch (2 in.), deck (8 in.), and barrier (32 in.). The wind force on structure (WS) is computed as follows. It should be noted that AASHTO LRFD Bridge BDS, Section 3.8.1.2.1 requires that the total wind loading on girder spans shall not be taken less than 0.3 klf.

$$WS = P_D H$$

$$WS = 0.065 \times \frac{(78 + 2 + 8 + 32)}{12}$$

$$WS = 0.65 \text{ klf} > 0.3 \text{ klf}$$

In the numerical model, the wind force on structure (WS) was applied as a uniform load on the exterior girder only as shown in Figure 4-14.

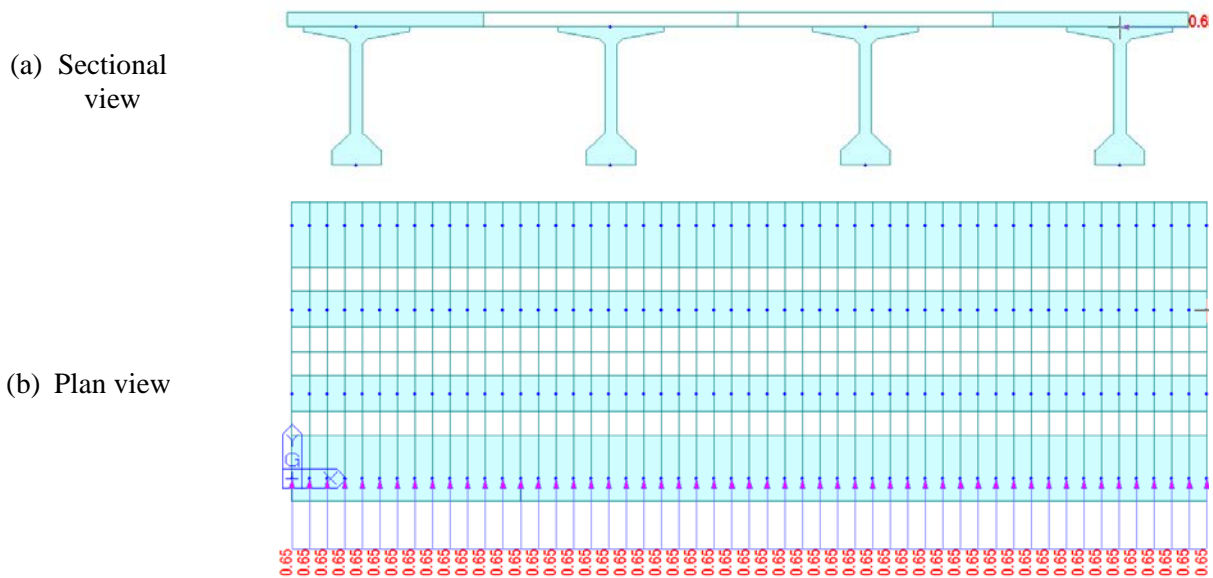


Figure 4-14: Application of wind pressure on structure (WS)

4.3.3—Wind Pressure on Vehicles (WL)

The design wind pressure on vehicles (WL) shall be applied to both structure and vehicles in the presence of vehicles. The effect of wind pressure on vehicles can be presented by an interruptible, moving force of 0.1 klf acting normal to, and 6.0 ft. above, the roadway. In the numerical model, the wind force on vehicle (WL) was applied as a uniform load on the exterior girder only as shown in Figure 4-15.

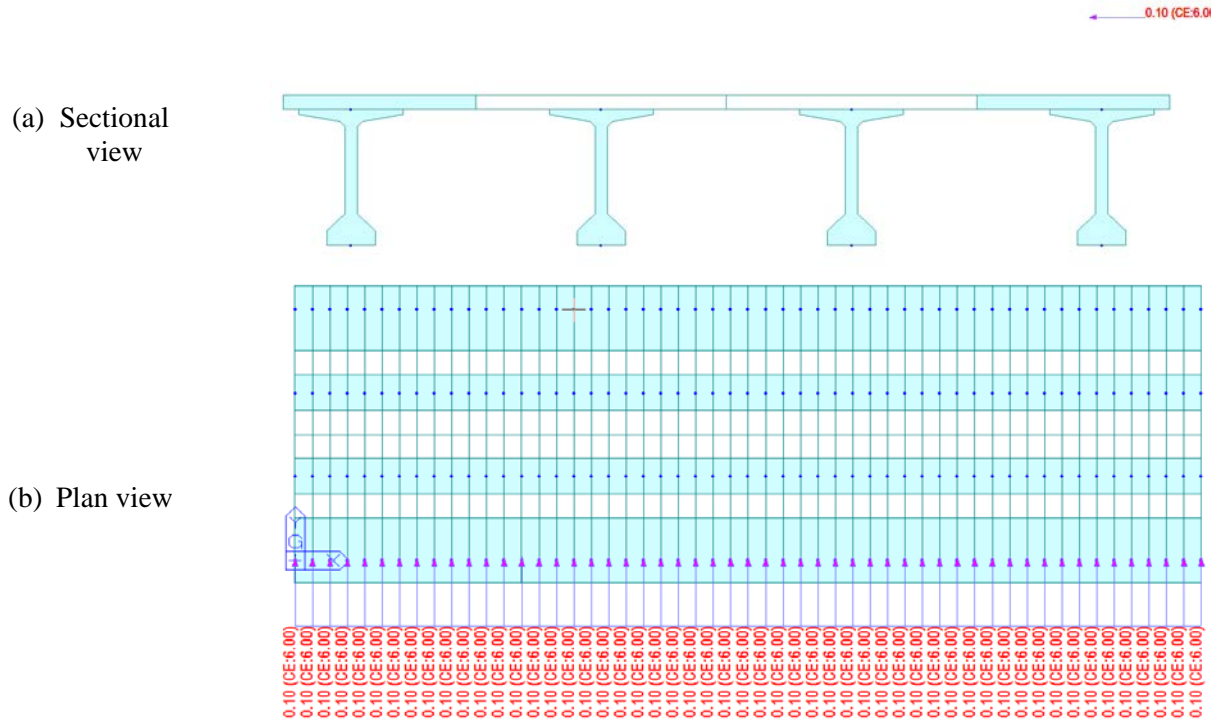


Figure 4-15: Application of wind pressure on vehicles (WL)

4.3.4—Wind Load Combinations and Load Factors

According to AASHTO LRFD Bridge BDS Table 3.4.1-1, Strength III and Strength V load combinations related to the bridge subjected to wind loading were investigated along with Strength I, which is basic load combination related to normal use of the bridge without wind.

$$\text{Strength I} = 1.25 \text{ DC} + 1.75 \text{ LL}$$

$$\text{Strength III} = 1.25 \text{ DC} + 1.40 \text{ WS}$$

$$\text{Strength V} = 1.25 \text{ DC} + 1.35 \text{ LL} + 0.40 \text{ WS} + 1.00 \text{ WL}$$

The factored flexural moments at mid-span of the exterior and interior girders for the three (3) different load combinations are summarized in Table 4-6. It can be readily seen from the results that despite that high wind pressure loading, the design of the interior and exterior girders is still governed by Strength I load combination.

Table 4-6: Factored flexure moments at mid-span (kip-ft.)

| Girder | Strength I | Strength III | Strength V |
|----------|------------|--------------|------------|
| Exterior | 13,459 | 6,125 | 11,823 |
| Interior | 13,573 | 7,139 | 12,114 |

4.4—Modeling of Elastomeric Bearings

4.4.1—Elastomeric Bearings Stiffness

Elastomeric bearing pads can resist translational movement (horizontal and vertical), and rotation. To reasonably accurately represent the boundary condition in the numerical model, the translational (two horizontal and one vertical), and rotation stiffness shall be estimated.

The horizontal stiffness (K_h) of the elastomeric bearing pads was derived based on the AASHTO LRFD Bridge Design Specifications (AASHTO LRFD BDS), equation 14.6.3.1-2 as follows:

$$K_h = \frac{GA}{h_{rt}}$$

Where,

K_h = horizontal stiffness of elastomeric bearing (kips/in)

G = shear modulus of the elastomer (ksi)

A = plan area of elastomeric bearing (in.²)

h_{rt} = total elastomer thickness (in.)

Similar to the horizontal stiffness, the vertical stiffness (K_v) was estimated as follows:

$$K_v = \frac{E_c A}{h_{rt}}$$

Where,

K_v = vertical stiffness of elastomeric bearing (kips/in),

E_c = effective modulus of elastomeric bearing in compression (ksi),

The rotational stiffness(K_r) is estimated in accordance with AASHTO LRFD BDS equation 14.6.3.2-3 as follows:

$$K_r = \frac{1.6(0.5E_c I)}{h_{rt}}$$

Where,

K_r = rotational stiffness of elastomeric bearing (kips-ft./rad)

I = moment of inertia of plan shape of bearing (in.⁴)

The effective modulus of elastomeric bearing in compression (E_c) was estimated using the stress-strain curves of reinforced bearings given in AASHTO LRFD BDS Figure C14.7.6.3.3-1, see Figure 4-16 using the shape factor (S_i), which is defined by AASHTO LRFD BDS equation 14.7.5.1-1 as follows:

$$S_i = \frac{LW}{2h_{ri}(L+W)}$$

Where,

S_i = the shape factor of a layer of a rectangular bearing without holes,

L = plan dimension of the bearing perpendicular to the axis of rotation under consideration (generally parallel to the global longitudinal bridge axis) (in.)

W = plan dimension of the bearing parallel to the axis of rotation under consideration (generally parallel to the global transverse bridge axis) (in.)

h_{ri} = thickness of i^{th} elastomeric layer (in.)

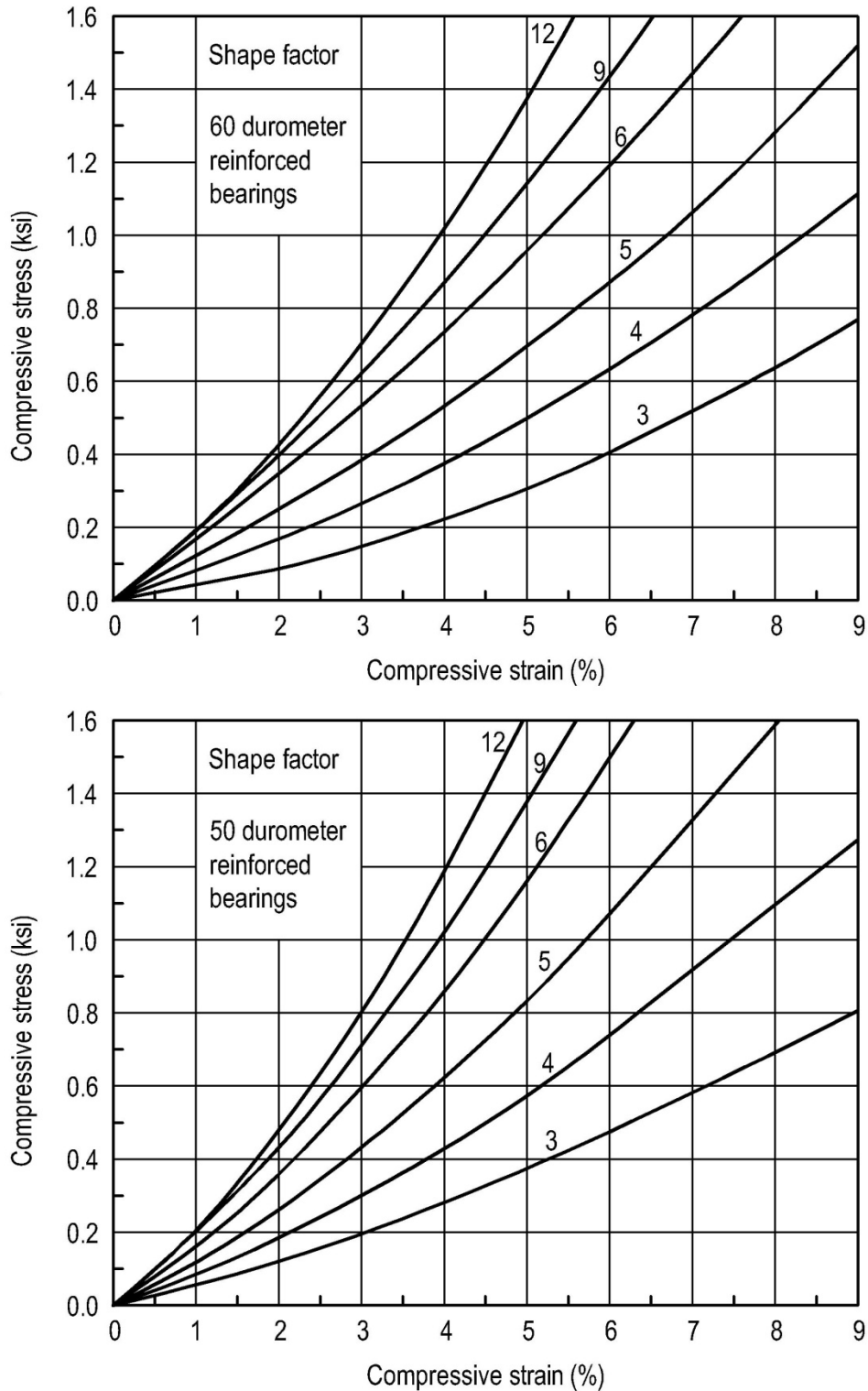


Figure 4-16: Stress-Strain Curves of elastomeric bearings in compression (C14.7.6.3.3-1)

The bearing pads of the bridge modeled in Section 4.2 of this report were designed according to AASHTO LRFD BDS Section 14.7.5. The design resulted in the following properties using Shear Modulus (G) of 150 psi:

$$L = 14 \text{ in.}$$

$$W = 22 \text{ in.}$$

$$h_{rt} = 6.25 \text{ in.}$$

using the geometrical and material properties of the bearing pads, the following values of translational and rotational stiffness were obtained:

$$K_h = 9.24 \text{ kips/in.}$$

$$K_v = 1,577 \text{ kips/in.}$$

$$K_{r-x} = 247,267 \text{ kips-ft./rad}$$

$$K_{r-y} = 610,600 \text{ kips-ft./rad}$$

4.4.2—Modeling of Bearing Pads

The bearing pads were represented in the numerical model using two (2) different approaches, to investigate the most accurate representation. In the first approach, the bearing pad was represented using one linear spring with three (3) translational and two (2) rotational stiffness, as shown in Figure 4-17. In the second approach, the bearing pad was represented using three linear springs with three (3) translational stiffness only, as shown in Figure 4-18. The rotational stiffness of the bearing pad is implicitly considered due to the use of three (3) springs. It should be noted that for vertical translational movement was considered as compression only, thus the bearing pad cannot resist tension.

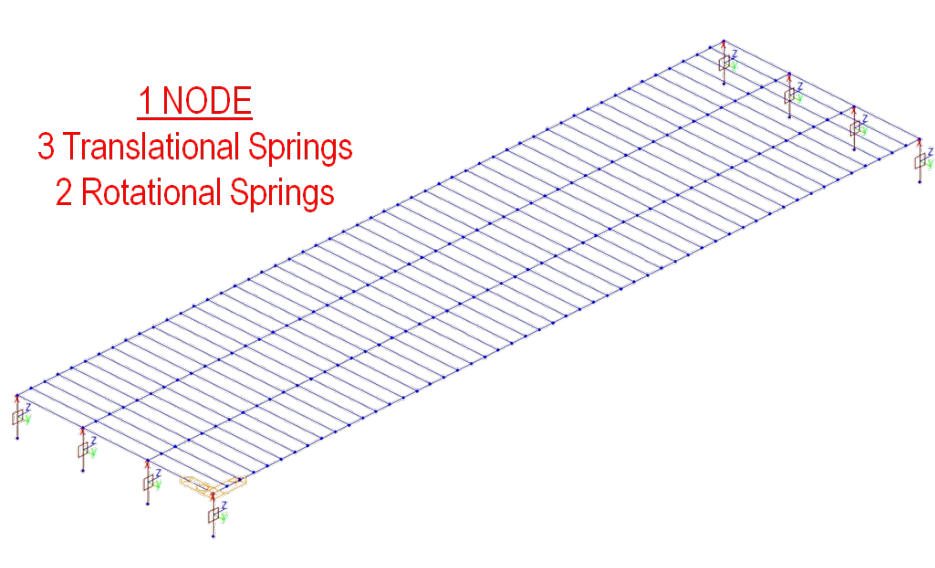


Figure 4-17: Modeling of bearings using one spring with three translational and two rotational stiffness

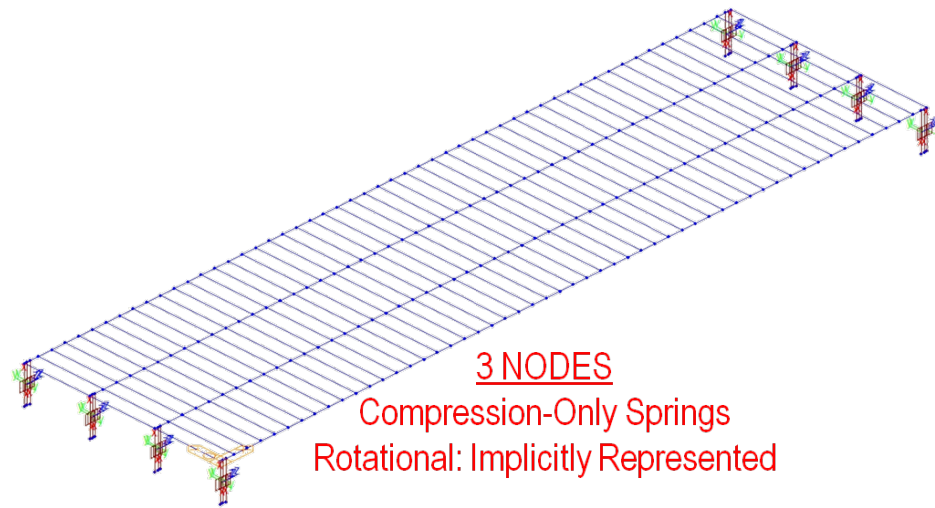


Figure 4-18: Modeling of bearings using three springs with translational stiffness only

By comparing the flexural moment diagrams of the different girders under the effect of live load for both approaches (Figure 4-19), it can be concluded that bearing pads are best represented using 3 compression-only springs. This is mainly due to the development of high values of negative flexural moment (approximately 25% of mid-span positive moment) at the end of the girders when using rotational stiffness.

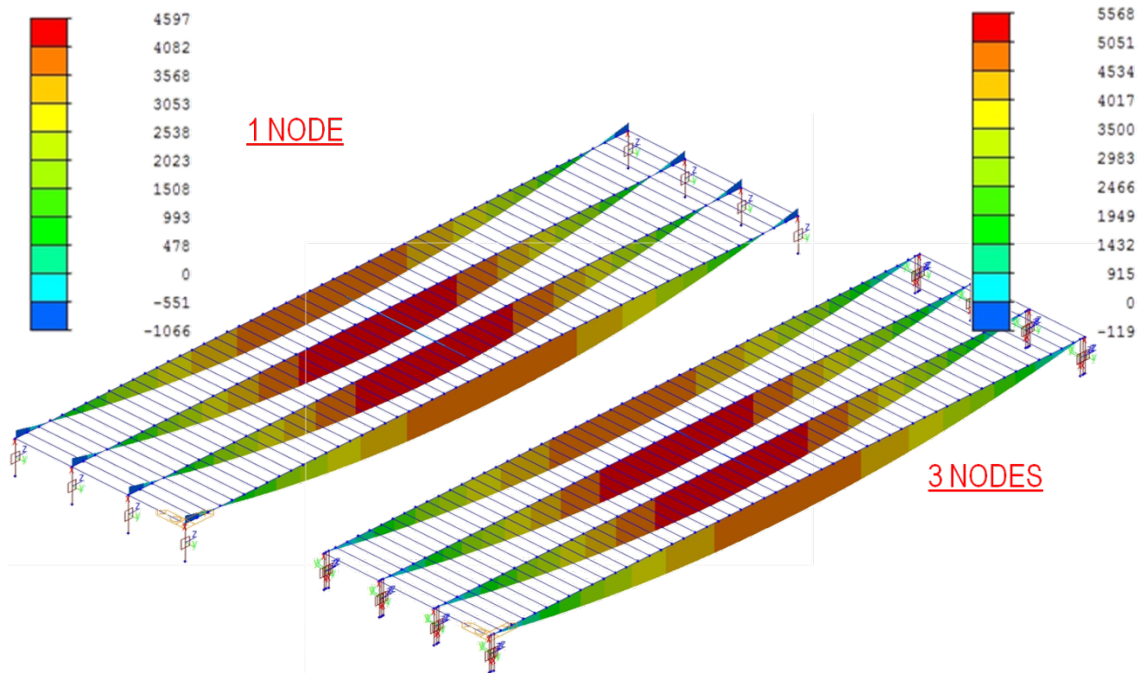


Figure 4-19: Live load BMD of girders for bearings two modeling approaches

4.5—Summary and Conclusions

The objective of the sensitivity study presented in Section 4 of this report is as follows:

- Determine appropriate modeling technique for straight, skew, and curved bridges.
- Investigate the effect of wind forces under normal loading conditions on bridge design.
- Decide on the best approach to represent the bearings pads in the numerical model.

Three (3) different modeling techniques using Finite Element Analysis were deployed to determine the most appropriate technique for straight, skew, and curved bridges. The three (3) investigated modeling techniques are Grillage Model (2-D using beam elements only), Planar Model (3-D using beam and plate elements), and Solid Model (3-D using solid elements).

The effect of wind pressure on structures (WS) and wind pressure on vehicles (WL) on the design of bridges under normal loading conditions was investigated utilizing a straight bridge and grillage modeling technique.

The modeling of bearing pads was investigated using two (2) different approaches. In the first approach, each bearing pad was represented using one linear spring with three (3) translational and two (2) rotational stiffness. In the second approach, the bearing pad was represented using three linear springs with three (3) translational stiffness only. In the second approach, the rotational stiffness of the bearing pad is implicitly considered due to the use of three (3) springs. For both approaches the vertical translational movement was considered as compression only, thus the bearing pad cannot resist tension.

Based on the observations and the findings of the sensitivity study, the following conclusion can be drawn:

- Grillage modeling technique (2-D using beam elements only) is appropriate for straight bridges.
- Planar modeling technique (2-D using beam and plate elements) is appropriate for skewed and curved bridges.
- Wind load forces and wind load combinations do not govern the design of bridges under normal loading conditions.
- Bearing pad is best modeled utilizing three (3) linear springs with translational (horizontal and vertical) stiffness only.

5—PARAMETRIC STUDY

5.1—Methodology

5.1.1—General

The new LADOTD Bridge Design and Evaluation Manual (BDEM) refined the intermediate diaphragm (ID) policy as given in Part II, Vol. 1, Chapter 5, Section 5.13.2.2. The policy requires one (1) ID at mid-span to be used for spans supported by BT-78 girder, LG-25 girder, and Quad beam under normal loading conditions (Case 1), and for spans on curve (Case 3). In addition, the new LADOTD BDEM requires ID to be full-height (extend from bottom of deck to the top of bottom flange) with a minimum width of eight (8) in.

The effect of removing ID on the design and behavior of the bridge was investigated by examining two conditions for each bridge. In the first condition, one (1) ID at mid-span was considered in accordance with BDEM, while in the second condition the ID was removed. For both conditions, end diaphragms with full-height and width of eight (8) in. were included.

5.1.2—Parameters

The parametric study was designed to investigate the effect of several parameters believed to influence the role of ID on the behavior of bridges in addition to the girder type. The parameters were selected to consider different possible configurations of bridges. The matrix developed for the parametric study is shown in detail in Table 5-1 with a total of 169 bridge models.

Table 5-1: Matrix of parametric study

| Connection Rigidity | | | | | | | | | | | | | | |
|---------------------|---------|------|---------------------|---------|-----|-----|-----|-----|-----|-----|-----|-----|---|------|
| Geometry: Straight | | | | | | | | | | | | | | |
| Girder | Spacing | Span | Connection Rigidity | | | | | | | | | | | |
| | | | Pin | Partial | | | | | | | | | | Full |
| | | | | 10% | 20% | 30% | 40% | 50% | 60% | 70% | 80% | 90% | | |
| BT-78 | 12'-0" | 130' | √ | √ | √ | √ | √ | √ | √ | √ | √ | √ | √ | |

| Connection Rigidity | | | | |
|---------------------|---------|------|---------------------|-----|
| Geometry: Straight | | | | |
| Girder | Spacing | Span | Connection Rigidity | |
| | | | Full | Pin |
| QUAD | 5'-0" | 40' | √ | √ |
| LG-25 | 9'-0" | 44' | √ | √ |
| BT-78 | 12'-0" | 130' | √ | √ |

| Span Length & Girder Spacing | | | | |
|-------------------------------------|---------|--------|---------|---------|
| Straight and Full-Moment Connection | | | | |
| QUAD | Spacing | 5'-0" | 4'-4.5" | 3'-6" |
| | Span | 40' | 40' | 40' |
| LG-25 | Spacing | 9'-0" | 7'-2.5" | 6'-0" |
| | Span | 44' | 47' | 50' |
| BT-78 | Spacing | 12'-0" | 9'-0" | 7'-2.5" |
| | Span | 130' | 146' | 156' |

| Span Length | | | | | | | |
|-------------------------------------|---------|--------|-----|------|------|------|------|
| Straight and Full-Moment Connection | | | | | | | |
| BT-78 | Spacing | 12'-0" | | | | | |
| | Span | 70' | 85' | 100' | 115' | 130' | 145' |

| Girder Spacing | | | | | | |
|-------------------------------------|---------|-------|---------|-------|--------|--------|
| Straight and Full-Moment Connection | | | | | | |
| BT-78 | Spacing | 6'-0" | 7'-2.5" | 9'-0" | 10'-0" | 12'-0" |
| | Span | 130' | | | | |

| Skew Angle | | | | | | | | |
|------------|---------|------|-------------|----|----|------------|----|----|
| Girder | Spacing | Span | Full-Moment | | | Pinned | | |
| | | | Skew Angle | | | Skew Angle | | |
| | | | 0 | 30 | 60 | 0 | 30 | 60 |
| QUAD | 5'-0" | 40' | √ | √ | √ | √ | √ | √ |
| LG-25 | 9'-0" | 44' | √ | √ | √ | √ | √ | √ |
| BT-78 | 12'-0" | 130' | √ | √ | √ | √ | √ | √ |

| Curvature / Cross-Slope | | | | | | | | | | | | | | |
|-------------------------|---------|------|---------------|---------|---------|---------|---------|---------|---------------|---------|---------|----|---|----|
| Girder | Spacing | Span | Full-Moment | | | | | | Pinned | | | | | |
| | | | Cross-Slope % | | | | | | Cross-Slope % | | | | | |
| | | | 8 | 10 | 8 | 10 | 8 | 10 | 8 | 10 | 8 | 10 | 8 | 10 |
| QUAD | 5'-0" | 40' | R1=500 | R2= 800 | R3=1000 | R1=500 | R2= 800 | R3=1000 | R1=500 | R2= 800 | R3=1000 | | | |
| LG-25 | 9'-0" | 44' | R1=500 | R2= 800 | R3=1000 | R1=500 | R2= 800 | R3=1000 | R1=500 | R2= 800 | R3=1000 | | | |
| BT-78 | 12'-0" | 130' | R1=1200 | R2=1400 | R3=2100 | R1=1200 | R2=1400 | R3=2100 | R1=1200 | R2=1400 | R3=2100 | | | |

The investigated parameters are as follows:

- Girder type (BT-78, LG-25, and Quad)
- Rigidity of connection between ID and girders (full-moment connection, partial-moment connection, and pinned connection)
- Skew angle (0, 30, and 60 degrees)
- Curvature of the bridge (radius of curvature = 1200 ft., 1400 ft., and 2100 ft. for BT-78 and 500 ft., 800 ft., 1000 ft. for LG-25 and Quad)
- Cross-slope for curved bridges (8% and 10%)

The effect of rigidity of connection between ID and the girders was investigated. Different levels of rigidity were considered including full moment connection, partial-moment connection, and pinned connections. The current standard detail given in the old LADOTD Bridge Design Manual, which is widely used in Louisiana bridges, lends itself to a pinned connection.

The effect of removal of ID on bridges with BT-78, LG-25 and Quad beams was studied. For each bridge type, three (3) girder spacing were investigated and the span lengths were varied accordingly to satisfy design requirements.

The effect of the skew angle of the bridge on the removal of ID was considered. In addition, curved bridges with different radii of curvature and cross-slopes were investigated.

The bridges considered in the parametric study were numerically modeled using Finite Element Analysis. The commercial software package “Midas Civil” was employed for this study. Grillage modeling (2-D using beam elements only) and planar models (3-D using beam and plate elements) were used to model the bridges. Refer to Section 4 (Sensitivity Study) of this report for full details about modeling techniques and the validation of the different modeling techniques for each bridge type.

The following material properties were used for all bridges considered in the parametric study:

- Concrete compressive strengths (f_c')
 - Girders: 8.5 ksi
 - Deck and diaphragms. 4.0 ksi
- Concrete unit weight for loads: 0.155 kcf
- Concrete unit weight for modulus: 0.145 kcf
- Prestressing Strands
 - 0.6 in. diameter
 - ASTM A416, Grade 270
 - Low-relaxation
- Structural deck thickness: 8.0 in.
- Barrier weight: 0.3 klf

5.1.3—Live Load Cases

5.1.3.1—General

Louisiana Design Vehicle Live Load 2011 (LADV-11) was used according to LADOTD BDEM Section 3.6. LADV-11 is the product of the standard design vehicle HL-93, specified by AASHTO LRFD BDS, and a magnification factor. Since the bridges considered in this study are simply supported, a magnification factor of 1.3 was used, according to the Magnification Factor Table given in LADOTD BDEM for positive moment effect and span lengths less than 240 ft. The Multiple presence factor was considered and was taken according to *AASHTO LRFD BDS Table 3.6.1.1.2-1*.

Several load cases were investigated for the three (3) different girders types to produce maximum effect in exterior and interior girders. LADOTD BDEM requires ID to be located at mid-span of girders, where the flexure moments are maximum for simply supported bridges. Accordingly, the investigated live load cases were concerned with the mid-span flexure moment only. In addition, due to the presence of full-height end diaphragms, ID has virtually no effect on shear forces (reactions); therefore, investigating the load cases to produce maximum shear forces was not considered.

5.1.3.2—BT-78 Girder Bridges

The BT-78 girder bridge was analyzed under four (4) different load cases to determine the load case that would produce maximum mid-span flexure moment in the exterior and interior girders.

For the exterior girder (G1), the loading case shown in Figure 5-1 with two lanes loaded, as expected produces the maximum mid-span flexural moment in the girder.

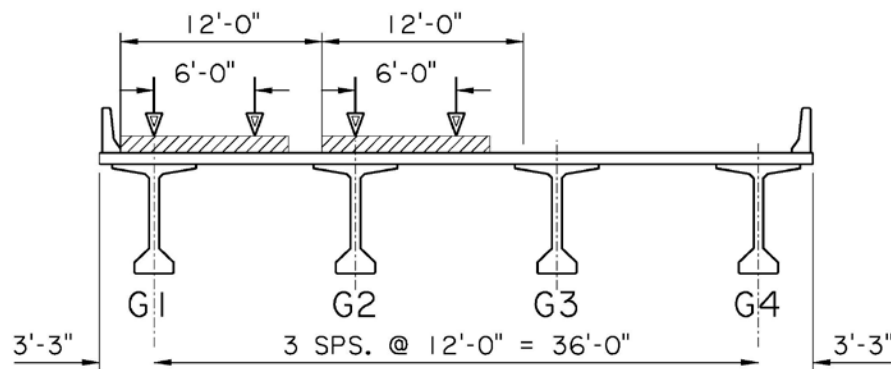


Figure 5-1: Live load case of BT-78 exterior girder (G1)

Three (3) different load cases were investigated for the interior girder (G2), as shown in Figure 5-2. The mid-span flexure moment of each girder for each load case is given in Table 5-2. It can be readily seen from Table 5-1 that load case A (three (3) lanes loaded) produces the maximum mid-span moment in the interior girder (G2). Accordingly, the two load cases shown in Figure 5-1 and Case A in Figure 5-2 were selected as the controlling load cases for the exterior and interior girders of BT-78 girder bridges, respectively.

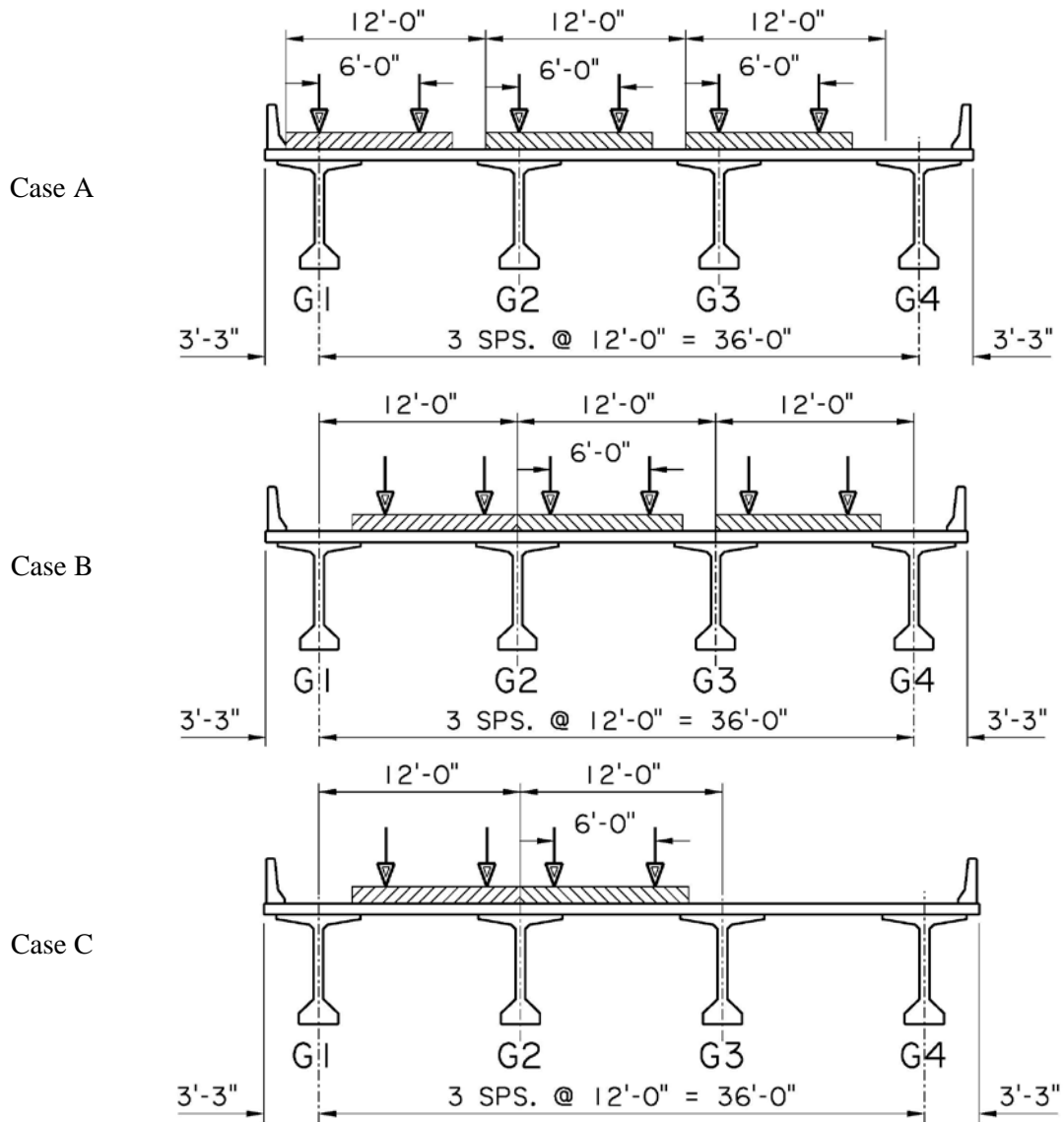


Figure 5-2: Live load cases of BT-78 interior girder (G2)

Table 5-2: Live load moments of BT-78 interior girder (G2)

| Live Load Case | Mid-Span Moment (kip-ft.) | | | |
|----------------|---------------------------|------|------|------|
| | G1 | G2 | G3 | G4 |
| A | 3767 | 3782 | 3365 | 2950 |
| B | 3451 | 3585 | 3477 | 3235 |
| C | 4053 | 3451 | 2290 | 1239 |

5.1.3.3—LG-25 Girder Bridges

Similar to the BT-78 girder bridges, the LG-25 girder bridges were analyzed under four (4) load cases to determine the maximum mid-span flexure moment in the exterior and interior girders.

For the exterior girder (G1), the load case shown in Figure 5-3 produces the maximum mid-span moment in the girder.

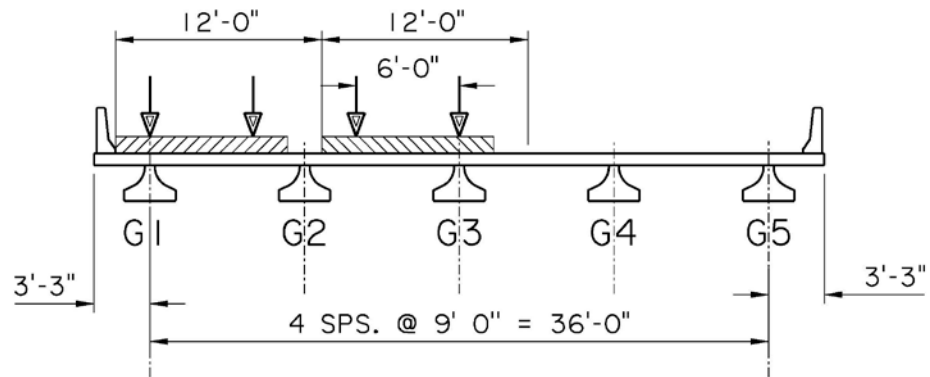


Figure 5-3: Live load cases of LG-25 exterior girder (G1)

Figure 5-4 shows the three (3) load cases investigated to determine the extreme case for the interior girder (G2). The flexure moment at mid span of each girder under each loading case is given in Table 5-2. The load case with the three lanes loaded (Case A) produced the maximum moment at mid-span of girder (G2).

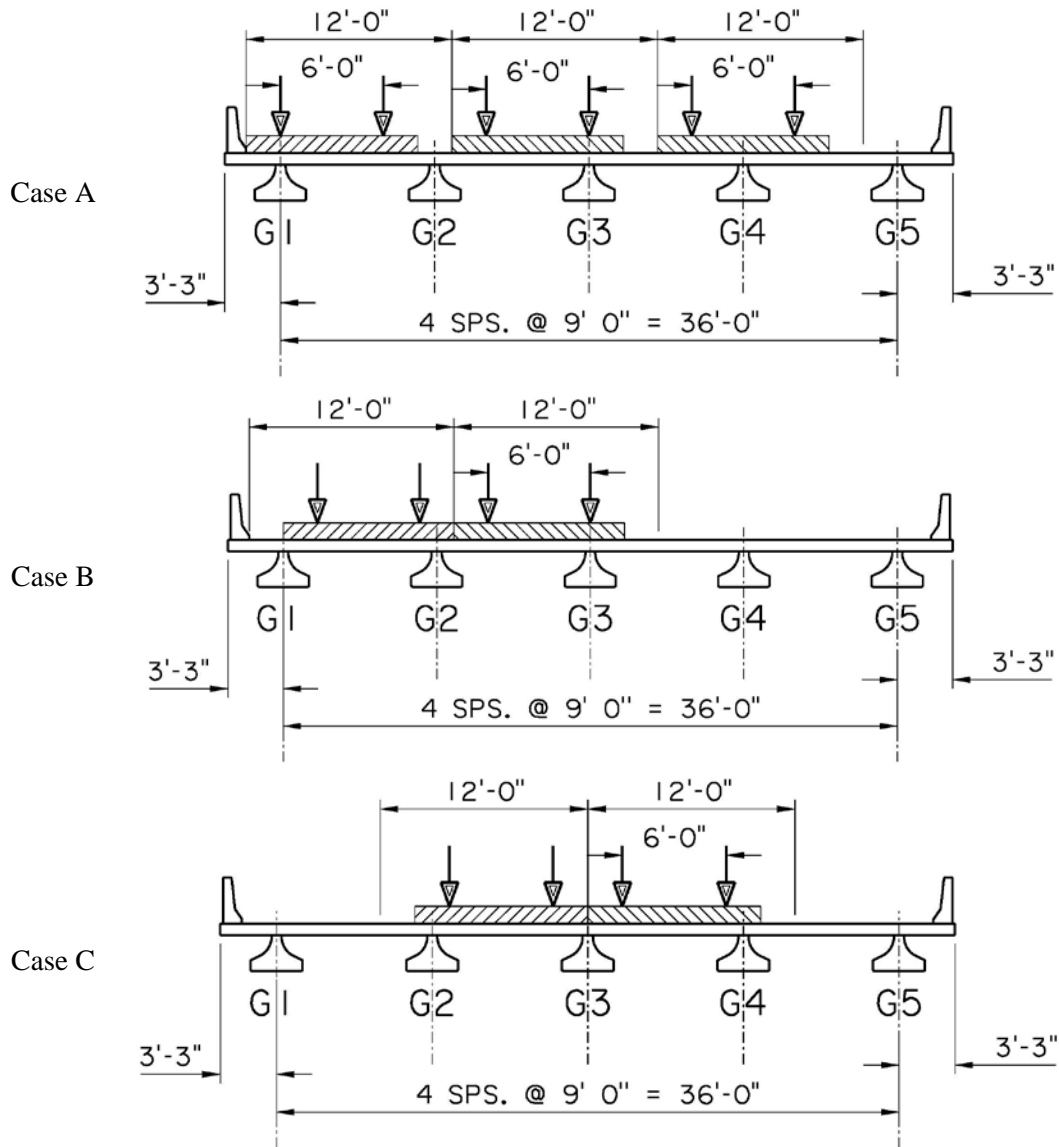


Figure 5-4: Live load cases of LG-25 interior girder (G2)

Table 5-3: Live load moments of LG-25 interior girder (G2)

| Live Load Case | Mid-Span Moment (kip-ft.) | | | | |
|----------------|---------------------------|-----|-----|-----|-----|
| | G1 | G2 | G3 | G4 | G5 |
| A | 649 | 644 | 605 | 523 | 511 |
| B | 730 | 618 | 491 | 294 | 170 |
| C | 449 | 463 | 534 | 462 | 447 |

5.1.3.4—Quad Beam Bridges

The Quad beam bridges were analyzed under two (2) load cases to determine the maximum mid-span moment in the exterior and interior girders. Figure 5-5 and Figure 5-6 show the load cases that produced the maximum mid-span moment in the exterior girder (G1) and the interior girder (G2), respectively.

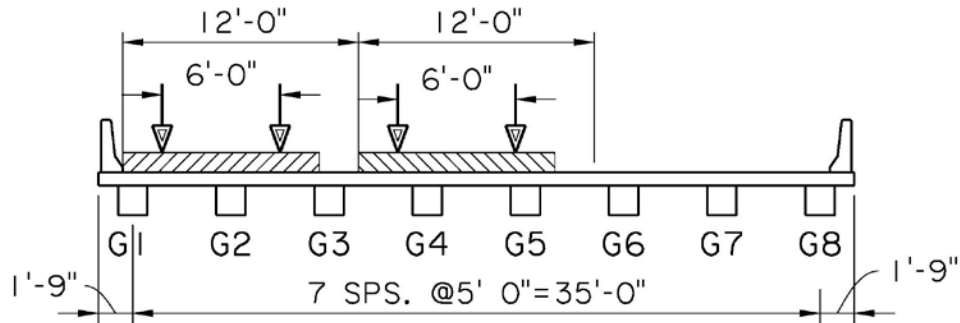


Figure 5-5: Live load case of Quad exterior beam (G1)

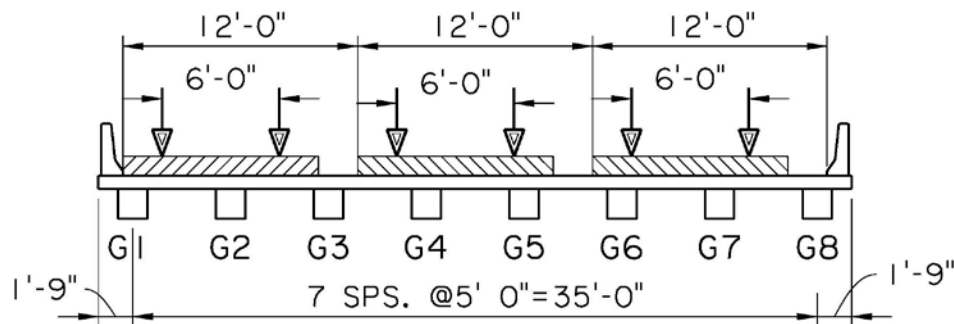


Figure 5-6: Live load case of Quad interior beam (G2)

The two governing load cases for the exterior and interior girders of the BT-78, LG-25 and Quad bridges were used throughout the parametric study. This enabled direct comparisons and examining the effect of the geometry of the bridge without interaction with the loading effects.

5.2—Evaluation Criteria: Live load Moment Envelope

This section presents the criteria adopted in this study to evaluate the impact of the ID removal on the design and behavior of the bridges under normal loading conditions. For each investigated bridge in the parametric study, the mid-span moment of each girder was considered for the two controlling load cases demonstrated in Section 5.1.3. As explained in Section 5.1.1, each bridge was investigated under two conditions, with ID and without ID.

For demonstration purposes, the development of the live load moment envelope for the BT-78 girder bridge under the two conditions, with ID and without ID is illustrated. Figure 5-7 shows the mid-span flexure moment of each girder for the two (2) load cases for a BT-78 girder bridge with ID. The three (3) lanes (Lane 1+2+3) load cases produces the maximum moment in the interior girder (G2), while the two (2) lanes (Lane 1+2) load produces the maximum moment in the exterior girder (G1). In addition, Figure 5-7 shows the moment envelope developed for the two load cases (Lane 1+2 and Lane 1+2+3) at each girder. The envelope was developed by connecting the maximum moment for the exterior girder (G1) from load case “Lane 1+2” and the maximum moment for the interior girder (G2) from load case “Lane 1+2+3”. Due to the symmetry of the bridge, the maximum moments for girders G3 and G4 are equal to that of G2 and G1, respectively.

Similarly, Figure 5-8 shows the mid-span flexure moment of each girder for the two load cases (Lane 1+2 and Lane 1+2+3) for the same bridge without ID. Following the same procedure for the condition with ID, the moment envelope for the condition without ID was developed as shown in Figure 5-8.

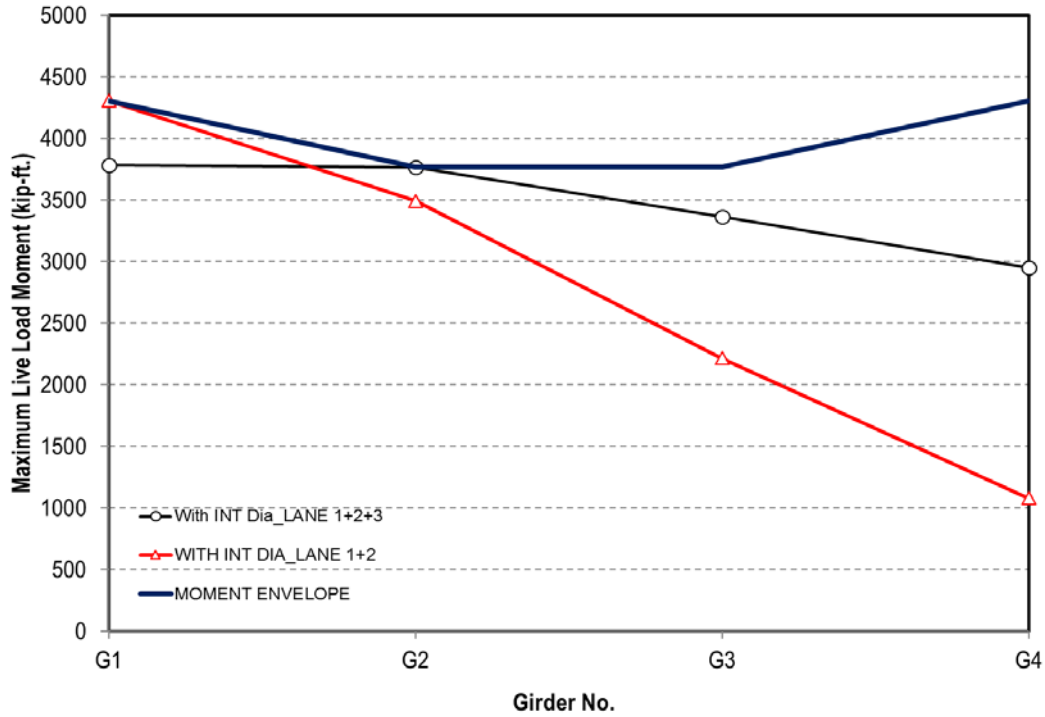


Figure 5-7: Moment envelope of a representative BT-78 girder bridge with ID

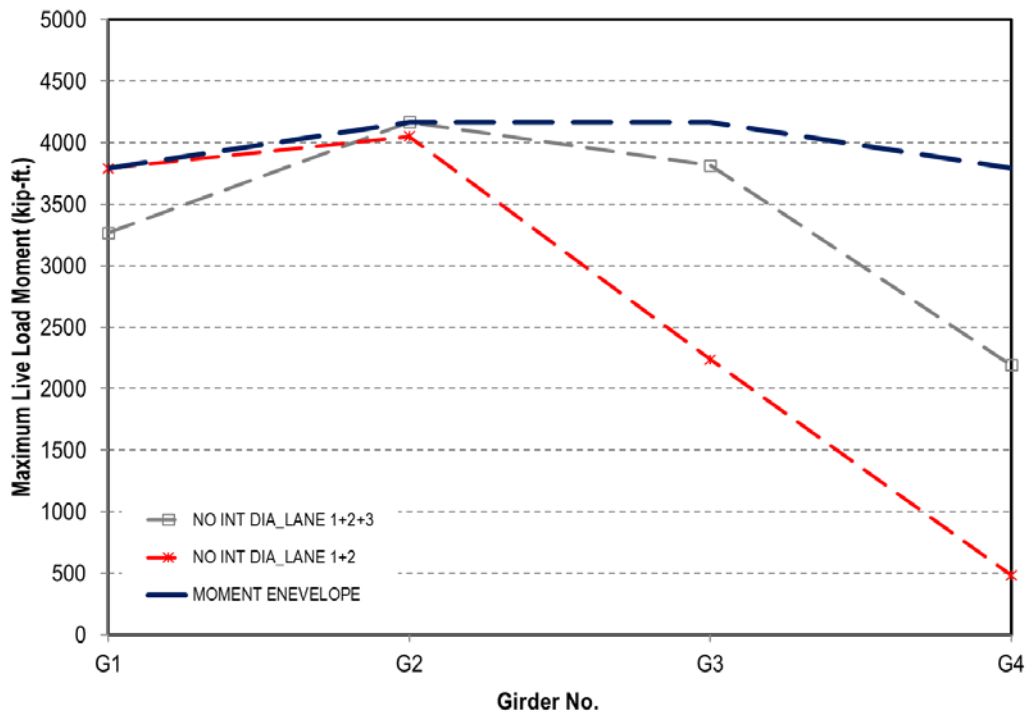


Figure 5-8: Moment envelope of a representative BT-78 girder bridge without ID

The two moment envelopes, shown in Figure 5-7 and Figure 5-8, are compared in Figure 5-9 for clarification and to demonstrate the significance of developing the moment envelopes. Figure 5-9 reveals that removal of ID resulted in 11% increase in mid-span moment of the interior girder (G2) and 12%

decrease in the mid-span moment of the exterior girder (G1). This moment increase or decrease in value at mid-span will be referred to in subsequent sections as “Moment Difference Due to Removal of ID”.

This moment difference shown in Figure 5-9 clearly illustrate that while presence of ID reduces the demand on interior girders, it increases the demand on exterior girders. In other words, the gain obtained by the interior girder is offset by the increased demand on the exterior girder. The moment envelopes for the two conditions, with and without ID, were compared for every analyzed bridge. This comparison served as the basis of the evaluation criteria for determining the impact of removing ID on the design and behavior of the bridge.

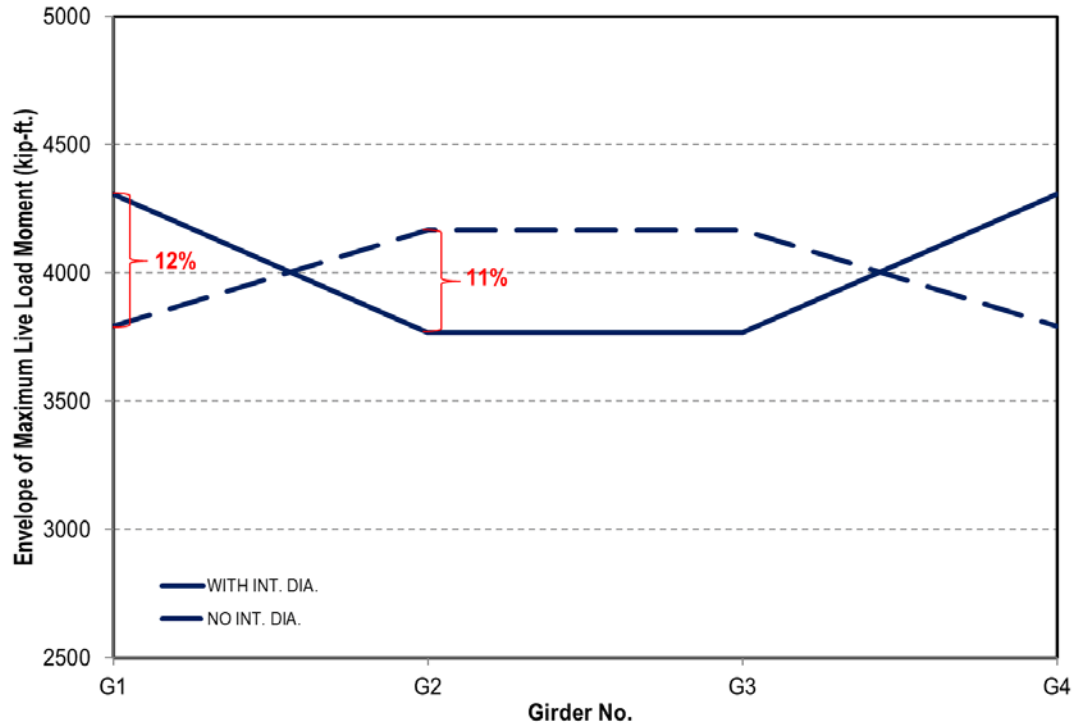


Figure 5-9: Moment envelope of BT-78 girder bridge with and without ID

5.3—Effect of Connection Rigidity

5.3.1—General

The influence of the rigidity of connection between the ID and the girders was investigated for the BT-78, LG-25, and Quad beam bridges. Different types of connection rigidities were investigated, namely full moment, partial-moment, and pinned connections. The full moment connection assumes full moment transfer between ID and the girder, which requires continuous reinforcement and monolithic casting or transverse post-tensioning. The pinned connection represents full moment release (no moment transfer between ID and the girder), which is the best representation of the current detail used in the State of Louisiana. Typically, ID is connected to the webs of longitudinal girders using coil inserts as shown in Figure 5-10, which does not enable full moment transfer between ID and the girder. The possibility of partial-moment transfer from ID to the girder was also assessed. To evaluate the influence of partial-moment connection, nine (9) BT-78 girder bridges with ID that enable partial moment transfer between ID and the girders were analyzed. The level of moment transfer was incrementally increased from 10% to 90% as given in Table 5-4. The same BT-78 girder bridge was modelled using ID with full moment and pinned connections, and without ID.

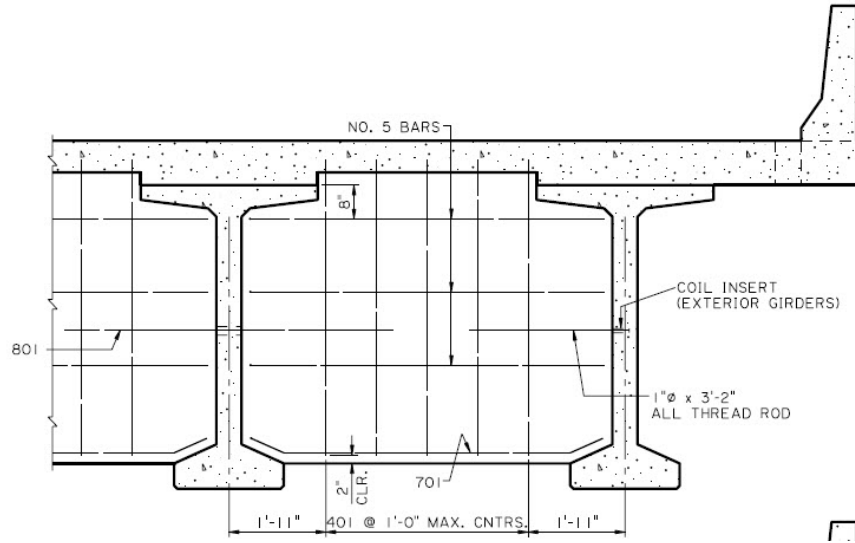


Figure 5-10: Typical connection between ID and girder using coil insert

Table 5-4: Bridges models investigated for the effect of partial-moment connection rigidity (12 models)

| Connection Rigidity | | | | | | | | | | | | | |
|---------------------|---------|------|---------------------|---------|-----|-----|-----|-----|-----|-----|-----|-----|------|
| Geometry: Straight | | | | | | | | | | | | | |
| Girder | Spacing | Span | Connection Rigidity | | | | | | | | | | |
| | | | Pin | Partial | | | | | | | | | Full |
| | | | | 10% | 20% | 30% | 40% | 50% | 60% | 70% | 80% | 90% | |
| BT-78 | 12'-0" | 130' | √ | √ | √ | √ | √ | √ | √ | √ | √ | √ | √ |

The moment envelopes developed for the nine levels of partial-moment connection are compared to those of the full moment connection, pinned connection, and the bridge without ID, as shown in Figure 5-11

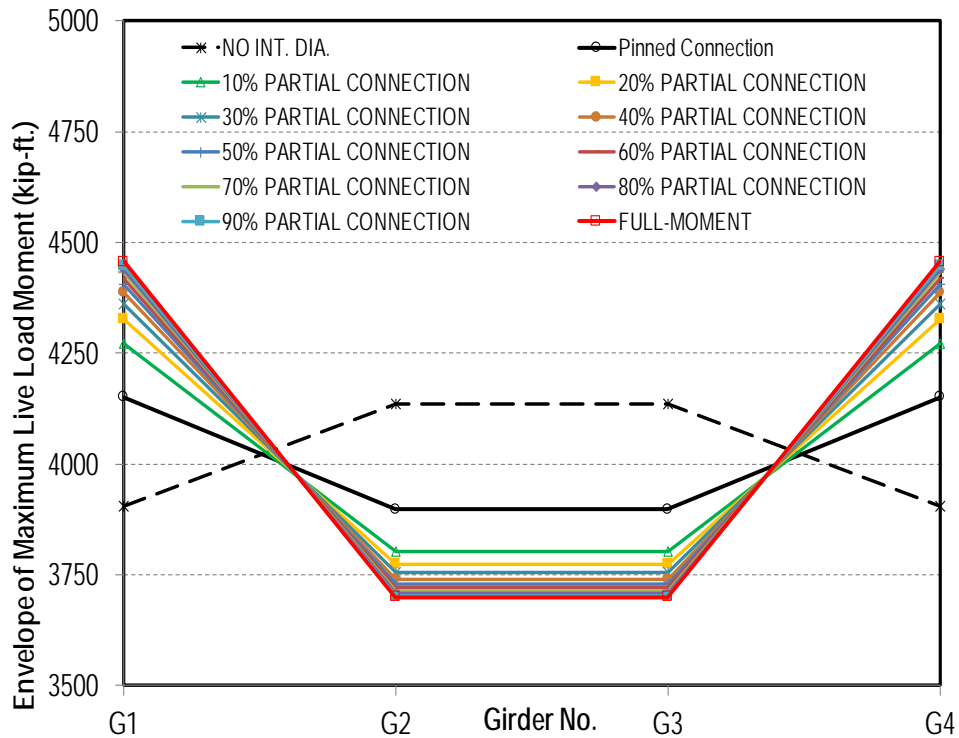


Figure 5-11: Moment envelope of BT-78 girder bridges with partial-moment connection

The results also indicate that the removal of ID resulted in an increase in the moment of the interior girder and a decrease in the moment of the exterior girder for different levels of connection rigidity. Moreover, the ID showed less effect on the moments of the exterior and interior girders for the case of pinned connection when compared to full moment connection. This concludes that ID with pinned connection is less effective compared with full moment connection.

Since the full moment and pinned connections were shown to be the two bounds for this parameter and in the lack of definition of partial-moment connection, it is intuitive to consider these two cases only to evaluate the influence of the connection rigidity for different types of bridges. The following sections present the results for the connection rigidity for BT-78, LG-25, and Quad beam bridges. The investigated bridge models are detailed in Table 5-5.

Table 5-5: Bridges models investigated for the effect of connection rigidity (9 models)

| Connection Rigidity | | | | |
|---------------------|---------|------|---------------------|-----|
| Geometry: Straight | | | | |
| Girder | Spacing | Span | Connection Rigidity | |
| | | | Full | Pin |
| QUAD | 5'-0" | 40' | √ | √ |
| LG-25 | 9'-0" | 44' | √ | √ |
| BT-78 | 12'-0" | 130' | √ | √ |

5.3.2—BT-78 Girder Bridges

The BT-78 girder bridge with the cross-section shown in Figure 5-12 was considered to investigate the influence of the rigidity of connection between the ID and the girder. Same bridge was modelled using two different connection rigidities; ID with full moment connection and ID with pinned connection. The bridge was also modelled without ID. The moment envelope diagrams were developed for each case. Figure 5-13 shows a comparison between the moment envelopes developed for BT-78 bridges with ID for the cases of full moment and pinned connections, and the case of the bridge without ID.

As shown in Figure 5-13, for the case of ID with full moment connection, removal of the ID resulted in 12% increase in the moment of the interior girder and 12% decrease in the moment of the exterior girder. For the case of ID with pinned connection, removal of the ID resulted in 7% increase in the moment of the interior girder and 5% decrease in the moment of the exterior girder.

These results show that ID with pinned connection has less impact on the bridge in comparison with ID having full moment connection. Given that current practice utilizes pinned connection, it can be concluded that the use of ID introduces 5% reserved capacity only in the interior girder and 6% more demand on the exterior girder. Accordingly, removal of ID shall not have significant effect on the live load demand of interior and exterior BT-78 girder bridges.

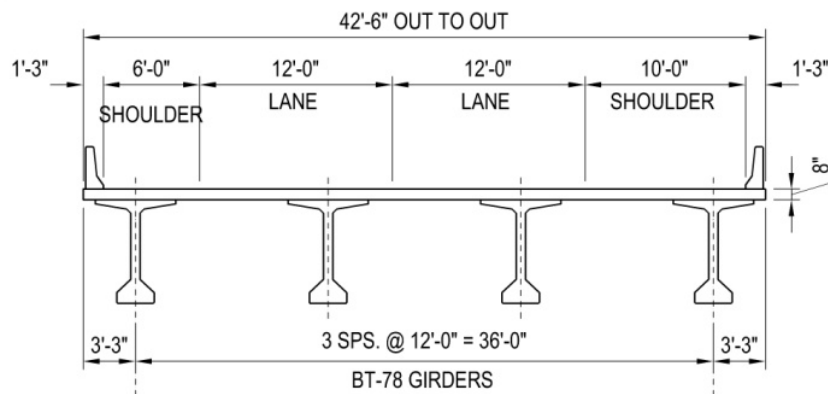


Figure 5-12: Cross-section of BT-78 girder bridge with different connection rigidities

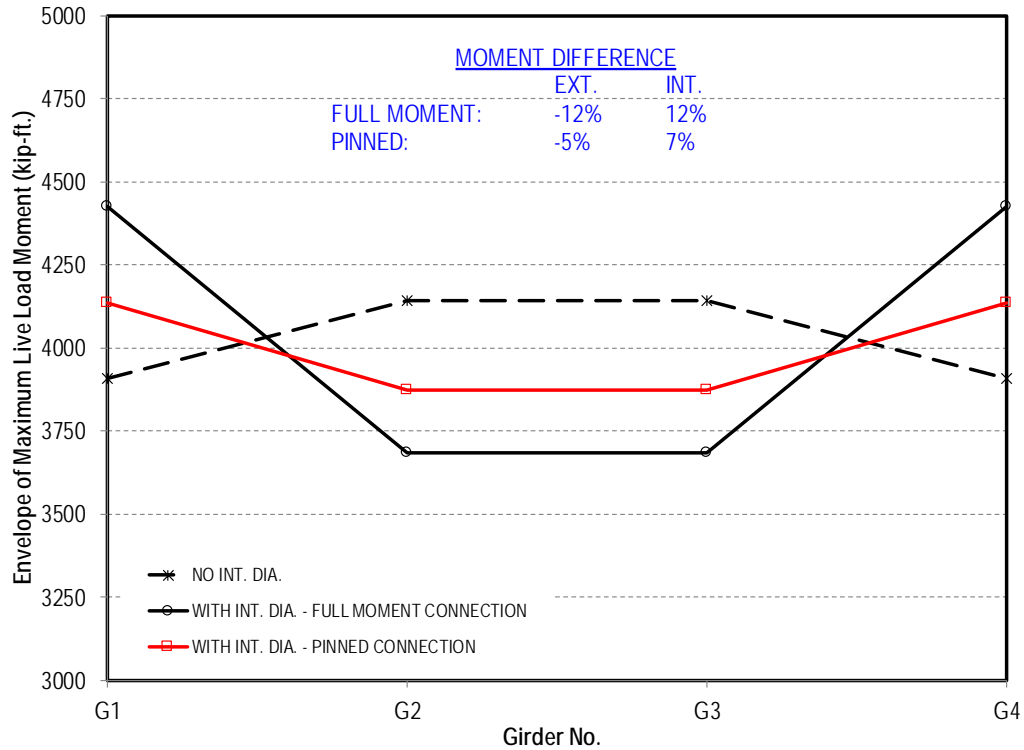


Figure 5-13: Moment envelopes of BT-78 girder bridges with different connection rigidities

5.3.3—LG-25 Girder Bridges

Similar to the BT-78 bridge, same cases were investigated for the LG-25 girder bridge with the cross-section shown in Figure 5-14. Same behavior observed for the BT-78 bridges, applies to the LG-25 girder bridges. The moment envelopes developed for the cases of full moment connection, pinned connection, and without ID are compared in Figure 5-15. The results show 1% increase in moment of the interior girder and 1% decrease in moment of the exterior girder when using ID with pinned connection in comparison to the case without ID. However, for the bridge with ID utilizing full moment connection, removal of the ID resulted in 3% increase in moment for the interior girder and 4% decrease in moment for the exterior girder. These results clearly indicate that the impact of using ID is less significant for the case of pinned connection compared to full moment connection. Accordingly, removal of ID shall not have significant effect on the live load demand of interior and exterior LG-25 girder bridges.

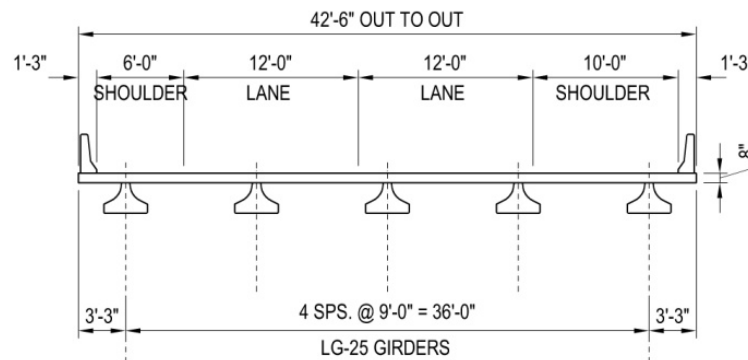


Figure 5-14: LG-25 girder bridge with different connection rigidities

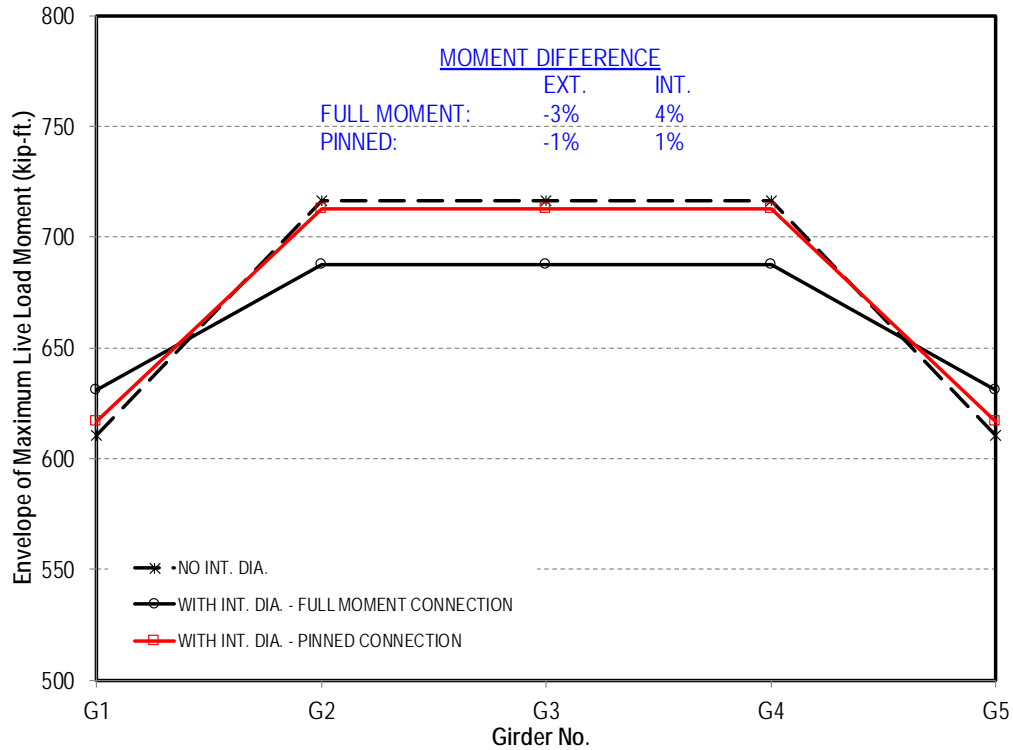


Figure 5-15: Moment envelopes of LG-25 girder bridges with different connection rigidities

5.3.4—Quad Beam Bridges

Same cases were studied for the Quad beam bridge with the cross-section shown in Figure 5-16. The moment envelopes developed for the cases of full moment pinned connections, and without ID are compared in Figure 5-17. It can be seen from Figure 5-17 that the removal of the ID resulted in 3% increase in the moment of the interior girder and 4% decrease in the moment of the exterior girder for the case of ID with full moment connection. As expected, for the case of ID with pinned connection, removal of the ID exhibited minimal effect on moments of both exterior and interior girders.

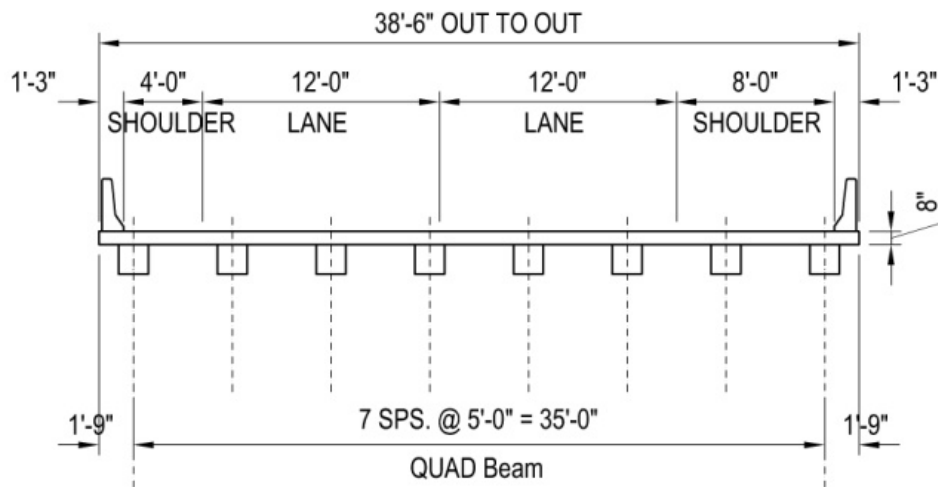


Figure 5-16: Quad beam bridges with different connection rigidities

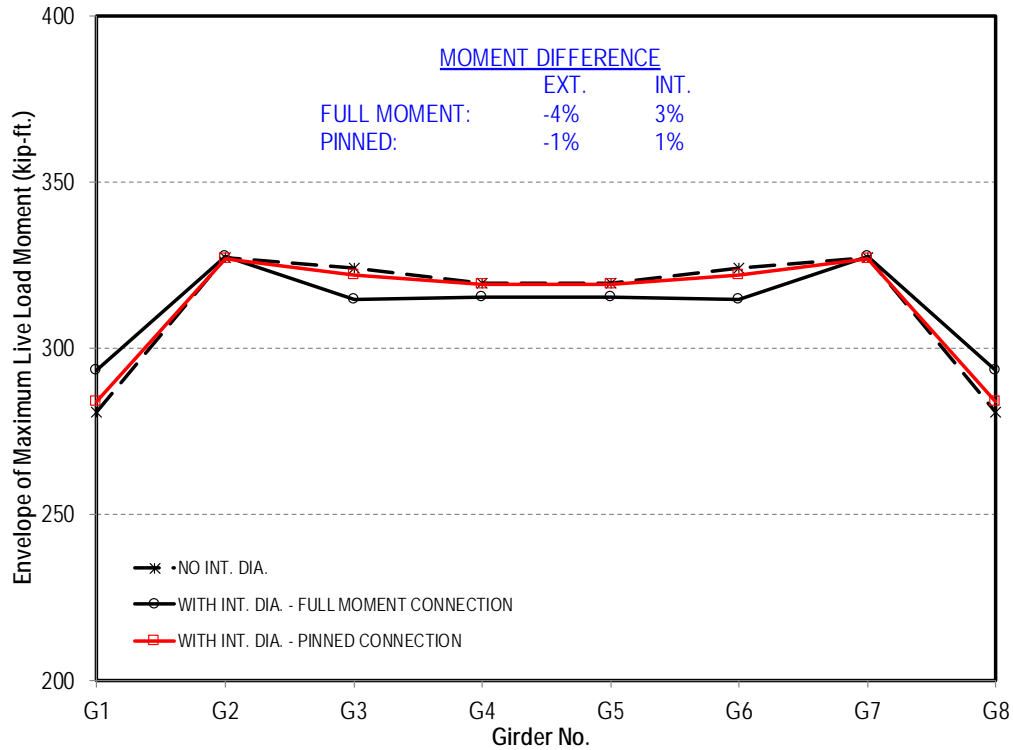


Figure 5-17: Moment envelopes of Quad beam bridges with different connection rigidities

5.4—Effect of Girder Spacing and Span Length

5.4.1—Combined Effect of Girder Spacing and Span Length

5.4.1.1—BT-78 Girder Bridges

The effect of removing ID on the design and behavior of BT-78 straight bridges was evaluated for bridges with different configurations. The investigated cases, shown in Table 5-6, comprised three different girder spacing and the corresponding span lengths to meet the design requirements. Full moment connection between ID and the girders was assumed in all models. Bridge cross-sections are shown in Figure 5-18.

Table 5-6: BT-78 girder bridge models with variable girder spacing and span length (6 models)

| Span Length & Girder Spacing | | | | |
|-------------------------------------|---------|--------|---------|---------|
| Straight and Full-Moment Connection | | | | |
| QUAD | Spacing | 5'-0" | 4'-4.5" | 3'-6" |
| | Span | 40' | 40' | 40' |
| LG-25 | Spacing | 9'-0" | 7'-2.5" | 6'-0" |
| | Span | 44' | 47' | 50' |
| BT-78 | Spacing | 12'-0" | 9'-0" | 7'-2.5" |
| | Span | 130' | 146' | 156' |

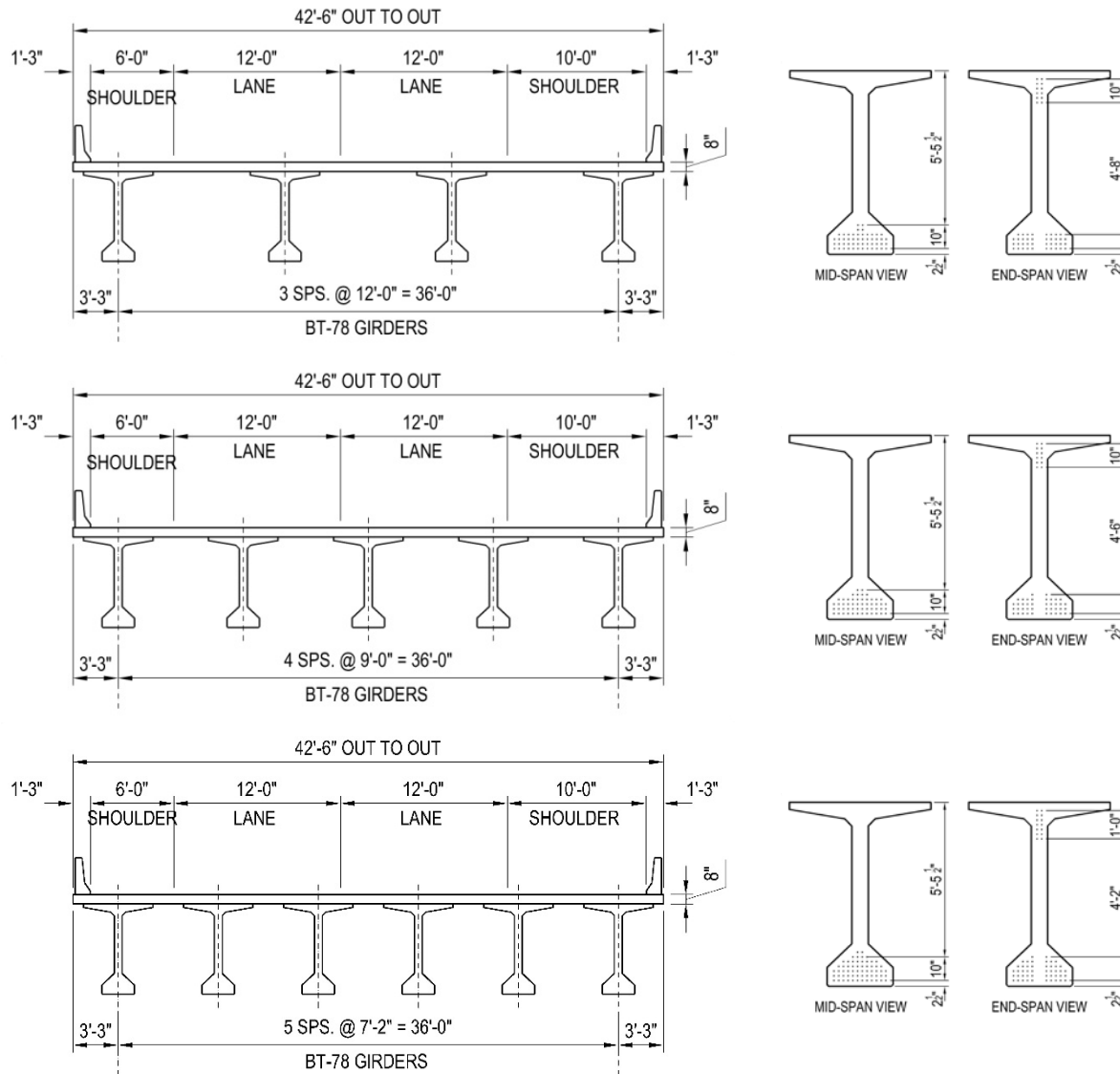


Figure 5-18: Cross-sections of BT-78 girder bridges with variable girder spacing and span length

The effect of removal of the ID on the mid-span moments of the exterior and interior girders of BT-78 bridges with different girder spacing and span length is demonstrated in Figure 5-19. For example, for the spacing of 7.2 ft., the difference in moment in the interior girder (G2) is 2% which means that the live load moment demand on the interior girder (G2) increased by 2% due to removing the ID. However, for the same spacing and span length, the live load moment demand on the exterior girder (G1) decreased by 11% due to removing the ID. This observation can be explained due to the decrease of girder spacing which results in adding more interior girders since the bridge width is constant. The moment difference of each interior girder required to offset the moment difference of the exterior girder, decreases as their number increases. As shown in Figure 5-19, the removal of ID results in an increase in the moment of the interior girder and a decrease in the moment of the exterior girder. Moreover, the results indicate that, when using larger girder spacing coupled with reducing span length, the change in mid-span moment of both interior and exterior girders increases. These results imply that the effect of ID on mid-span moment of BT-78 girder bridge decreases as the spacing between the girders decreases and span lengths increase.

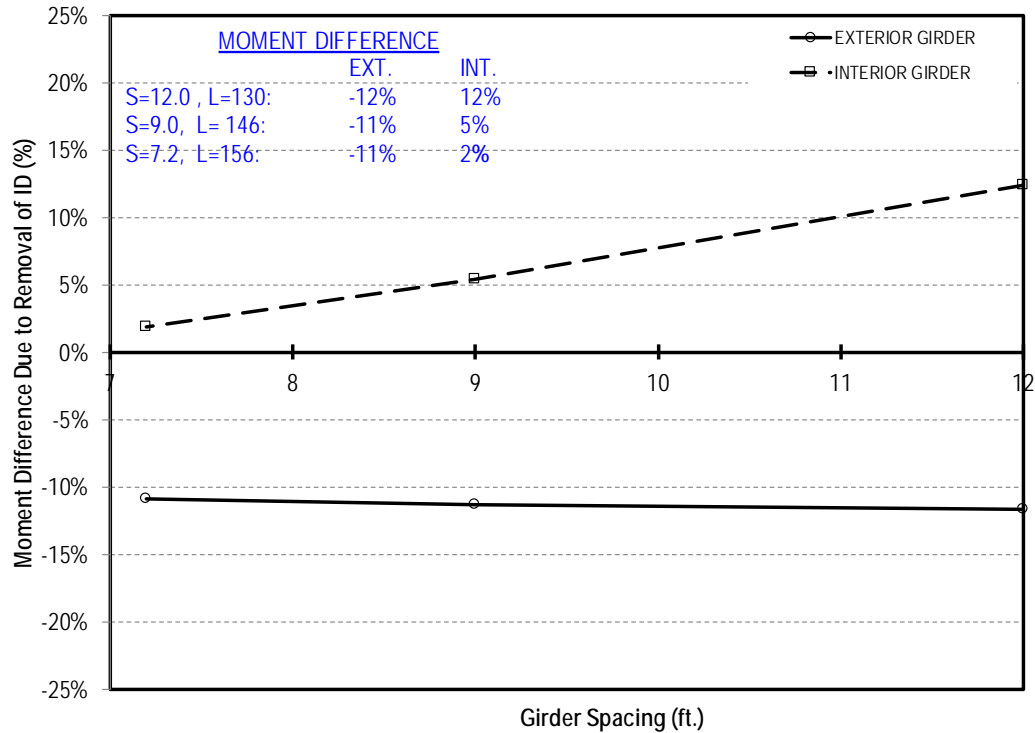


Figure 5-19: Moment difference of BT-78 girder bridges with variable girder spacing and span length

5.4.1.2—LG-25 Girder Bridges

The effect of the removal of ID was investigated for three (3) LG-25 girder bridges with different girder spacing and span lengths as detailed in Table 5-7. Full moment connection between ID and the girders was used for all models. Figure 5-20 shows the typical cross-section of the LG-25 girder bridges.

Table 5-7: LG-25 girder bridge models with variable girder spacing and span length (6 models)

| Span Length & Girder Spacing | | | | |
|-------------------------------------|---------|--------|---------|---------|
| Straight and Full-Moment Connection | | | | |
| QUAD | Spacing | 5'-0" | 4'-4.5" | 3'-6" |
| | Span | 40' | 40' | 40' |
| LG-25 | Spacing | 9'-0" | 7'-2.5" | 6'-0" |
| | Span | 44' | 47' | 50' |
| BT-78 | Spacing | 12'-0" | 9'-0" | 7'-2.5" |
| | Span | 130' | 146' | 156' |

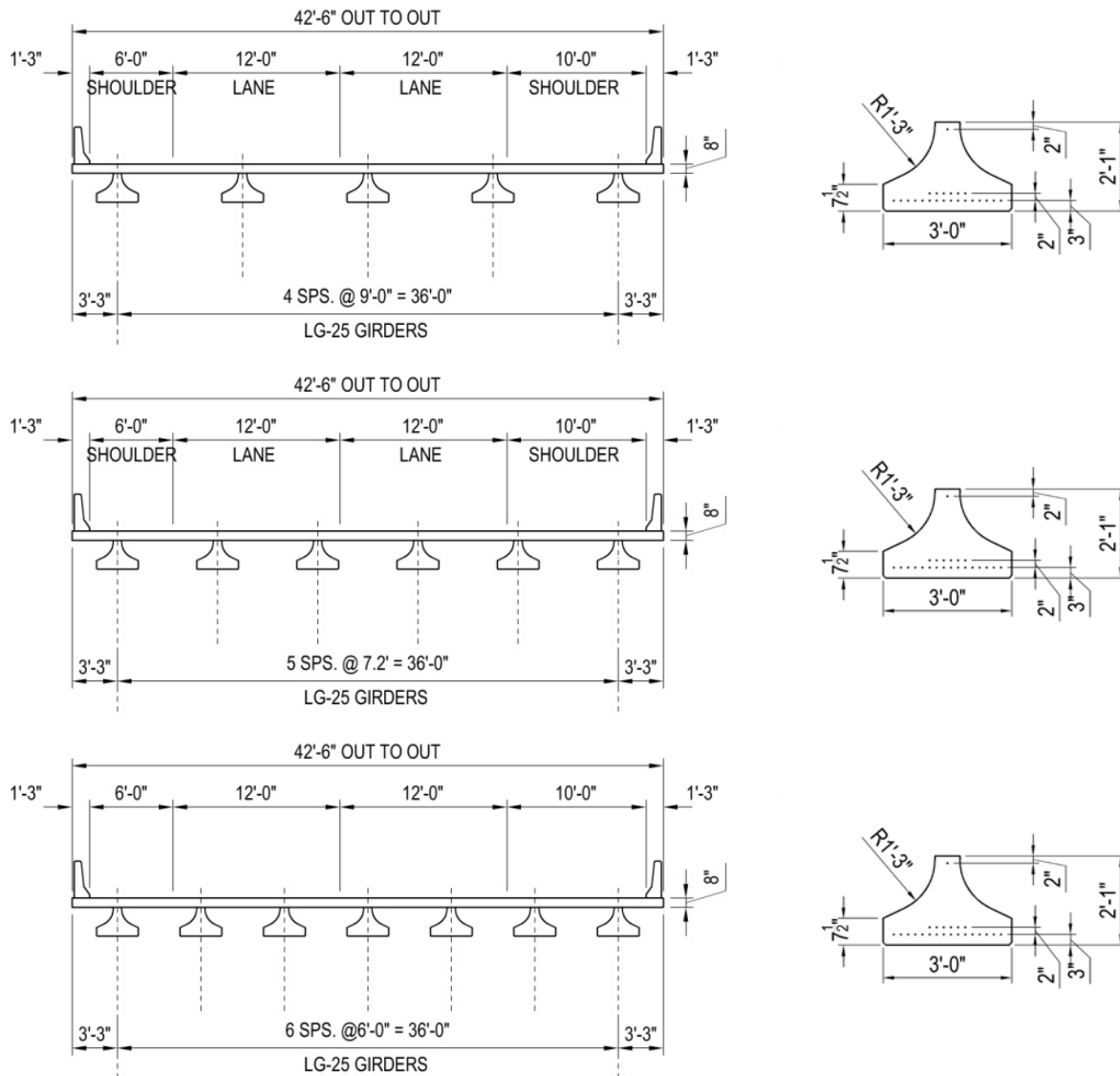


Figure 5-20: Cross-sections of LG-25 girder bridges with variable girder spacing and span length

Figure 5-21 shows the effect of removal of ID on the moments of the exterior and the interior girders of the LG-25 girder bridges. The horizontal axis represents the girder spacing, whereas the vertical axis represents the moment difference (%). As shown in Figure 5-21, when the girder spacing is 9 ft. (Span is 44 ft.), the removal of ID results in 4% increase in the interior girder moment and a 3% decrease in the exterior girder moment. Note that the decrease in the exterior girder moment due to removal of ID is about 3% for the three different girder spacing, however, the increase in the interior girder moment varies from 4% (6 ft. spacing) to 2% (9 ft. spacing). This observation is also valid for the BT-78 bridges and indicate that the effect of the ID decreases as the girder spacing decreases.

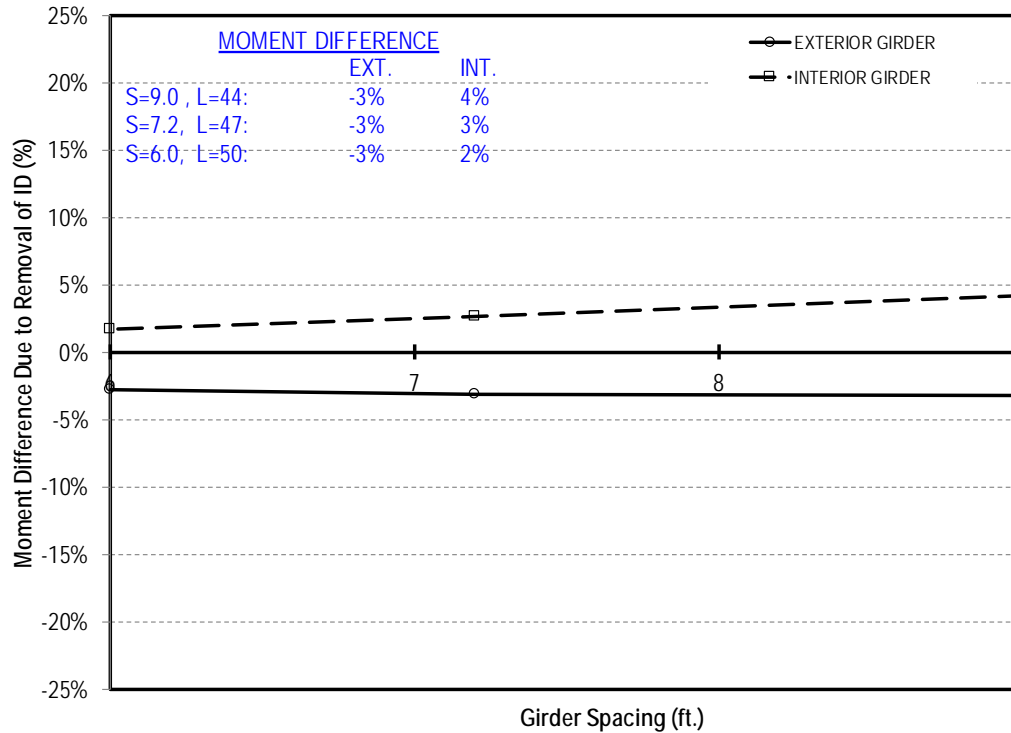


Figure 5-21: Moment difference of LG-25 girder bridges with variable girder spacing and span length

5.4.1.3—Quad Beam Bridges

The effect of removal of ID in Quad beam bridges was investigated for three different girder spacing. The investigated bridge models shared the same span of 40 ft. Full moment connection between the ID and the Quad beams was assumed for all the cases shown in Table 5-8. The cross-sections of the investigated bridges are also shown in Figure 5-22.

Table 5-8: Quad beam bridge models with variable girder spacing and span length (6 models)

| Span Length & Girder Spacing | | | | |
|-------------------------------------|---------|--------|---------|---------|
| Straight and Full-Moment Connection | | | | |
| QUAD | Spacing | 5'-0" | 4'-4.5" | 3'-6" |
| | Span | 40' | 40' | 40' |
| LG-25 | Spacing | 9'-0" | 7'-2.5" | 6'-0" |
| | Span | 44' | 47' | 50' |
| BT-78 | Spacing | 12'-0" | 9'-0" | 7'-2.5" |
| | Span | 130' | 146' | 156' |

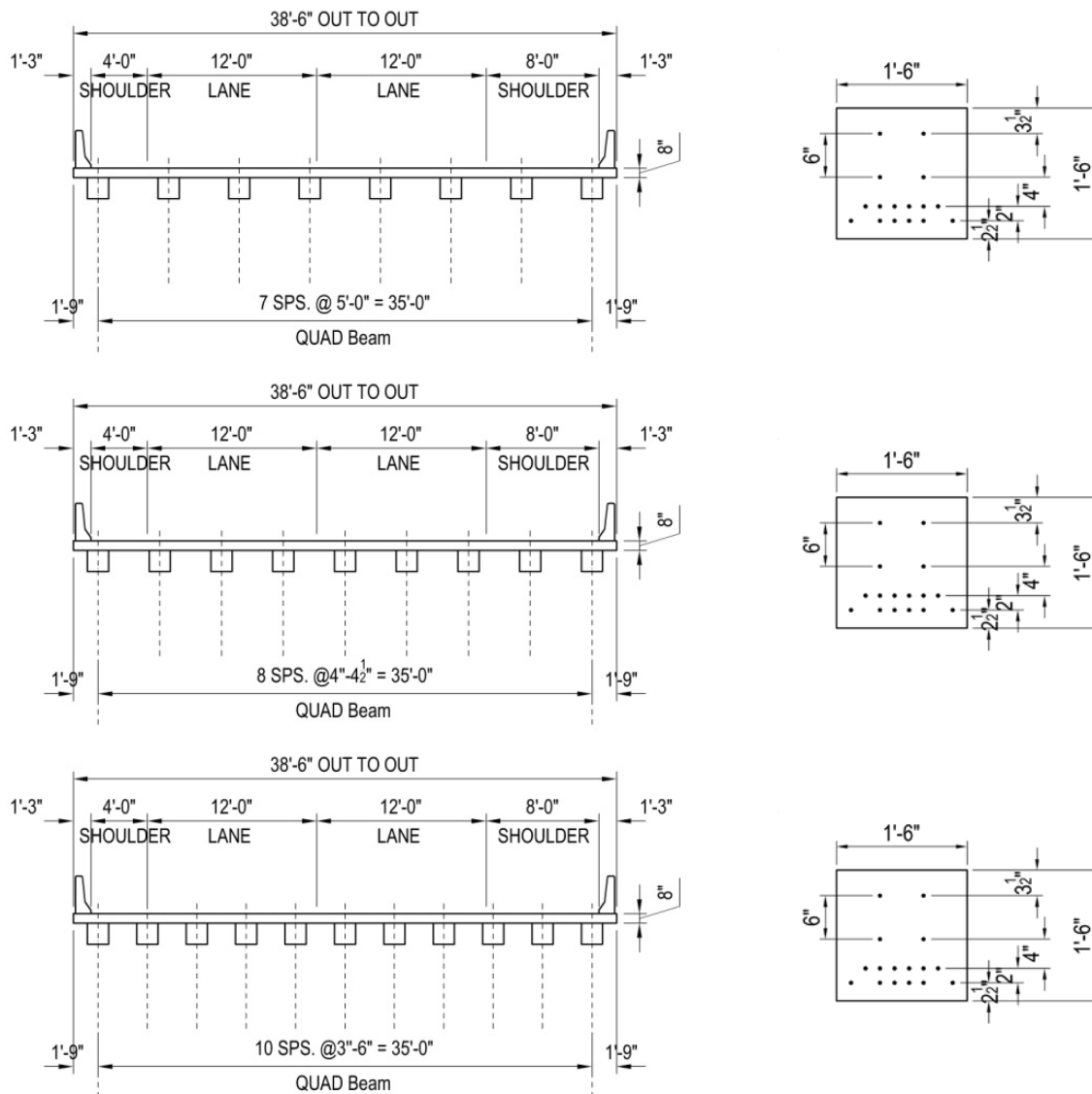


Figure 5-22: Cross-sections of Quad beam bridges with variable girder spacing and span length

The effect of the removal of the ID on the mid-span moments of the exterior and interior girders in Quad beam bridges is demonstrated in Figure 5-23. The maximum increase in interior girder moment is 5% and the maximum decrease in the exterior girder moment is 8% and they both occur when the spacing between the girders is 4.4 ft. Moreover, the results indicate that, due to the large number of Quad beams in the bridge (8, 9, and 11) and the high relative stiffness of the deck to the Quad beams, the presence of ID is insignificant for Quad beam bridge regardless of the girder spacing.

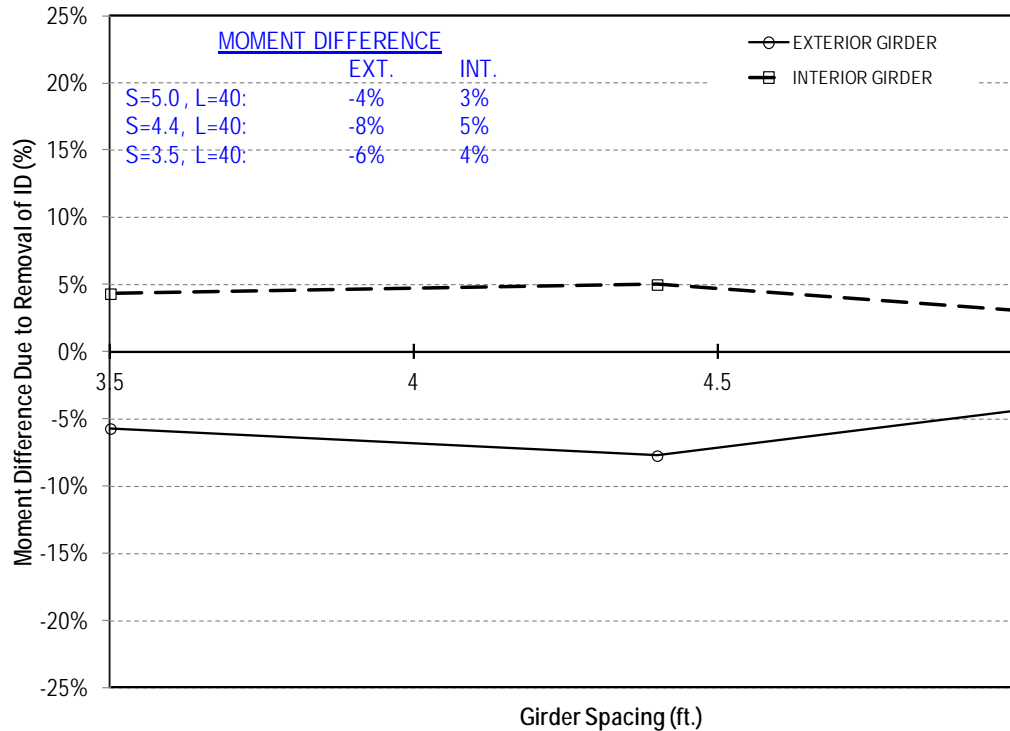


Figure 5-23: Moment difference of Quad beam bridges with different girder spacing and span length

5.4.2—Effect of Span Length

In Section 5.4.1, the girder spacing varied for each bridge and the span length was altered accordingly to simulate an actual design practice. This section presents the effect of removal of ID on bridges with various span lengths while maintaining the girder spacing. In other words, the girder spacing remained constant for all the investigated bridges. BT-78 girder bridge shown in Figure 5-24 with girder spacing of 12 ft. was investigated for six (6) different span lengths of 70, 86, 100, 115, 130, and 145 ft. as shown in Table 5-9. Full moment connection between the ID and girder was used for all models.

Table 5-9: BT-78 girder bridge models with constant girder spacing and variable span length (12 models)

| Span Length | | | | | | |
|-------------------------------------|---------|--------|-----|------|------|------|
| Straight and Full-Moment Connection | | | | | | |
| BT-78 | Spacing | 12'-0" | | | | |
| | Span | 70' | 85' | 100' | 115' | 130' |

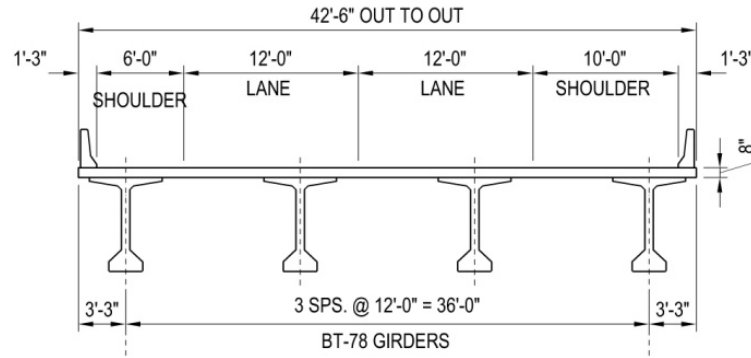


Figure 5-24: Cross-section of BT-78 girder bridges with constant girder spacing and variable span length

The moment difference due to removal of ID is plotted against the span length for the exterior and interior girders in Figure 5-25. The removal of ID resulted in increasing the moment for the interior girder and decreasing the moment for the exterior girder for all span lengths investigated. Further, Figure 5-25 indicates that the value of the moment difference decreases with the increase of the span length for both girders. This implies that the impact of the ID reduces for bridges with longer spans.

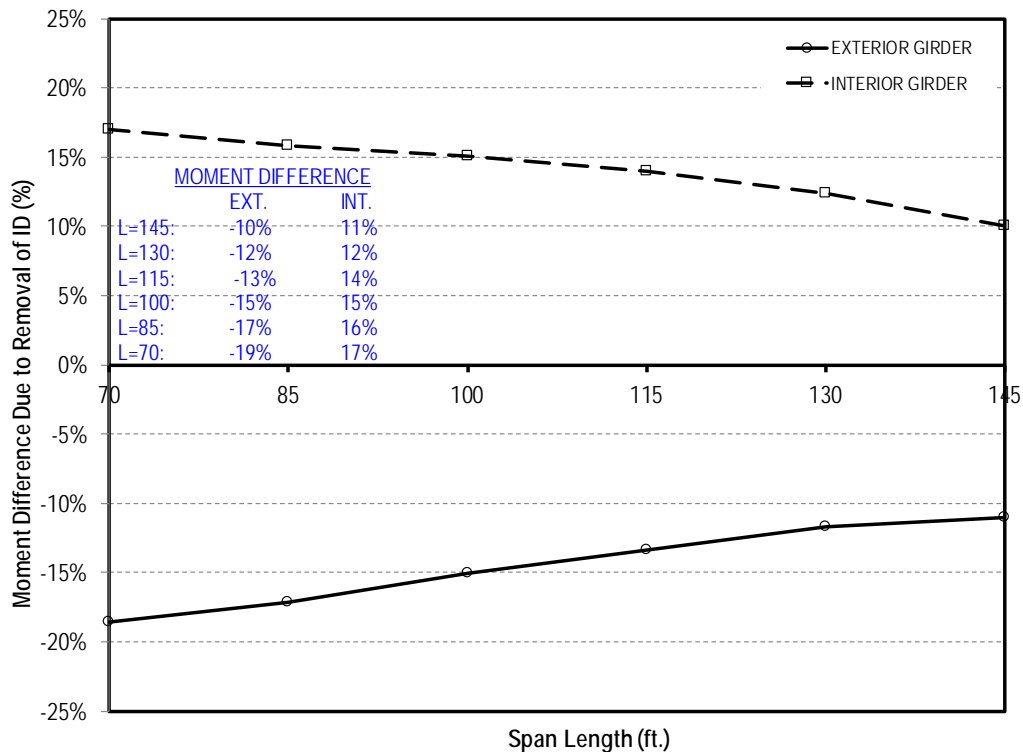


Figure 5-25: Moment difference of BT-78 girder bridges with constant girder spacing and variable span length

5.4.3—Effect of Girder Spacing

Similar to the approach adopted in section 5.4.2, this section presents the effect of removing the ID on bridges with variable girder spacing and having the same span length. This was achieved by maintaining

the span length constant as 130 ft. while varying the girder spacing. The bridge comprised of seven (7) BT-78 girders spaced at 6.0, 7.2, 9.0, 10.0, and 12.0 ft. as shown in Table 5-10, leading to a total bridge width of 42.5, 49.7, 60.5, 66.5, and 78.5 ft., respectively. Full moment connection between the ID and the girders was used for all bridges. The typical cross-section of the bridge is shown in Figure 5-26.

Table 5-10: BT-78 girder bridge models with variable girder spacing and constant span length (10 models)

| Girder Spacing | | | | | | |
|-------------------------------------|---------|-------|---------|-------|--------|--------|
| Straight and Full-Moment Connection | | | | | | |
| BT-78 | Spacing | 6'-0" | 7'-2.5" | 9'-0" | 10'-0" | 12'-0" |
| | Span | 130' | | | | |

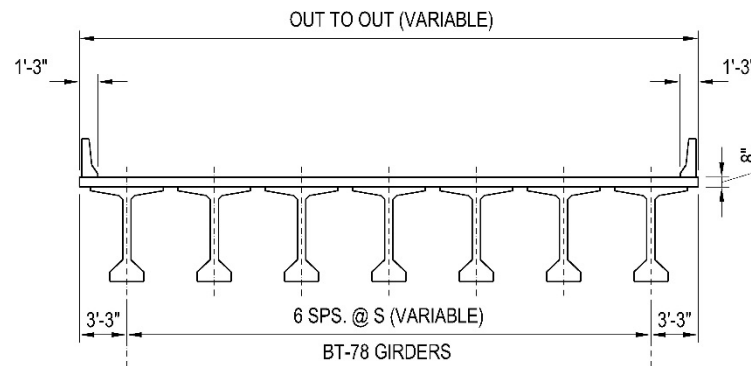


Figure 5-26: Cross-section of BT-78 girder bridges with variable girder spacing and constant span length

The moment difference due to the removal of ID were plotted against the girder spacing as given in Figure 5-27. As shown in Figure 5-27, increasing the girder spacing from 6 ft. to 12 ft. resulted in an increase in the moment difference up to 15% for the interior girder. On the other hand, increasing the girder spacing from 6 ft. to 12 ft. resulted in a decrease in the moment difference up to 12% for the exterior girder. These results imply that the impact of the ID is more significant for interior girder of bridges with large girder spacing, while it is more significant for exterior girder of bridges with small girder spacing.

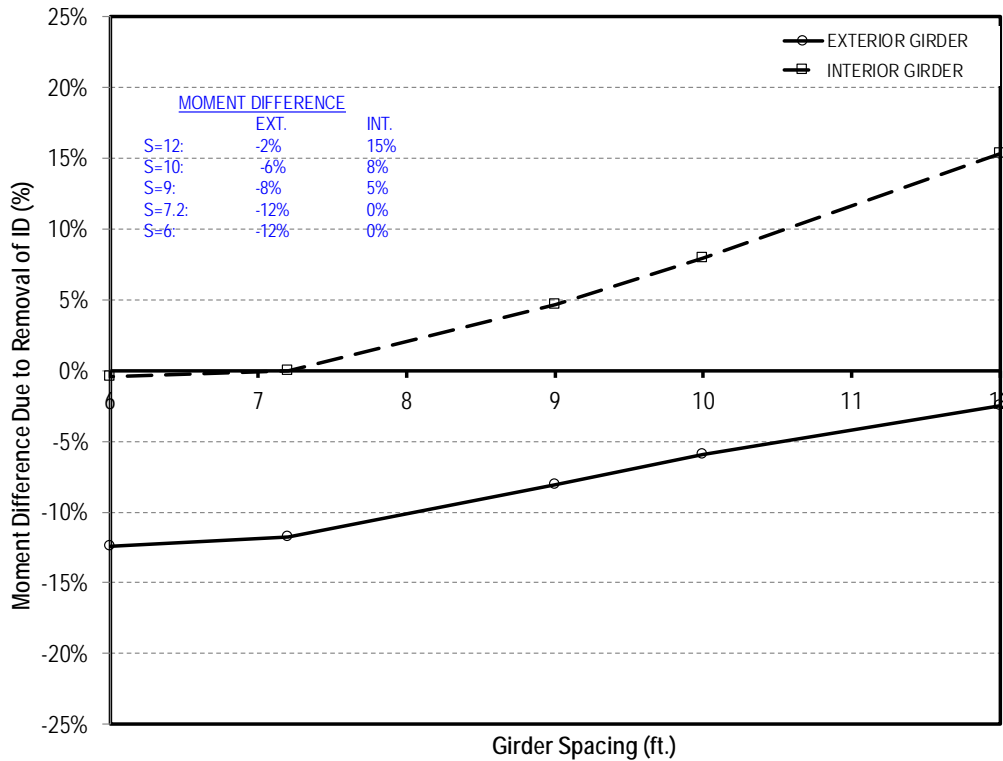


Figure 5-27: Moment difference of BT-78 girder bridges with variable girder spacing and constant span length

5.5—Effect of Skew Angle

5.5.1—General

The effect of ID of skewed bridges was evaluated for the BT-78, LG-25, and Quad beam bridges. Each bridge type was investigated using different skew angles of 0, 30 and 60 degrees. The two (2) connection rigidities, full moment and pinned connections, were considered for each bridge. In addition, each bridge was modelled for the two cases with and without ID. A total of 27 models were investigated as shown in Table 5-11.

Table 5-11: Skew bridge models (36 models)

| Girder | Spacing | Span | Skew Angle | | | | | |
|--------|---------|------|-------------|----|----|------------|----|----|
| | | | Full-Moment | | | Pinned | | |
| | | | Skew Angle | | | Skew Angle | | |
| | | | 0 | 30 | 60 | 0 | 30 | 60 |
| QUAD | 5'-0" | 40' | √ | √ | √ | √ | √ | √ |
| LG-25 | 9'-0" | 44' | √ | √ | √ | √ | √ | √ |
| BT-78 | 12'-0" | 130' | √ | √ | √ | √ | √ | √ |

5.5.2—BT-78 Girder Bridges

The plan views and cross-sections of the skewed BT-78 girder bridges are shown in Figure 5-28. Moment envelope diagrams were developed for each bridge for the conditions, with and without ID. The moment difference due to removal of ID was determined for both the exterior and interior girders for each bridge. The moment difference is plotted versus the skew angle in Figure 5-29 for the two connection rigidities.

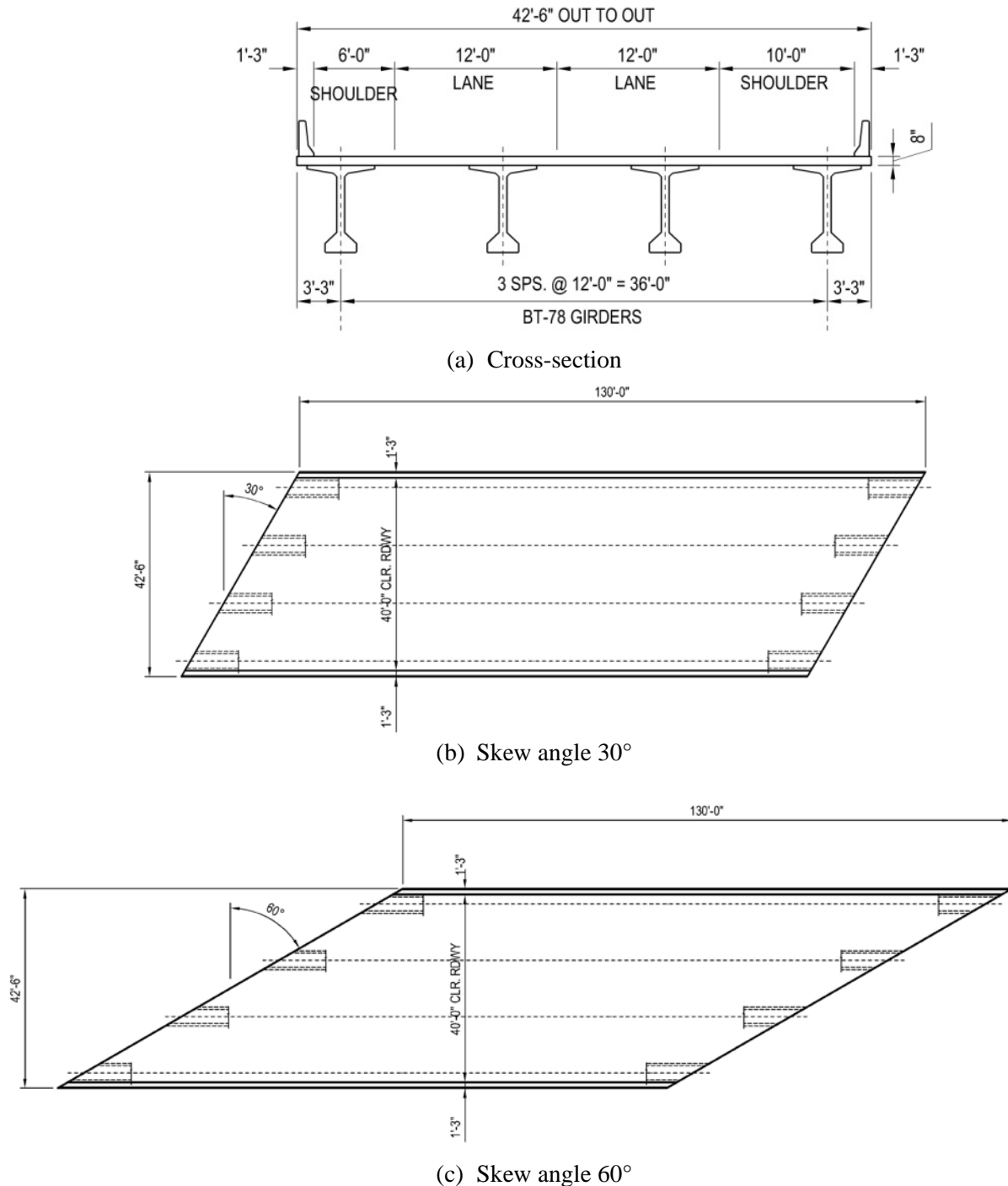


Figure 5-28: Details of skew BT-78 girder bridges

Typically, removal of the ID resulted in increasing the moment of the interior girder and decreasing the moment of the exterior girder in all cases. Figure 5-29 reveals that increasing the skew angle from 08 to 308 had minimal effect on the moment difference due to removal of ID. This implies that bridges with skew angle of 30° or less experience the same behavior as straight bridges. This behavior is in line with AASHTO LRFD BDS Table 4.6.2.2.2e-1, where for skew angles less than 30°, there is no reduction in live load moment.

As evident from Figure 5-29, increasing the skew angle from 308 to 608 significantly reduced the moment difference due to removal of ID. This is mainly attributed to the development of negative moment at the girder supports, thus reducing the mid-span moment.

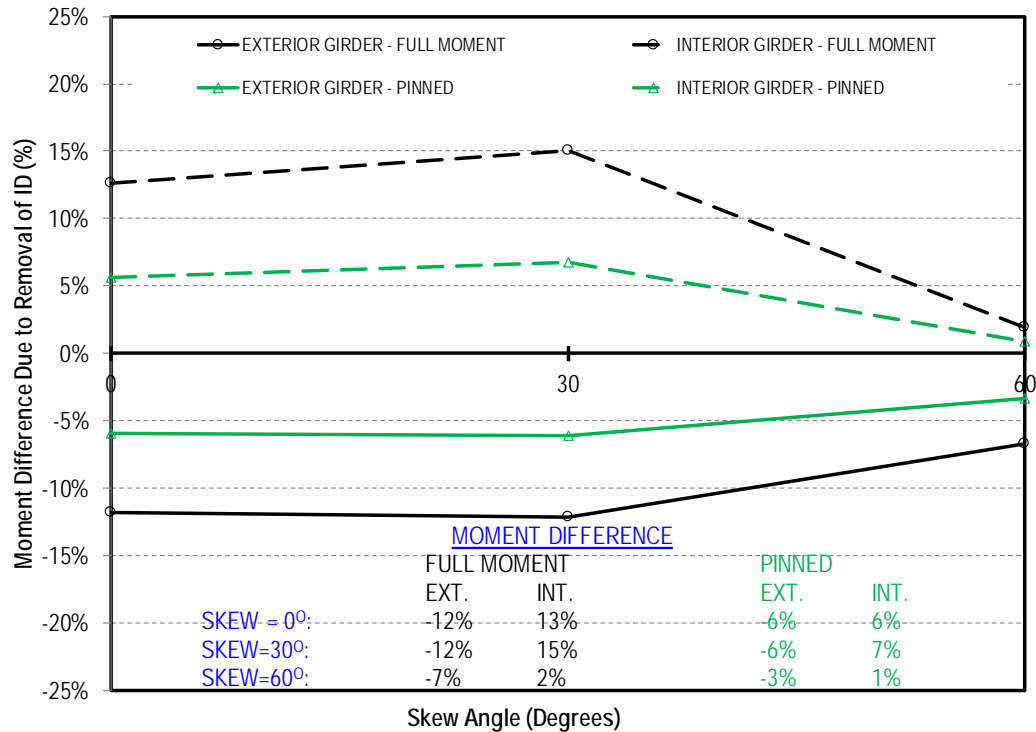


Figure 5-29: Moment difference of skew BT-78 girder bridges

5.5.3—LG-25 Girder Bridges

The plan views and cross-sections of the skewed LG-25 girder bridges are shown in Figure 5-30. Moment envelope diagrams were developed for each bridge for the conditions, with and without ID. The moment difference due to removal of ID was determined for both the exterior and interior girders for each bridge. The moment difference is plotted versus the skew angle in Figure 5-31 for the two connection rigidities. Same behavior observed for skewed BT-78 girder bridge was also observed for skewed LG-25 girder bridges, where increasing the skew angle from 08 to 308 exhibited minimal effect on the moment difference for both the exterior and interior girders. However, the moment difference in the girders dropped significantly for the 608 skewed bridges. It is also evident from Figure 5-31 that the effect of ID was less pronounced for the case of the pinned connection compared to the full moment connection for both, the exterior and interior girders.

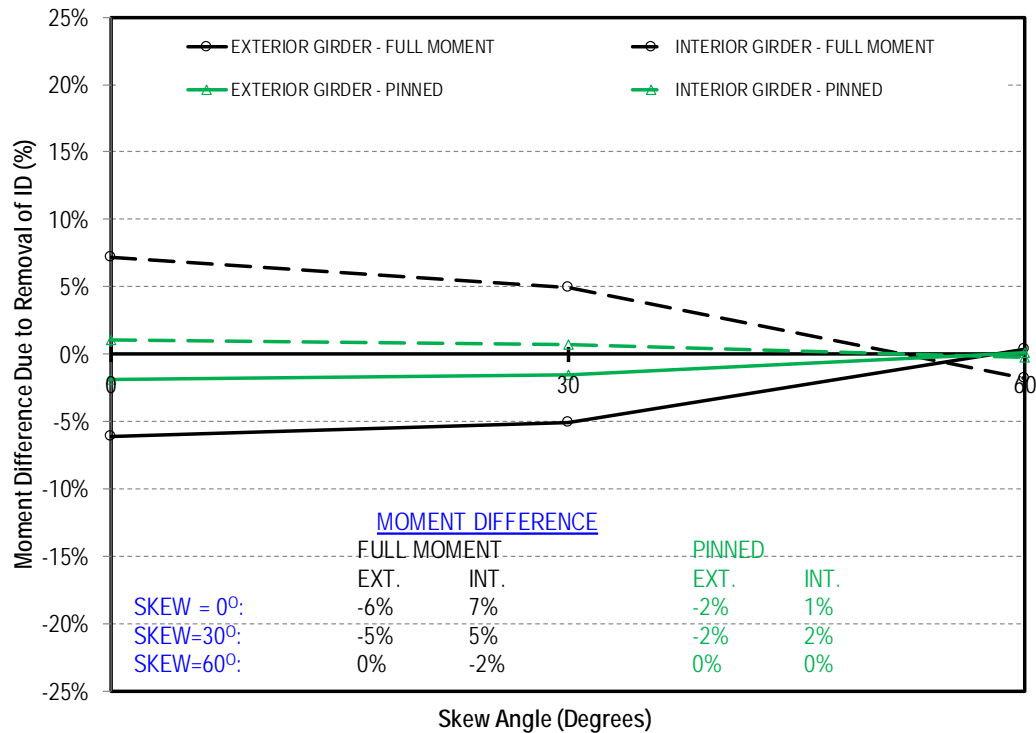


Figure 5-31: Moment difference of skew LG-25 girder bridges

5.5.4—Quad Beam Bridges

The plan views and cross-sections of the skewed Quad beam bridges are shown in Figure 5-32. Moment envelope diagrams were developed for each bridge for the conditions, with and without ID. The moment difference due to removal of ID was determined for both the exterior and interior girders for each bridge. The moment difference is plotted versus the skew angle for the Quad beam bridges for the two connection rigidities in Figure 5-33. Same behavior was observed for the skewed Quad beam bridges as in BT-78 and LG-25 girder bridges.

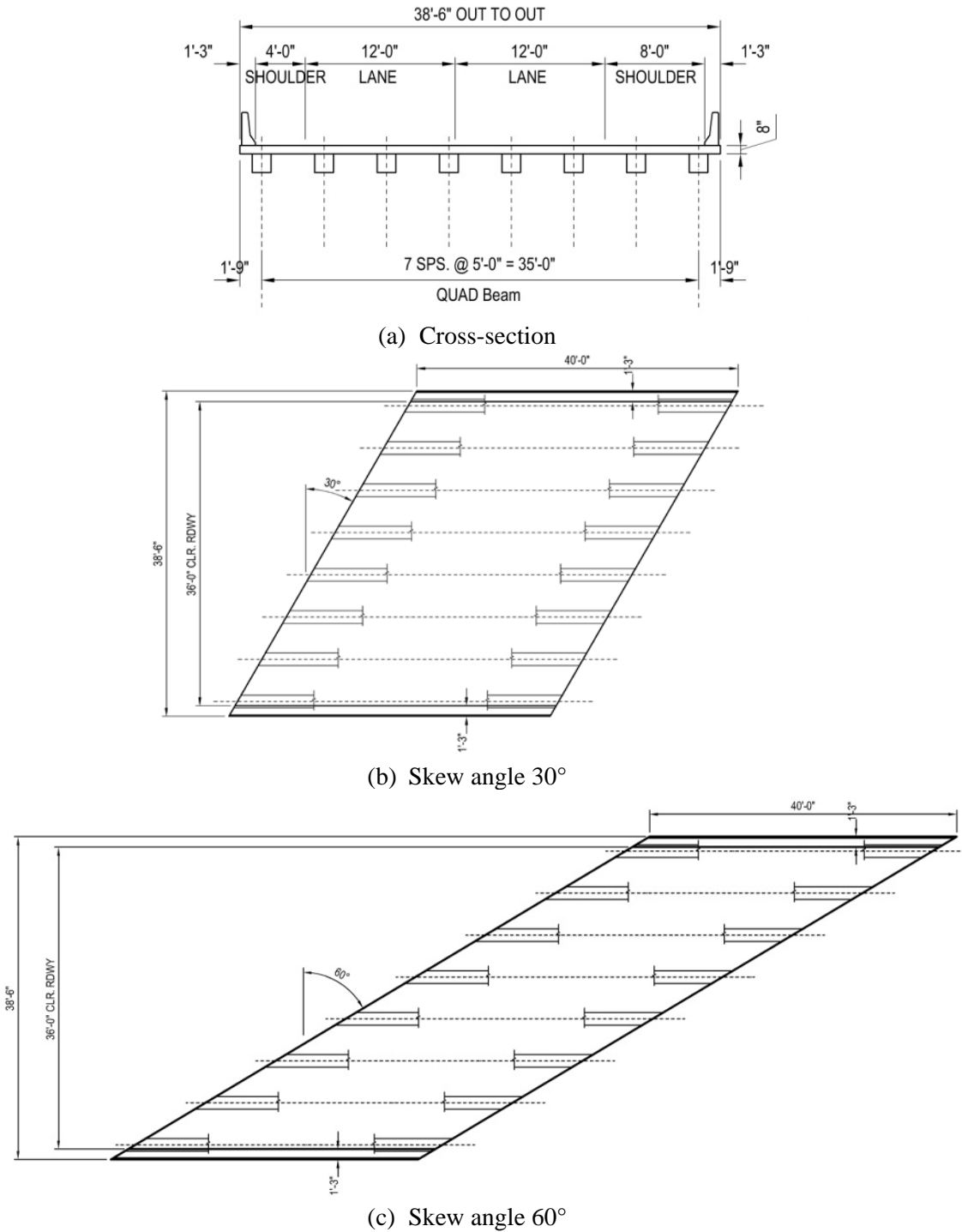


Figure 5-32: Details of skew Quad beam bridges

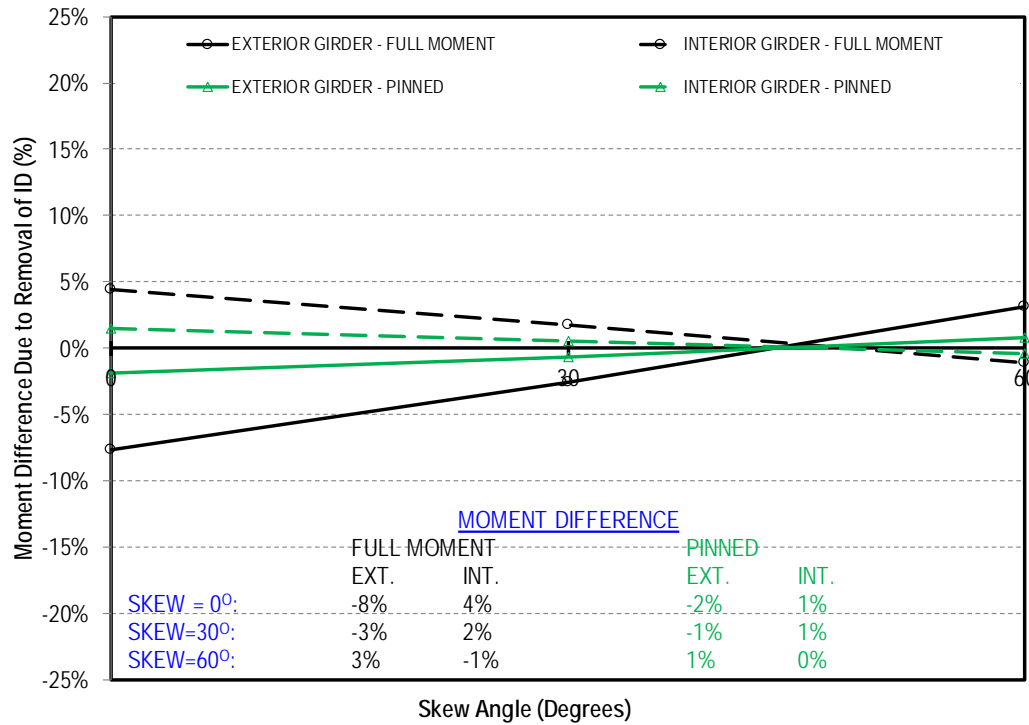


Figure 5-33: Moment difference of skew Quad beam bridges

5.6—Effect of Curvature and Cross-Slope

5.6.1—General

The effect of removing the ID on curved bridges (curved deck on chorded girders) was investigated for BT-78, LG-25 and Quad beam bridges. The study included investigating three different radii of curvature, two values of cross-slope, and two different connection rigidities as given in Table 5-12. A total of 72 models were completed to assess the effect of curvature and cross-slope.

Table 5-12: Curved bridge models (36 models)

| | | | Curvature / Cross-Slope | | | | | | | | | | | | | | | | | |
|--------|---------|------|-------------------------|----|---|---------|---|----|---------------|----|---|---------|---|----|---------|--|--|---------|--|--|
| Girder | Spacing | Span | Full-Moment | | | | | | Pinned | | | | | | | | | | | |
| | | | Cross-Slope % | | | | | | Cross-Slope % | | | | | | | | | | | |
| | | | 8 | 10 | 8 | 10 | 8 | 10 | 8 | 10 | 8 | 10 | 8 | 10 | | | | | | |
| QUAD | 5'-0" | 40' | R1=500 | | | R2= 800 | | | R3=1000 | | | R1=500 | | | R2= 800 | | | R3=1000 | | |
| LG-25 | 9'-0" | 44' | R1=500 | | | R2= 800 | | | R3=1000 | | | R1=500 | | | R2= 800 | | | R3=1000 | | |
| BT-78 | 12'-0" | 130' | R1=1200 | | | R2=1400 | | | R3=2100 | | | R1=1200 | | | R2=1400 | | | R3=2100 | | |

LADOTD BDEM specifies that in curved spans for chorded precast, prestressed concrete girders to be used, the offset between the arc and its chord shall not exceed 1 ft. (Part II, Vol. 1, Chapter 5, Clause 5.14.1.2). In addition, LADOTD BDEM presents maximum overhang length for exterior girders of 4'-9". A radii of curvature equal to 500, 800, and 1000 ft. were proposed to be investigated in this study. The

resulting arc offset from chord and maximum overhang length at mid-span of outer girder using the proposed radii of curvature for the different girder types are given in Table 5-13.

It is readily seen from Table 5-13 that despite using very sharp curves (small radius of curvature) for LG-25 girder and Quad beam bridges, the arc offset and overhang length did not exceed the maximum limits of LADOTD BDEM. This is due to the short spans of the LG-25 girder and Quad beam bridges. However, for BT-78 the use of small radius of curvature with 130 ft. span length yielded arc offsets from chord and overhang length, both well exceeding BDEM limits. Therefore, the framing plans of BT-78 girder curved bridges were developed by setting the span length (chord length) to 130 ft. at the centerline of the bridge and setting the arc offset from chord to three (3) different values of 1.00, 1.50, and 1.75 ft. The corresponding radius of curvature (R) and maximum overhang length were determined as given in the Table 5-13. In addition, a minimum overhang length at the joint for the outer beam and at mid-span for the inner beam were fixed at 3 ft. i.e. the deck extrudes 6 in. beyond the top flange as recommended by PCI Bridge Design Manual as minimum.

Figure 5-34, Figure 5-35, and Figure 5-36 show the framing plans and the cross-sections of the curved BT-78, LG-25, and Quad beams bridges, respectively.

Table 5-13: Framing plans details of curved bridges

| Girder | Span (Chord Length), ft. | Arc Offset from Chord (S) | Radius of Curvature (ft.) | Maximum Overhang Length |
|--------|--------------------------|--------------------------------------|---------------------------|-------------------------------------|
| BT-78 | 130 | 4'-3" | 500 | 7'-5 ¹ / ₁₆ " |
| | | 2'-7 ³ / ₄ " | 800 | 5'-8 ⁹ / ₁₆ " |
| | | 2'-1 ³ / ₈ " | 1000 | 5'-1 ⁵ / ₁₆ " |
| BT-78 | 130 | 1'-9 ¹ / ₈ " | 1200 | 4'-9 ¹ / ₂ " |
| | | 1'-6 ¹ / ₈ " | 1400 | 4'-6 ³ / ₈ " |
| | | 1'-0 ¹ / ₈ " | 2100 | 4'-0 ¹ / ₄ " |
| LG-25 | 44 | 0'-5 ³ / ₄ " | 500 | 3'-6" |
| | | 0'-3 ⁵ / ₈ " | 800 | 3'-6" |
| | | 0'-2 ⁷ / ₈ " | 1000 | 3'-6" |
| Quad | 40 | 0'-4 ¹³ / ₁₆ " | 500 | 2'-2" |
| | | 0'-3" | 800 | 2'-2" |
| | | 0'-2 ³ / ₈ " | 1000 | 2'-2" |

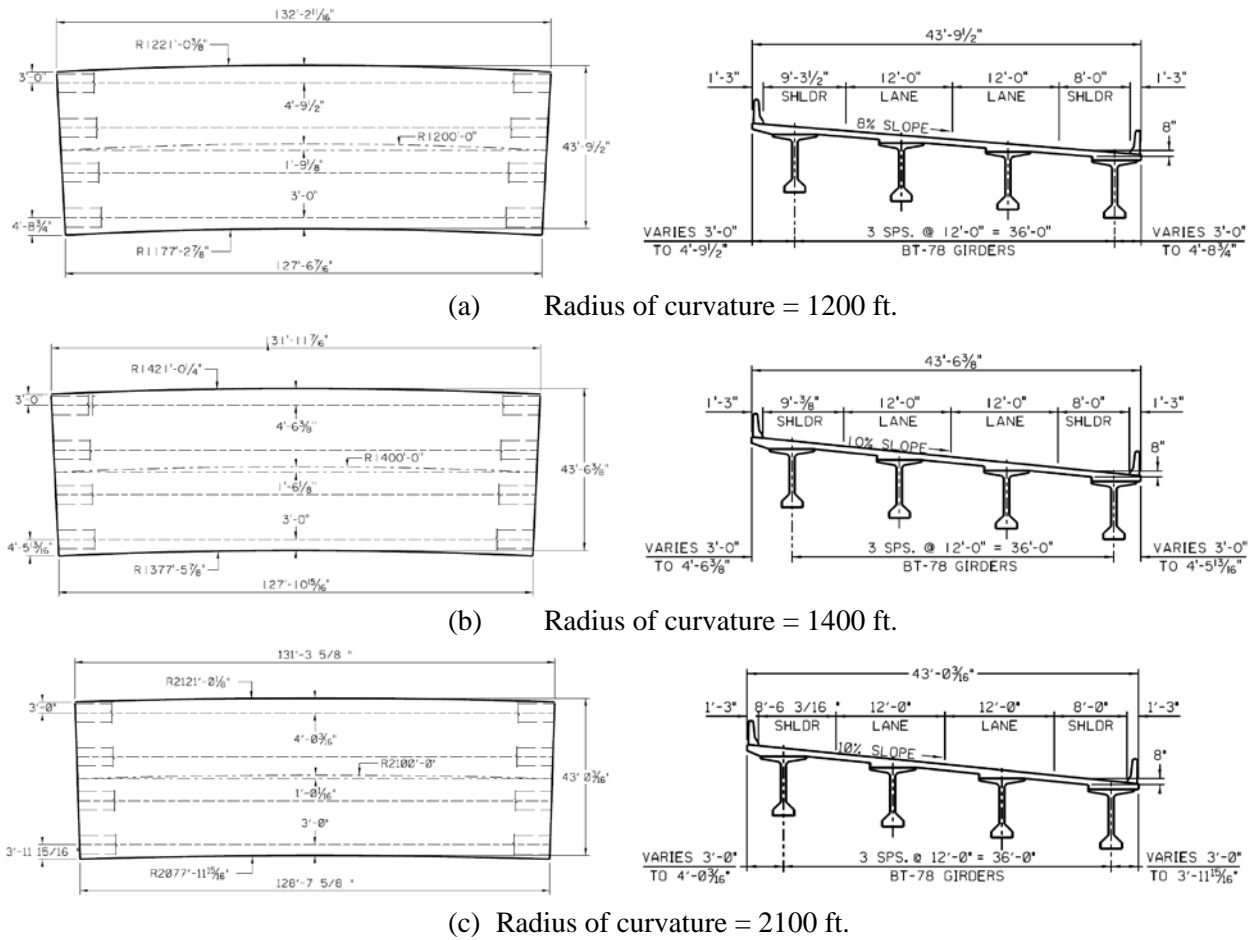
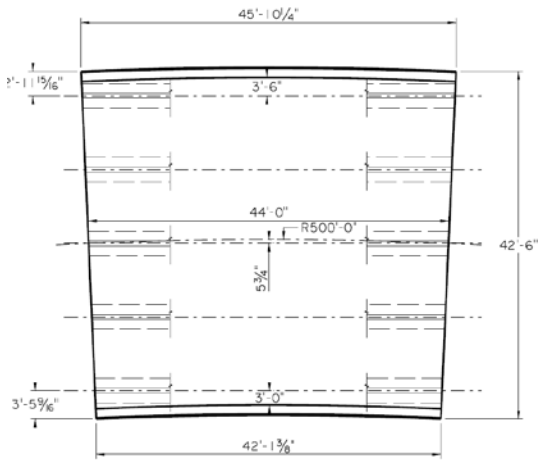
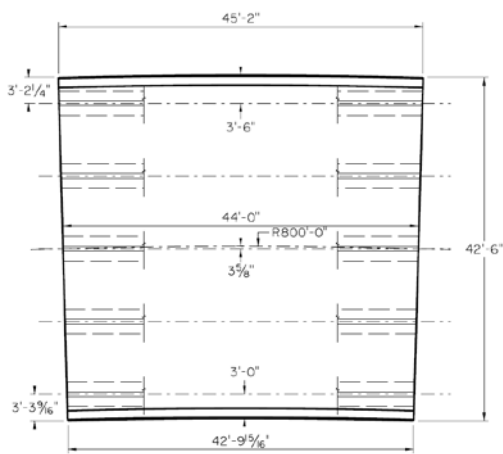
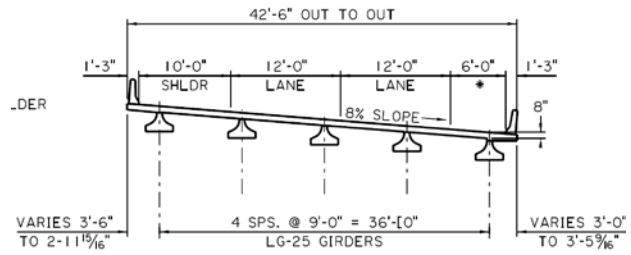


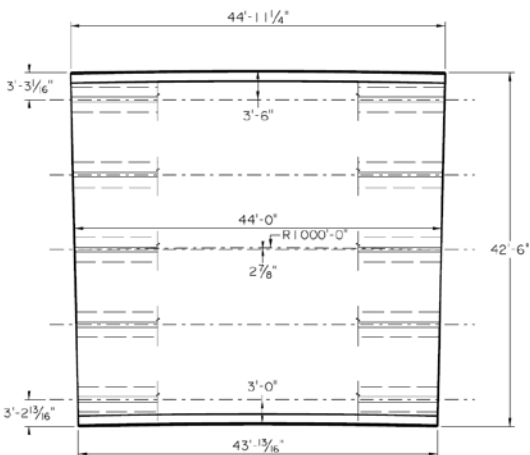
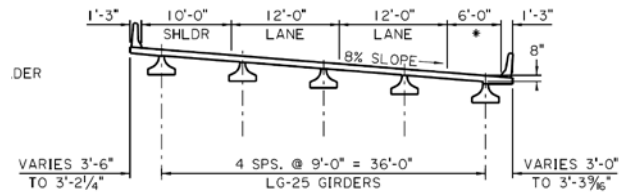
Figure 5-34: Framing plans of curved BT-78 girder bridges with different radii of curvature



(a) Radius of curvature = 500 ft.



(b) Radius of curvature = 800 ft.



(c) Radius of curvature = 1000 ft.

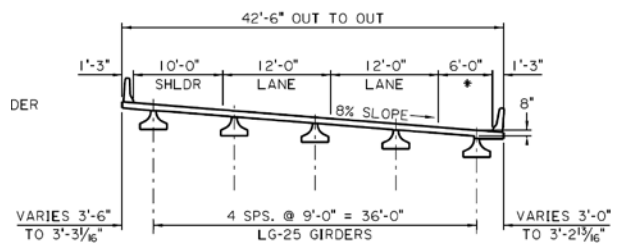


Figure 5-35: Framing plans of curved LG-25 girder bridges with different radii of curvature

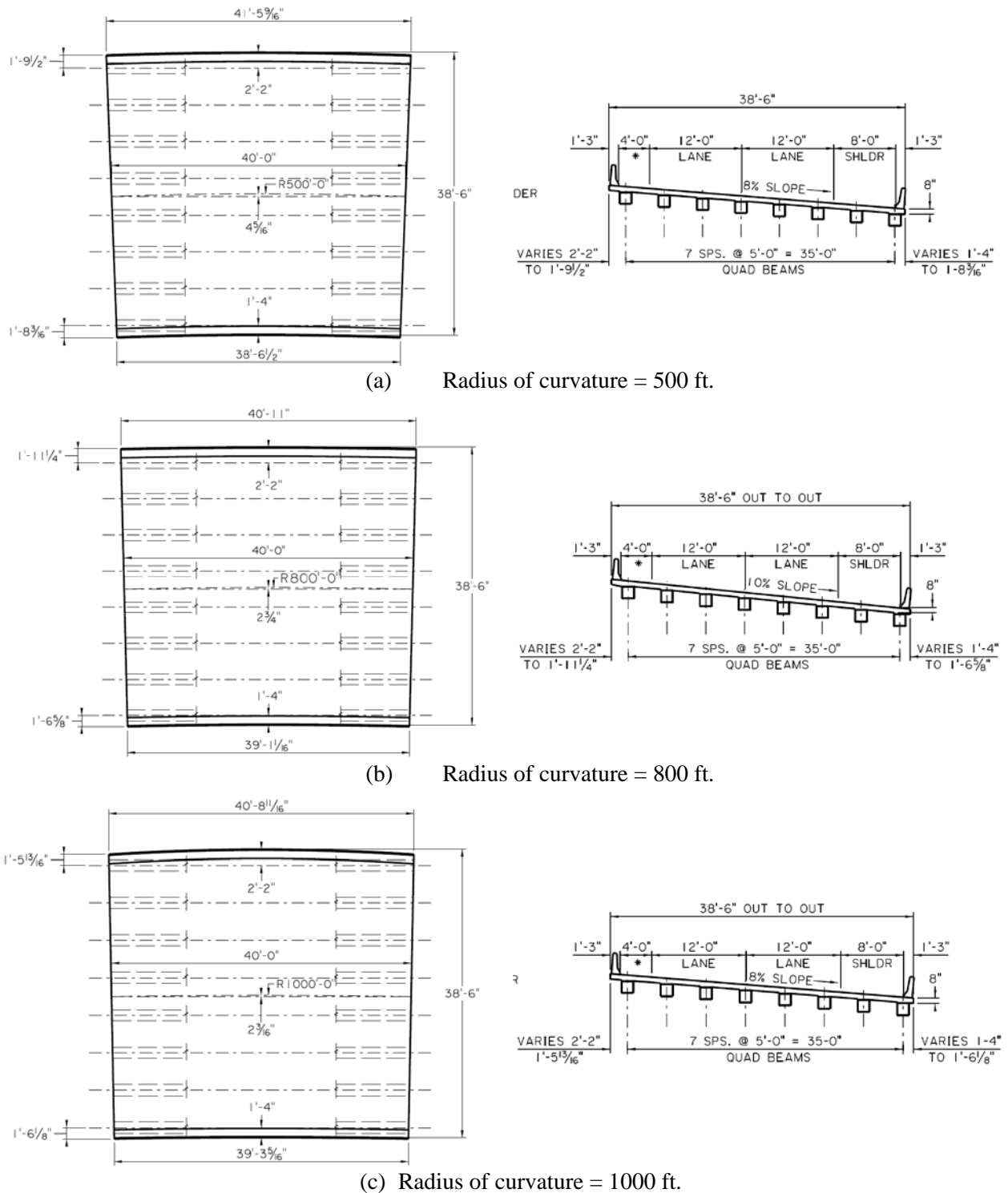
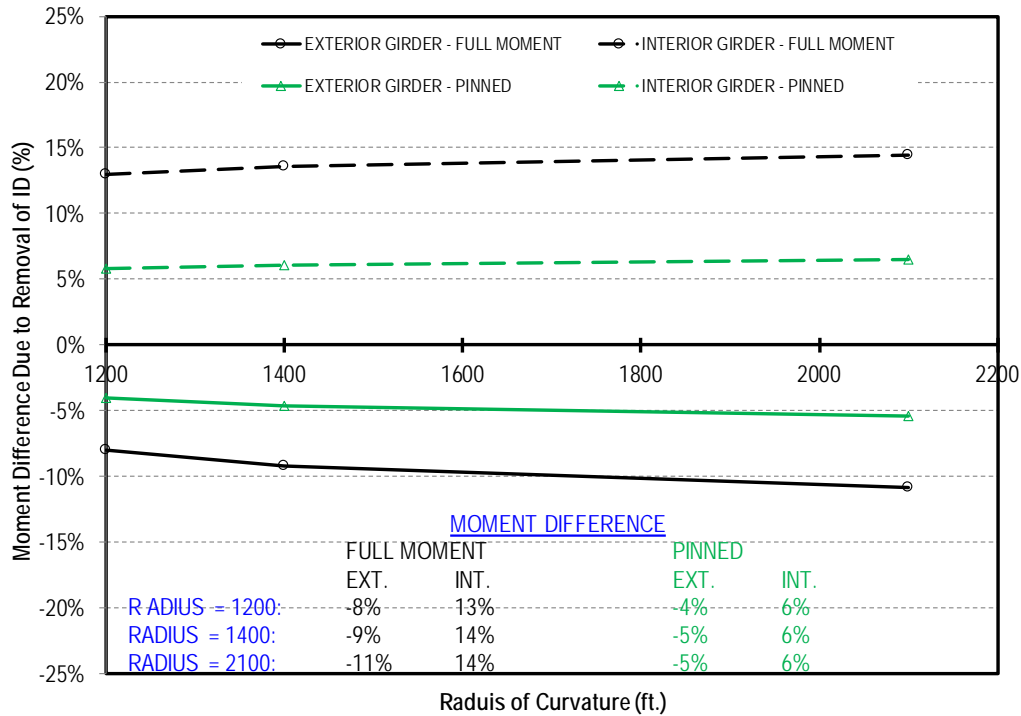


Figure 5-36: Framing plans of curved Quad beam bridges with different radii of curvature

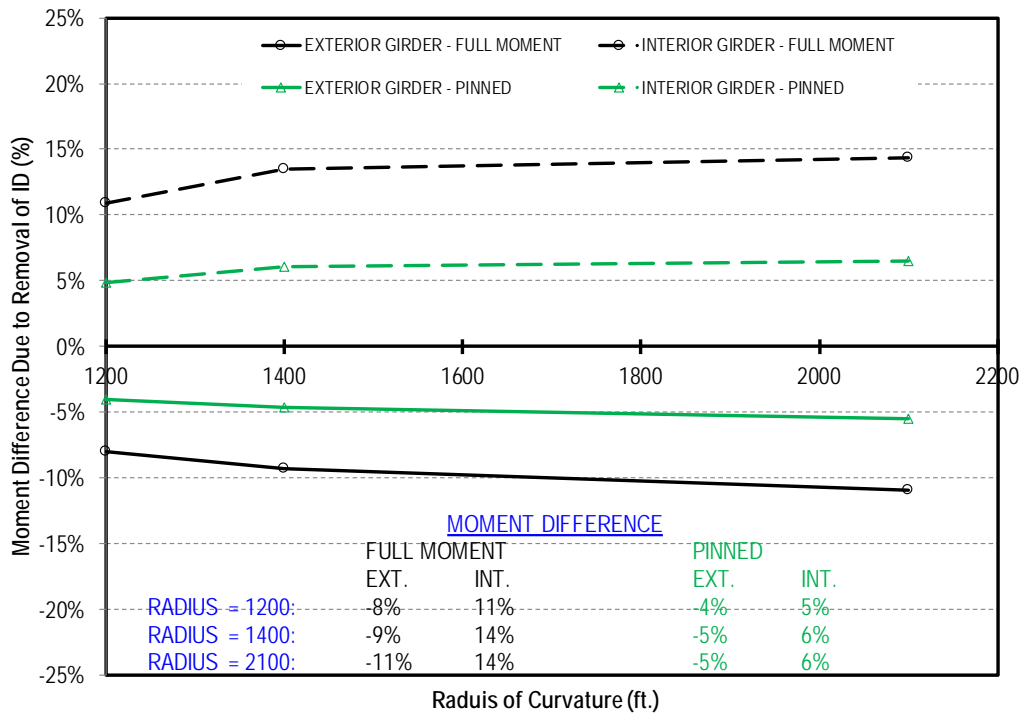
5.6.2—BT-78 Girder Bridges

The moment envelopes of the interior and exterior girders were developed for all investigated curved bridges using the procedure described in section 5.2. The difference in moment due to removal of the ID was determined for the exterior and interior girders for each case.

In order to demonstrate the effect of the radius of curvature of the bridge, the moment difference due to removal of ID is plotted against the radius of curvature for cross slopes of 8% and 10% in Figure 5-37. The results, shown in Figure 5-37, indicate that the radius of curvature of the bridge had virtually no effect on the moment difference due to removal of ID for both exterior and interior girders. This behavior implies that curved deck supported on chorded BT-78 girders with the range of curvature covered in this study act as straight bridges. Furthermore, the moment difference due to removal of ID was higher for the case of ID with full moment connection compared to pinned connection. This leads to the conclusion that ID with pinned connection has no significant impact on the design live load moment of curved spans made of curved deck and chorded girders. The influence of the cross slope of the bridge was investigated by plotting the moment difference due to removal of ID versus the cross-slope in Figure 5-38. Figure 5-38 (a) and (b) clearly indicate that increasing the cross slope of the bridge from 8% to 10% had a no effect on the moment difference due to removal of ID for the two connection rigidities.

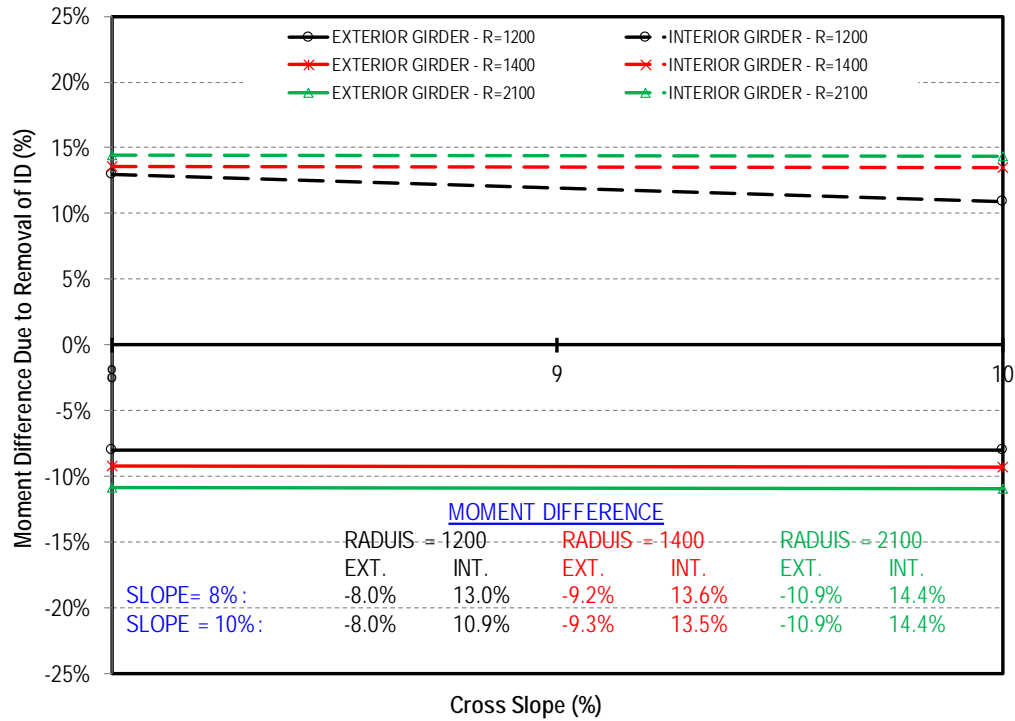


(a) Cross-slope 8%

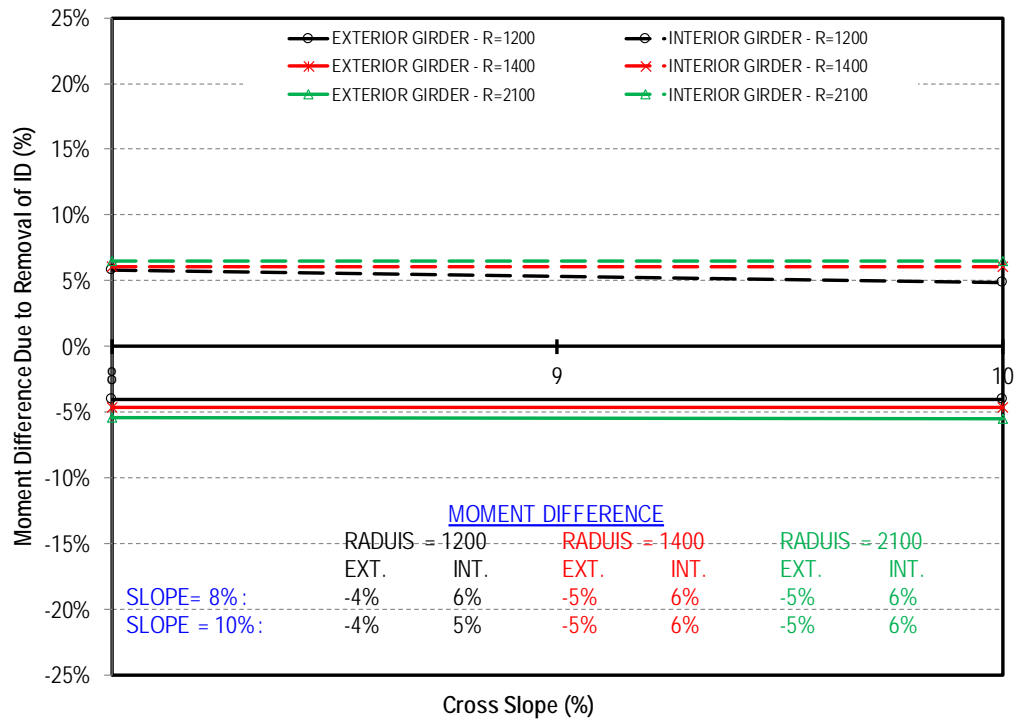


(b) Cross-slope 10%

Figure 5-37: Moment difference of curved BT-78 girder bridges with different radii of curvature



(a) Full moment connection



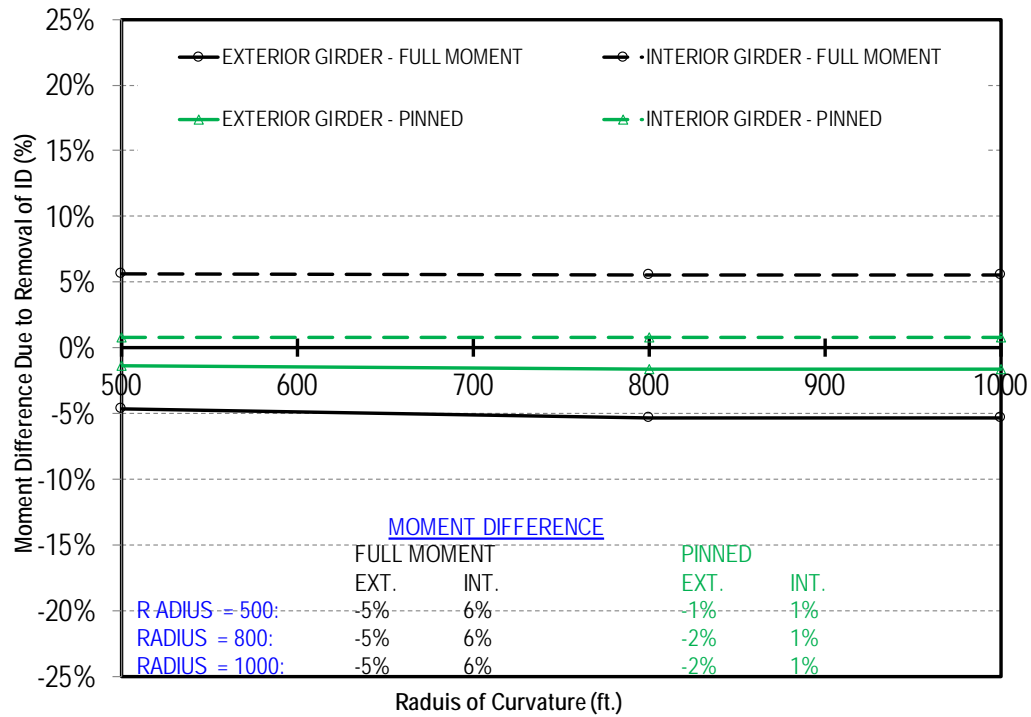
(b) Pinned connection

Figure 5-38: Moment difference vs. cross-slope for curved BT-78 girder bridges

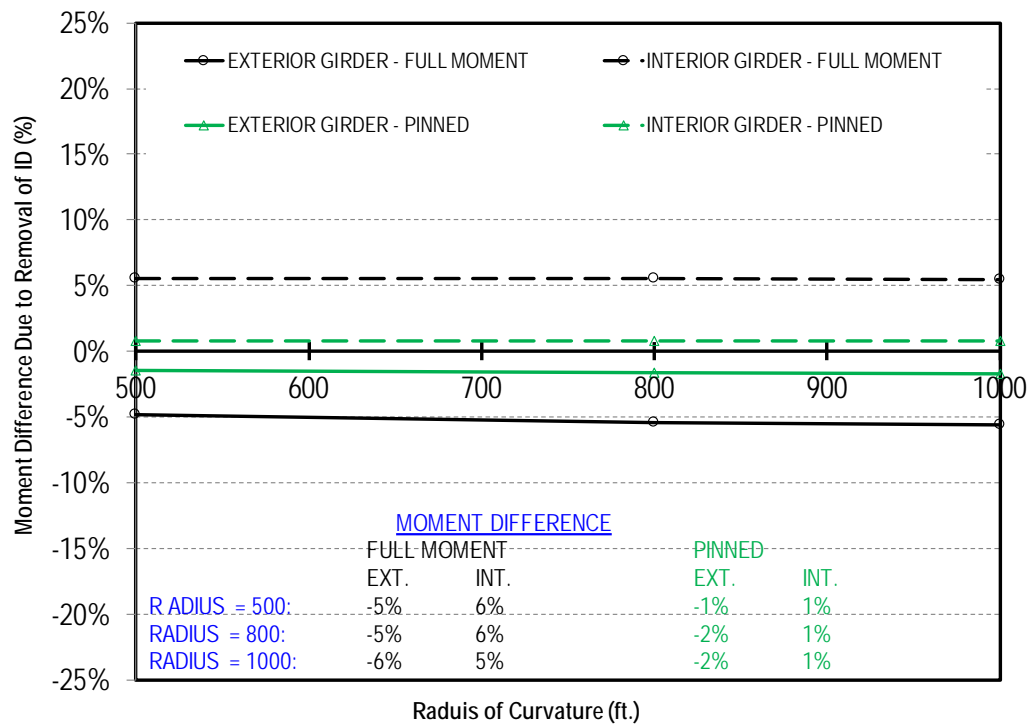
5.6.3—LG-25 Girder Bridges

The curved LG-25 girder bridges exhibited same behavior observed for BT-78 girder bridges. Figure 5-39 shows the moment difference due to removal of ID plotted against the radius of curvature of the bridge for the cases of cross slopes 8% and 10%. Radius of curvature showed minimal effect on the moment difference in both the exterior and interior girders. The effect of the removal of the ID was less significant for the case of the pinned connection when compared to the full moment connection. This behavior implies that curved spans where curved deck is supported on chorded LG-25 girders with the range of curvature covered in this study, act as straight bridges.

Figure 5-40 shows the moment difference due to removal of ID plotted versus the cross slope for bridges with different radii of curvature and connection rigidities. The cross slope showed virtually no effect on the behavior especially for the case of the ID with pinned connection.

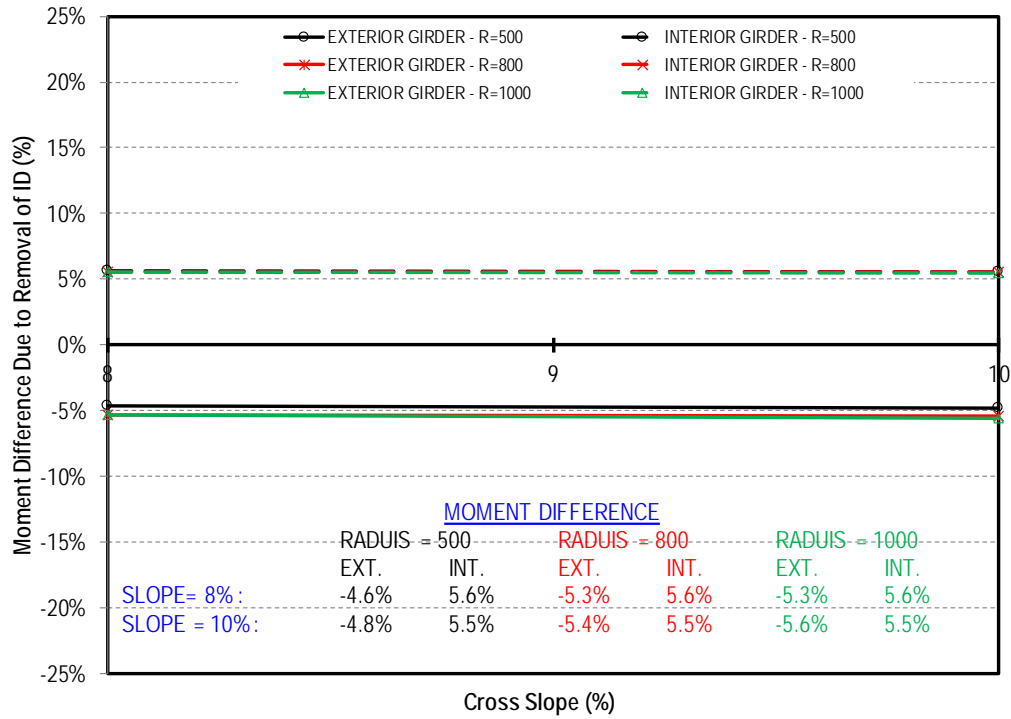


(a) Cross Slope 8%

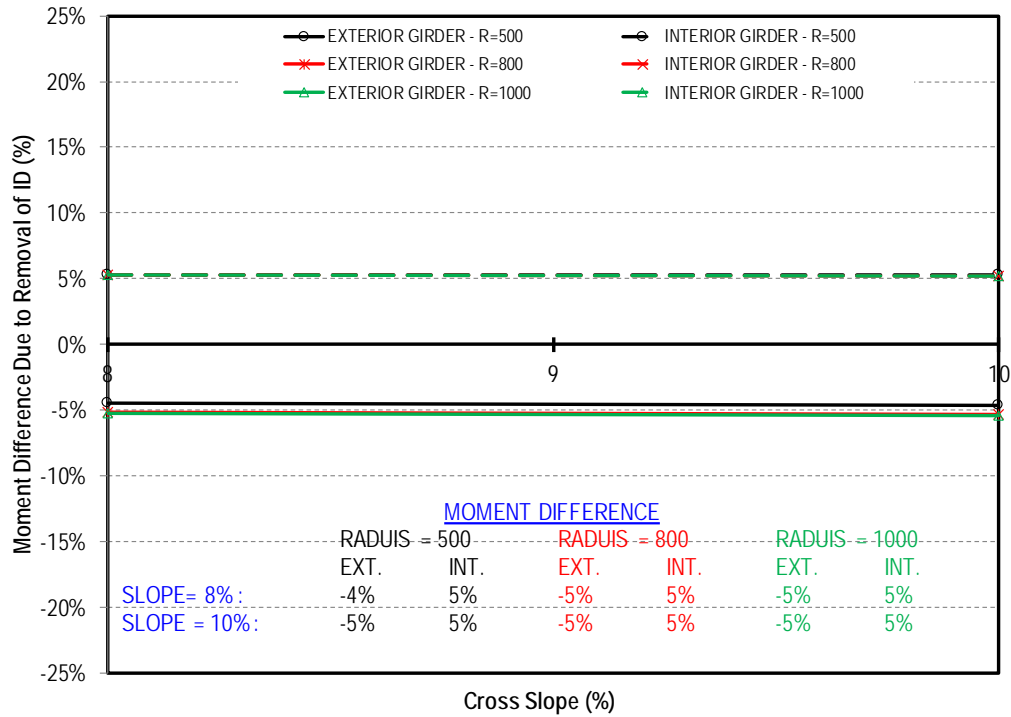


(b) Cross Slope 10%

Figure 5-39: Moment difference of curved LG-25 girder bridges with different radii of curvature



(a) Full moment Connection



(b) Pinned Connection

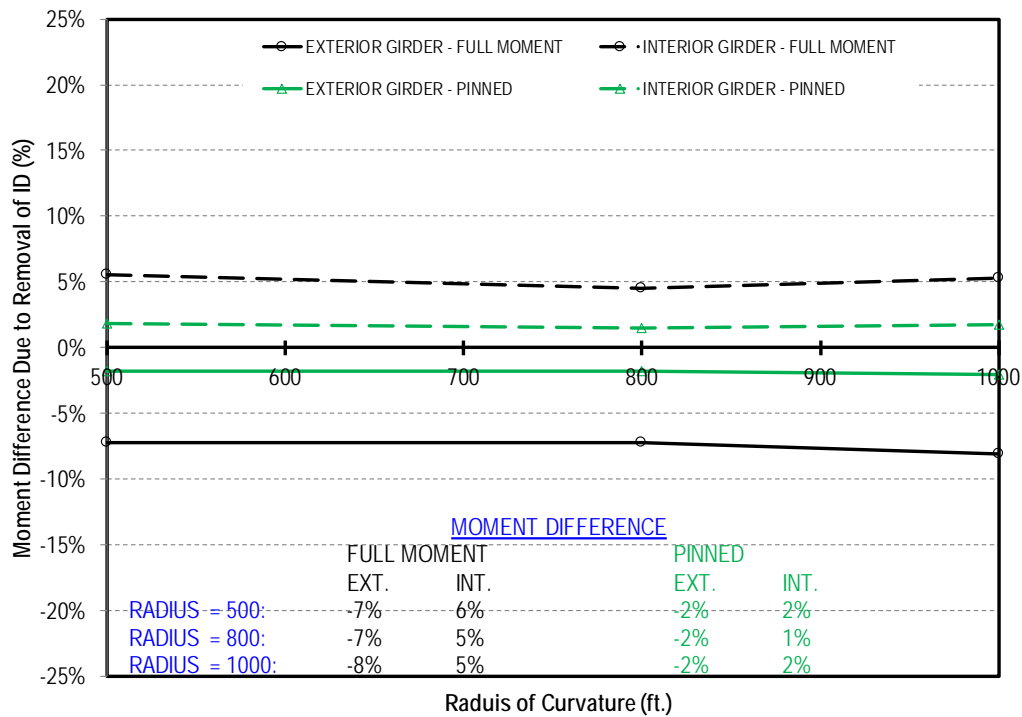
Figure 5-40: Moment difference vs. cross-slope for curved LG-25 girder bridges

5.6.4—Quad Beam Bridges

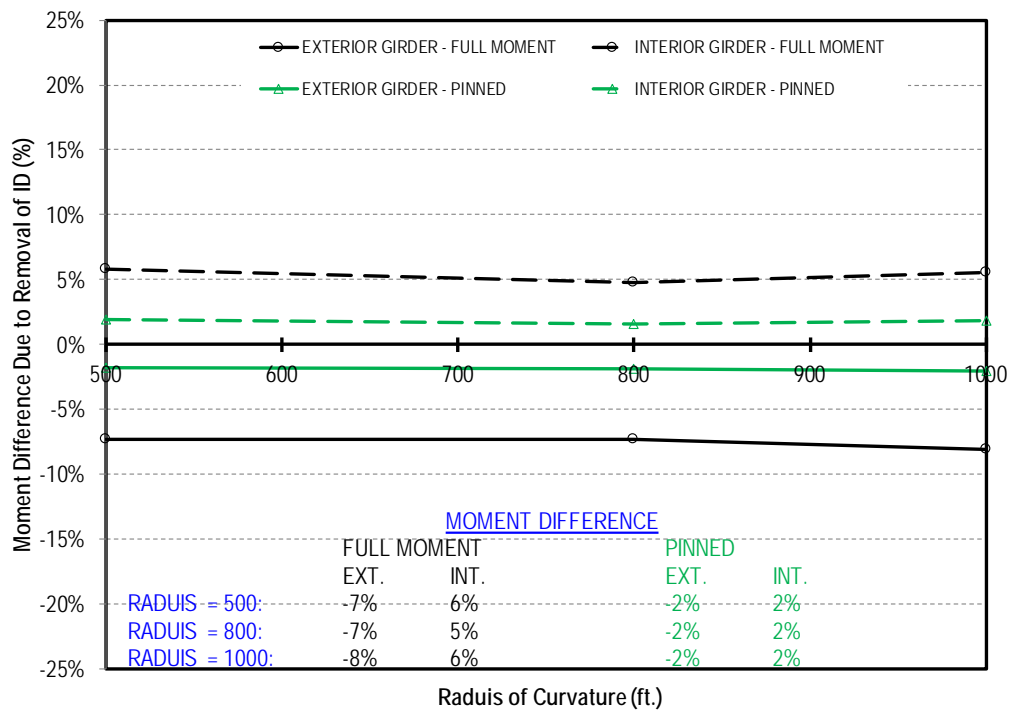
The moment difference due to removal of ID is plotted against the radius of curvature for different connection rigidities and cross slopes as shown in Figure 5-41. It can be seen from Figure 5-41 that increasing the radius of curvature of the bridge from 500 ft. to 1000 ft. resulted in 1% variation in the moment difference for the case of ID with full moment connection and had no effect for the case of the pinned connection. This observation indicates that the radius of curvature did not affect the moments of the exterior and interior girders.

It should be noted that the removal of the ID resulted in only 2% difference in the moments of the exterior and interior girders for the case of ID with pinned connection. This minor effect is expected, which is similar to BT-78 and LG-25 girder bridges results.

To evaluate the effect of cross slope of the bridge, the moment difference due to removal of intermediate diaphragms was plotted against cross slope for different connection types and radii of curvature as shown in Figure 5-42. As expected, the cross slope exhibited minimal effect on the moment difference due to removal of ID with a maximum variation less than one percent for different radii of curvature.

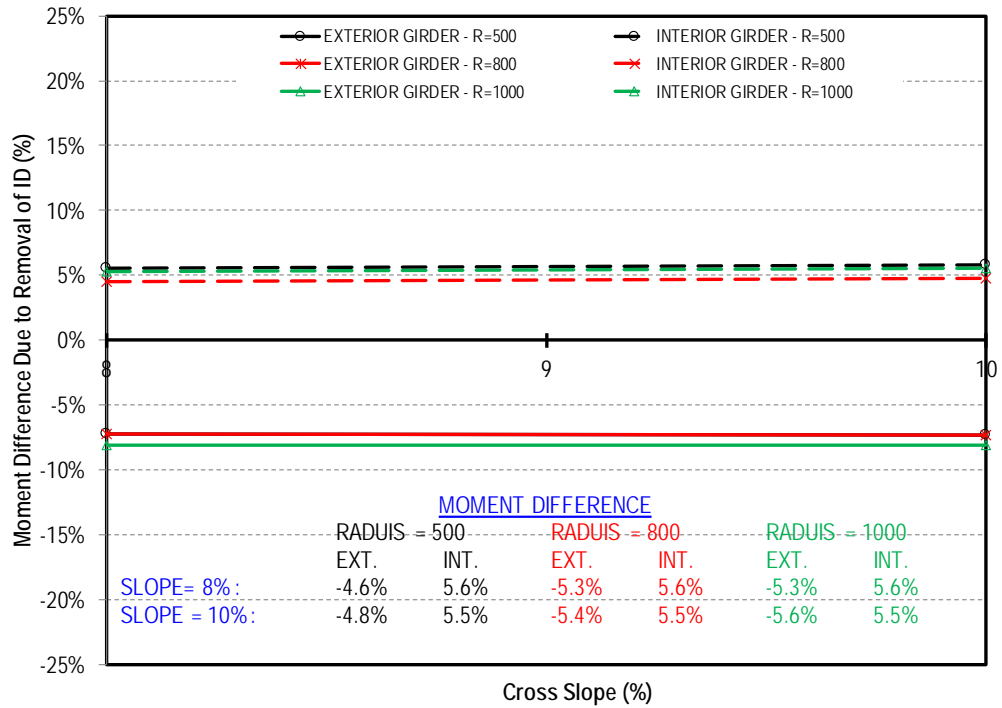


a) Cross-slope 8%

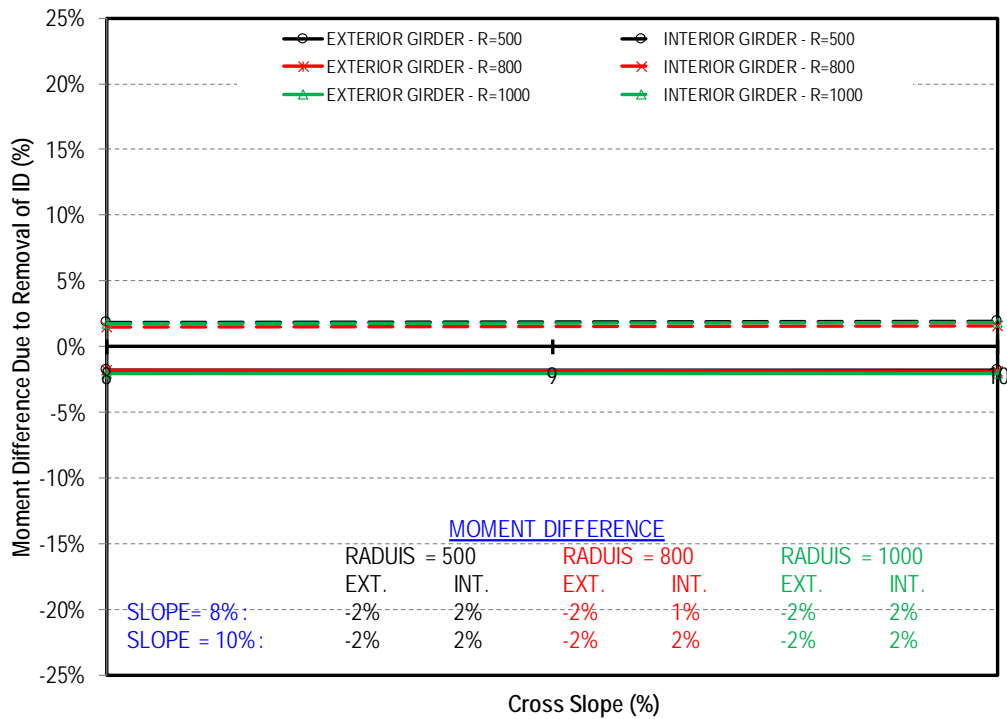


b) Cross-slope 10%

Figure 5-41: Moment difference of curved Quad beam bridges with different radii of curvature



a) Full Moment Connection



b) Pinned Connection

Figure 5-42: Moment difference vs. cross-slope for curved Quad beam bridges

5.7—Summary and Conclusions

A parametric study was conducted using Finite Element Analysis. The validated numerical modeling techniques (grillage model or planar model) were used to investigate the effect of different parameters that are believed to affect the contribution of ID in BT-78, LG-25 and Quad beam bridges.

The above three types of bridges were investigated for different geometric configurations including straight, skew, and curved bridges. The study also investigated the effect of the rigidity of the connection between ID and the girder assuming full moment and pinned connections.

To evaluate the role of the ID, each bridge was analyzed for two conditions, with and without ID. Moment envelopes were developed for each case and the moment difference due to removal of ID was determined for the exterior and interior girders of the bridge. The moment difference served as the basis for the evaluation of the role of ID. The effect of the investigated parameters on the moment difference was realized for each case. Based on the findings of the parametric study, the following conclusion could be drawn:

- Removal of ID results in increasing the mid-span moment of the interior girder and decreasing the mid-span moment of the exterior girder.
- The rigidity of the connection between ID and the girder impacts their role. ID with pinned connection showed to be less effective in comparison with ID with full moment connection.
- For BT-78, LG-25, and Quad beam bridges, contribution of ID to mid-span moment is insignificant when using pinned connection.
- Effectiveness of ID decreases with increasing span length and/or decreasing girder spacing.
- Skew bridges with skew angle less than 30° behave similarly to straight bridges. ID had virtually no effect on the mid-span moment of the exterior or interior girders when the skew angle was increased from 30° to 60°.
- For spans on curve with curved deck and straight (chorded) girders, the curvature of the deck has minimal effect on the mid-span moment of exterior and interior girders due to the removal of ID. In addition, cross-slope has absolutely no effect on the girders due the removal of ID.

6–DESIGN RECOMMENDATIONS

The results of the parametric study presented in Section 5 of this report showed that removal of intermediate diaphragm has insignificant effect on the live load moment at mid-span under normal loading conditions for BT-78 girder, LG-25 girder, and Quad beam bridges. Therefore, it is recommended to remove intermediate diaphragm from straight, skew and curved (curved deck on straight (chorded) girders) of BT-78 girder, LG-25 girder, and Quad beams bridges. The intermediate diaphragm policy given in Part II, Vol. 1, Chapter 5, Section 5.13.2.2 of LADOTD BDEM can be revised as follows:

| Case | Requirement for Intermediate Diaphragms (ID) |
|---|---|
| All spans unless otherwise specified as follows: | ID is not required. |
| <u>Case 1</u> : Spans over roadways, railroads, navigational channels, and water body with anticipated marine traffic under normal loading condition except for Cases <u>2</u> and <u>3</u> . | One ID shall be provided at center of span. |
| <u>Case 2</u> : Spans on curve with curved girders only. | Requirement of ID shall be determined for the design condition. Minimum one ID shall be provided. |
| <u>Case 3</u> : Spans subject to wave force, extreme high wind conditions, other anticipated lateral forces, or other unusual loading conditions. | Requirement of ID shall be determined for the design condition. Minimum one ID shall be provided. |

7—REFERENCES

- American Association of State Highway and Transportation Officials (AASHTO), (2012). "The Manual for Bridge Evaluation: Second Edition." *AASHTO Publications*, Washington, D.C., 1661.
- Abendroth, R. E., Klaiber, F. W., and Shafer, M. W. (1995). "Diaphragm Effectiveness in Prestressed-Concrete Girder Bridges." *Journal of Structural Engineering*, 121(9), 1362–1369.
- American Concrete Institute (ACI) Committee 440. (2003). "Guide for the Design and Construction of Concrete Reinforced with FRP Bars." ACI 440.1R-03. Farmington Hills, MI: ACI.
- Barr, P. J., Eberhard, M. O., and Stanton, J. F. (2001). "Live-load distribution factors in prestressed concrete girder bridges." *Journal of Bridge Engineering*, 6(5), 298–306.
- Cai, S., (2005). "Discussion on AASHTO LRFD Load Distribution Factors for Slab-on-Girder Bridges." *Practice Periodical on Structural Design and Construction*, 10(3), 171-176.
- Cai, S., and Avent, R. (2008). "Assessing the Needs for Intermediate Diaphragms in Prestressed Concrete Bridges." *Research Report*, Louisiana Transportation Research Center, 40.
- Cai, C. S., Shahawy, M., Peterman, R. J. (2002). "Effect of diaphragms on load distribution in prestressed concrete bridges." *Transportation Research Record*. 1814, Transportation Research Board, Washington D.C., 47-54.
- Cai, C. S., and Shahawy, M. (2004). "Predicted and measured performance of prestressed concrete bridges" *Journal of Bridge Engineering*, 9(1), 4-13.
- Dupaquier, S. (2014). " Investigation of the Use of Steel Intermediate Diaphragms and Temporary Bracing Alternatives for Prestressed Concrete Girder Bridges." MS Thesis, Auburn University, Auburn, Alabama.
- Eamon, C., and Nowak, A.S. (2002). "Effects of Edge-Stiffening Elements and Diaphragms on Bridge Resistance and Load Distribution." *ASCE Journal of Bridge Engineering*, 7(5), 258-266.
- Grace, N., Jensen, E.A., Enomoto, T., Matsagar, V.A., Soliman, E.M., and Hanson, J.Q., (2010). "Transverse Diaphragms and Unbonded CFRP Post-Tensioning in Box-Beam Bridges." *PCI Journal*, 55(2), 109-122.
- Green, T.M., Yazdani, N., and Spainhour, L. (2004). "Contribution of Intermediate Diaphragms in Enhancing Precast Bridge Girder Performance." *Journal of Performance of Constructed Facilities*, ASCE, 18(3), 142-146.
- Griffin, J. J. (1997). "Influence of diaphragms on load distribution in P/C I-girder bridges." Ph.D. dissertation, Univ. of Kentucky, Lexington.
- Kostem, C. N., and deCastro, E. S. (1977). "Effects of diaphragms on lateral load distribution in beam-slab bridges." *Transportation Research Record* 645, Transportation Research Board, Washington D.C., 6–9.
- Lin, C. S., and VanHorn, D. A., (1968). "The effect of midspan diaphragms on load distribution in a prestressed concrete box-beams bridge." *Fritz Engineering Laboratory Report No. 315.6*, Lehigh University Institute of Research, Bethlehem, Pa.
- Li, L., and Ma, Z., J., (2010). " Effect of Intermediate Diaphragms on Decked Bulb-Tee Bridge System for Accelerated Construction." *Journal of Bridge Engineering*, 15(6), 715-722.
- Midas Civil (2016), Version 1.1, MIDAS Information Technology Co., Ltd., Korea.
- Midas FEA (2015), Version 1.1, MIDAS Information Technology Co., Ltd., Korea.
- Newmark, N. M. (1938). "A Distribution Procedure for the Analysis of Slabs Continuous Over Flexible Beams." Engineering Experiment Station, Bulletin 304, University of Illinois, Urbana, Illinois.
- Pucket, J. A., et.al. (2006). "Simplified Live Load Distribution Factor Equations." *NCHRP Report for 12-62 TRB*, National Research Council, Washington, D.C.

- Sengupta, S., and Breen, J. E. (1973). "The Effect of Diaphragms in Prestressed Concrete Girder and Slab Bridges." *Research Report*, Ctr. for Hwy. Res., The University of Texas at Austin Center for Highway Research.
- Sithichaikasem, S., and Gamble, W. L. (1972). "Effect of diaphragms in bridges with prestressed concrete I-section girders." *Civil Engineering Studies, Struct. Res. Series No. 383*, Department of Civil Engineering, University of Illinois, Urbana, Ill.
- Sotelino, E. D., Lui, J., Chung, W., and Phuvoravan, K. (2004). "Simplified Load Distribution Factor for Use in LRFD Design." *Research Report No. FHWA/IN/JTRP-2004/2*, Joint Transportation Research Program, Purdue University, West Lafayette, IN.
- Stanton, J. F., and Mattock, A. H. (1986). "Load distribution and connection design for precast stemmed multibeam bridge superstructures." *NCHRP Rep. 287*, National Cooperative Highway Research Program, Washington, D.C.
- Zokaie T., et.al. (1993). "Distribution of Wheel Loads on Highway Bridges." *NCHRP Report 12-26 TRB*, National Research Council, Washington, D.C.

8—APPENDIX: LIVE LOAD MOMENT OF PARAMETRIC STUDY BRIDGE MODELS

8.1—Effect of Connection Rigidity

8.1.1—BT-78 Girder Bridges

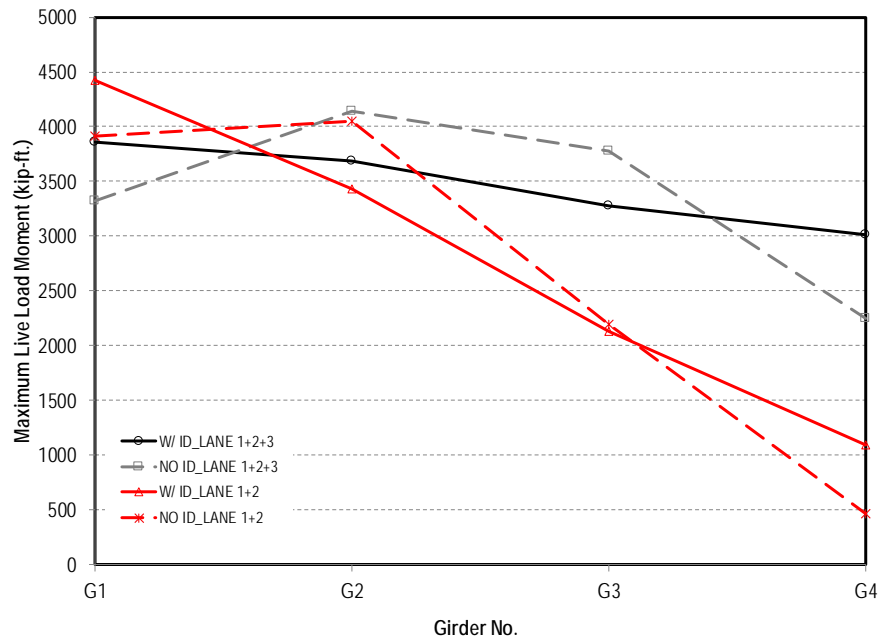


Figure 8-1: BT-78 girder bridge – ID with full moment connection

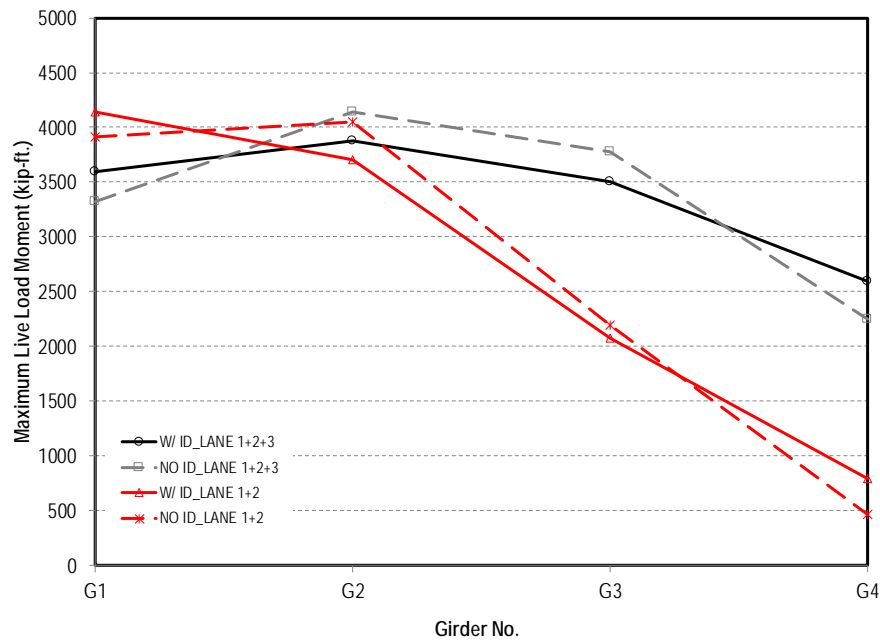


Figure 8-2: BT-78 girder bridge – ID with pinned connection

8.1.2—LG-25 Girder Bridges

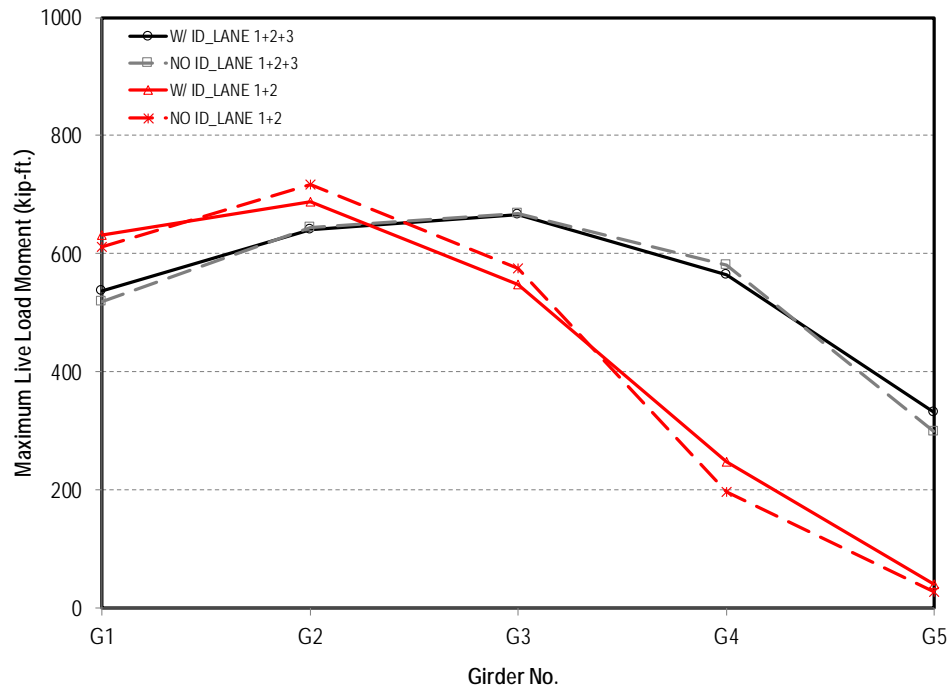


Figure 8-3: LG-25 girder bridge – ID with full moment connection

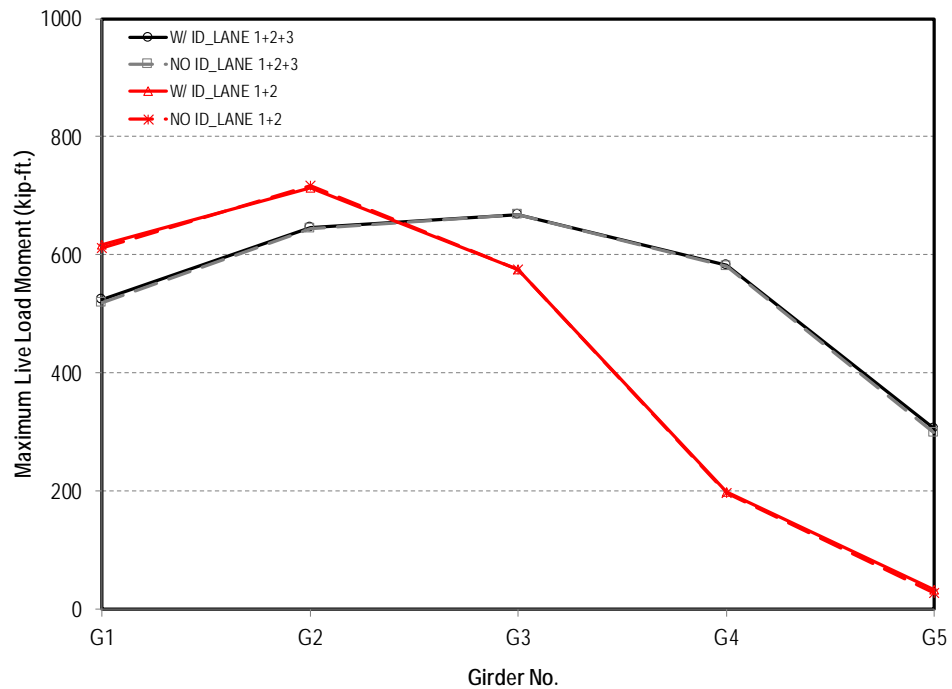


Figure 8-4: LG-25 girder bridge – ID with pinned connection

8.1.3—Quad Beam Bridges

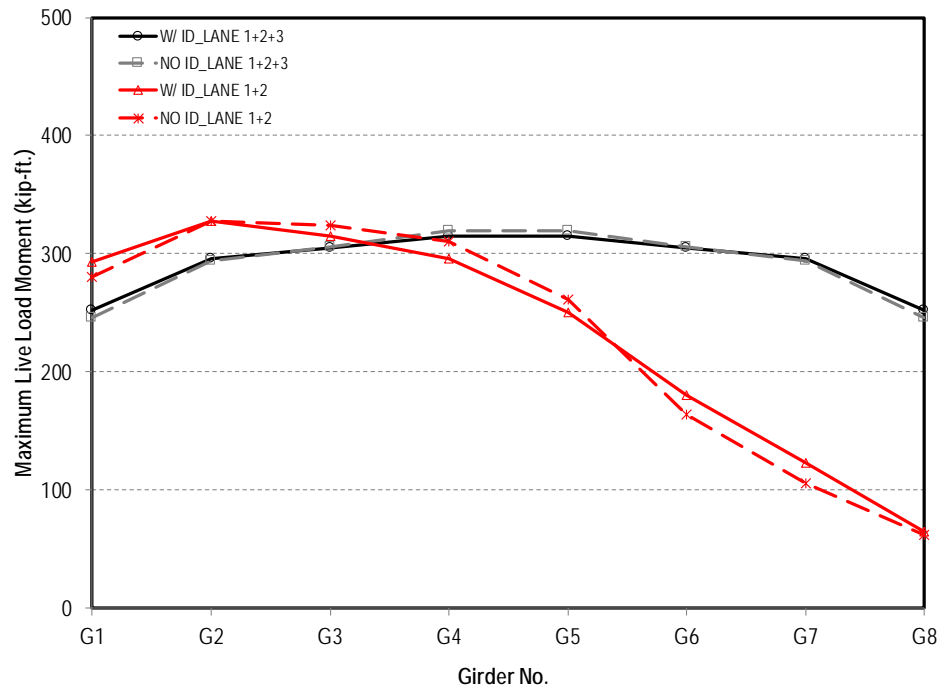


Figure 8-5: Quad beam bridge — ID with full moment connection

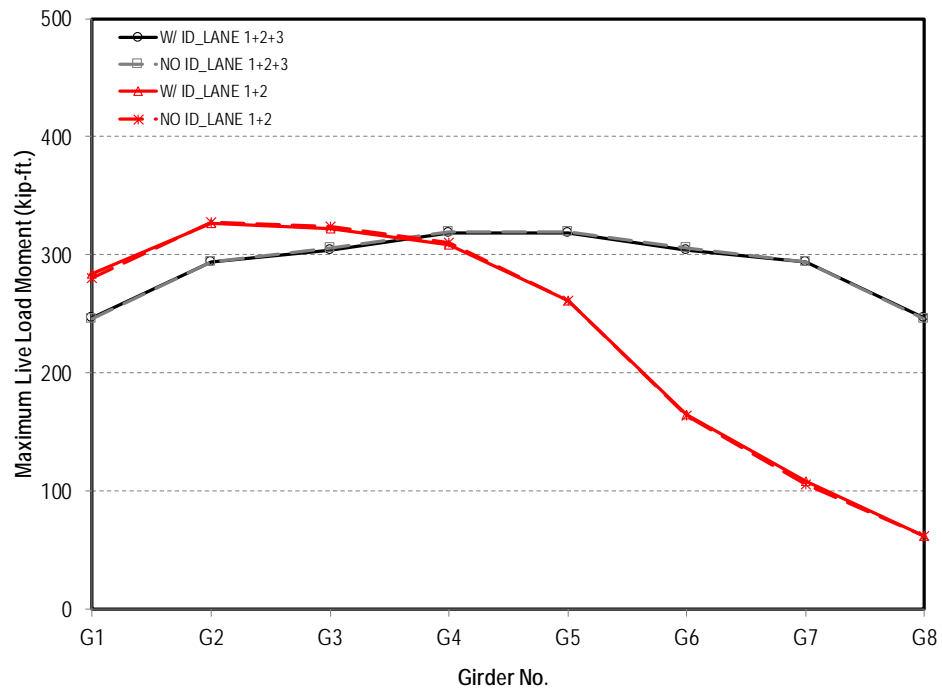


Figure 8-6: Quad beam bridge — ID with pinned connection

8.2—girder spacing and span length

8.2.1—Combined Effect of Girder Spacing and Span Length

8.2.1.1—BT-78 Girder Bridges

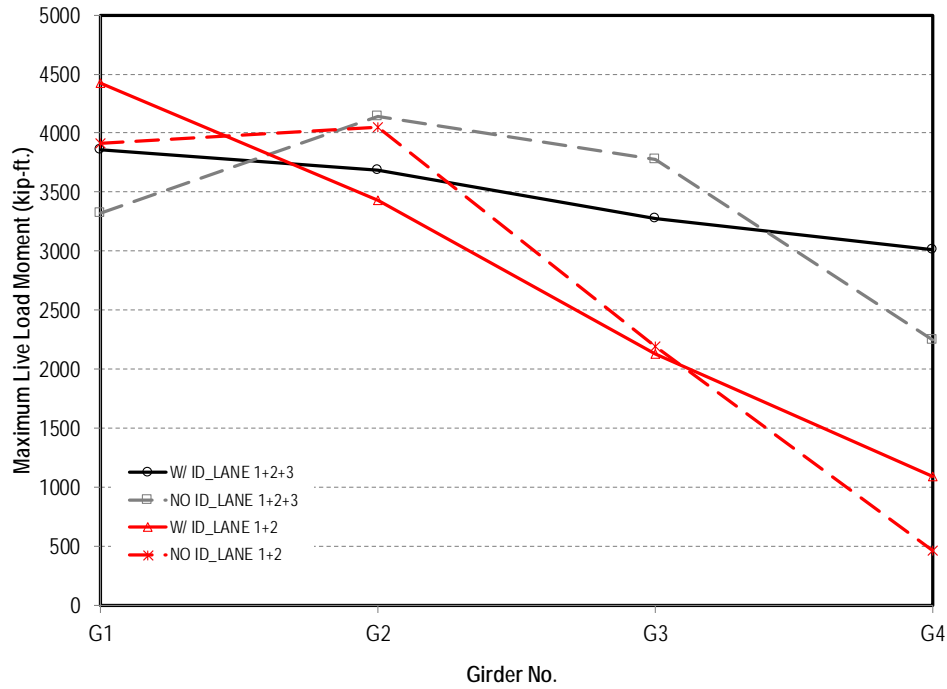


Figure 8-7: BT-78 girder bridge — 12 ft. girder spacing and 130 ft. span length

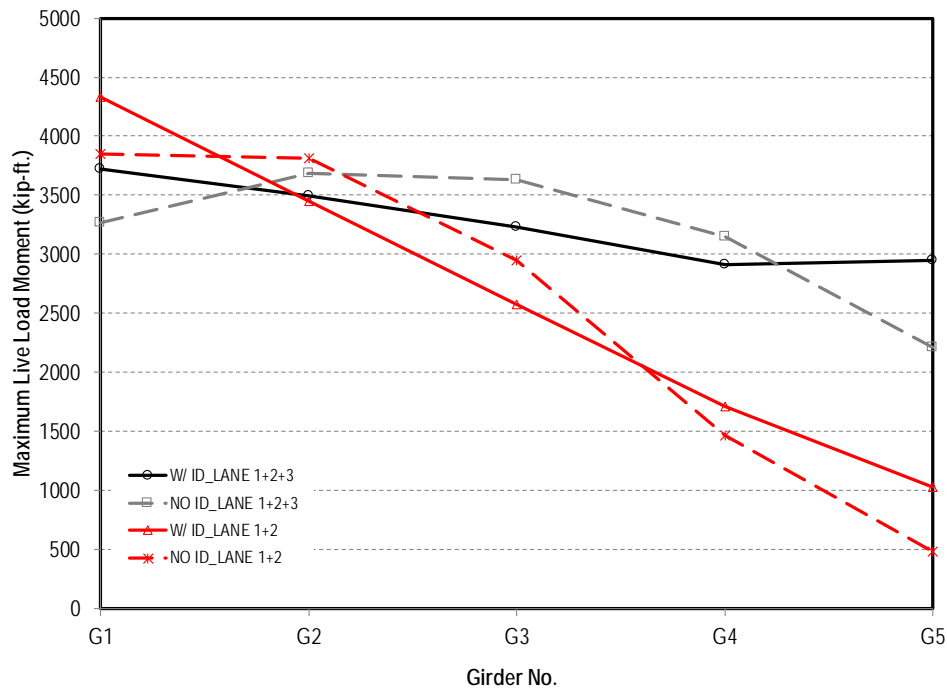


Figure 8-8: BT-78 girder bridge — 9 ft. girder spacing and 146 ft. span length

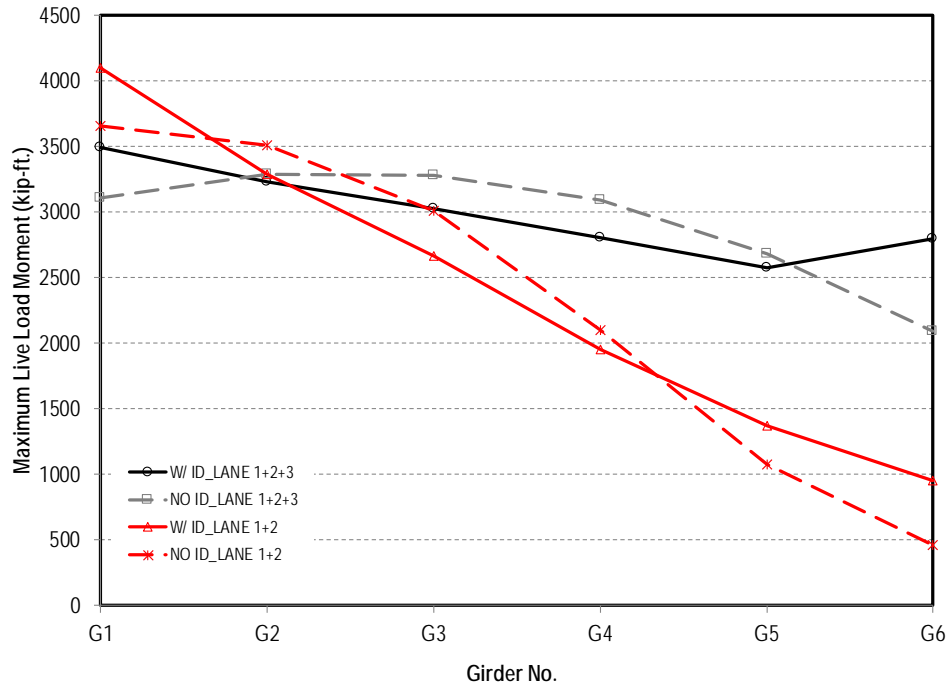


Figure 8-9: BT-78 girder bridge — 7.2 ft. girder spacing and 156 ft. span length

8.2.1.2—LG-25 Girder Bridges

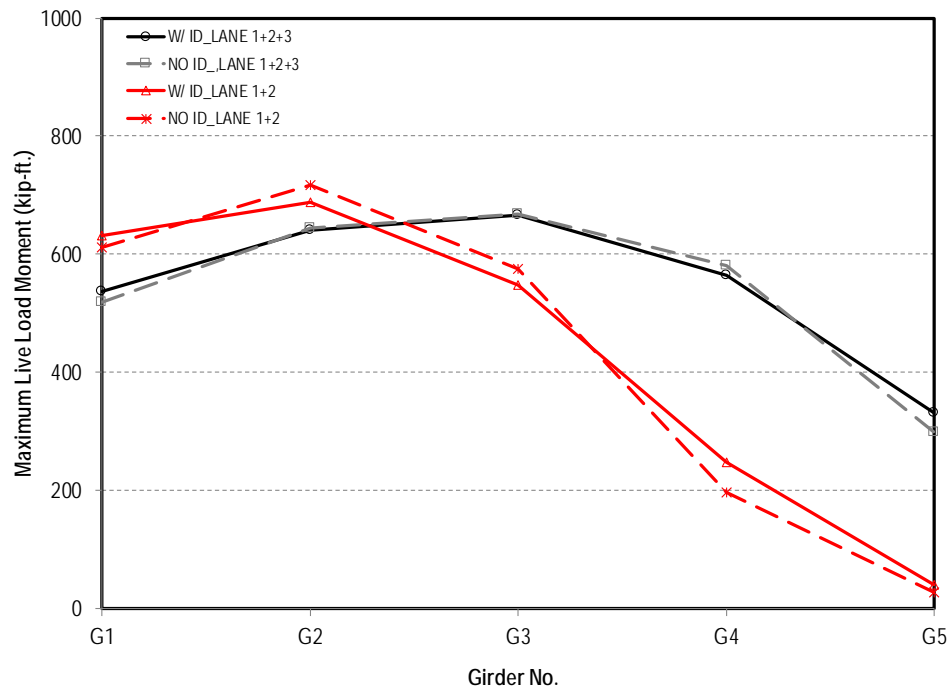


Figure 8-10: LG-25 girder bridge — 9 ft. girder spacing and 44 ft. span length

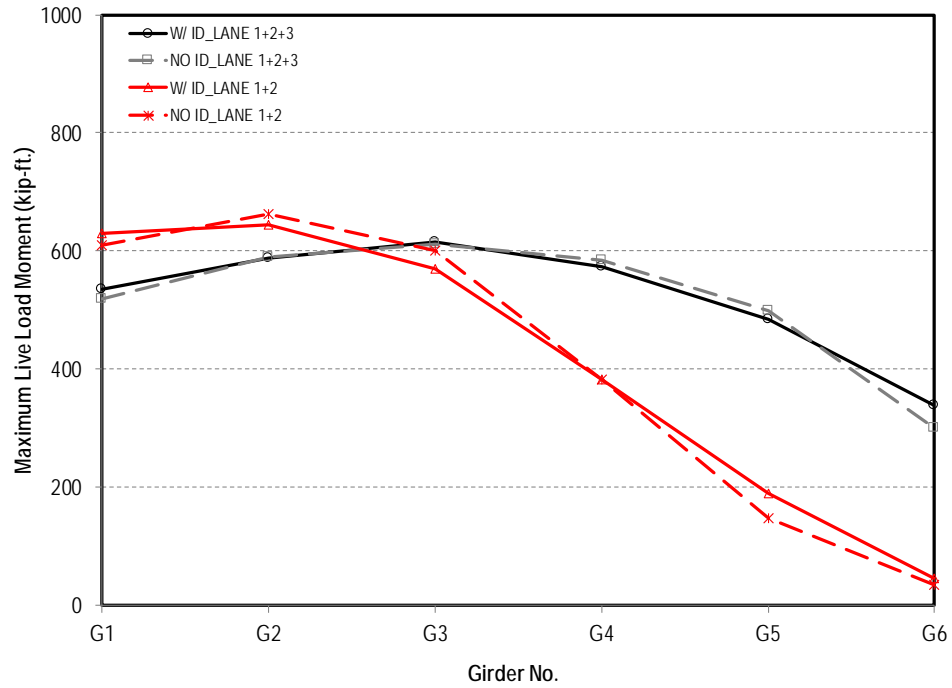


Figure 8-11: LG-25 girder bridge — 7.2 ft. girder spacing and 47 ft. span length

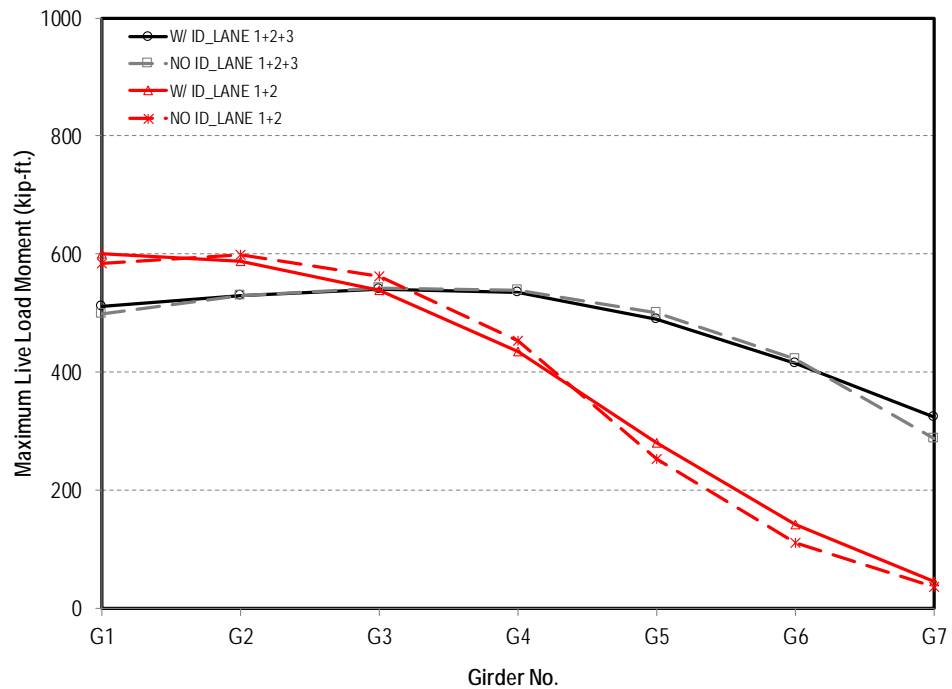


Figure 8-12: LG-25 girder bridge — 6 ft. girder spacing and 50 ft. span length

8.2.1.3—Quad Beam Bridges

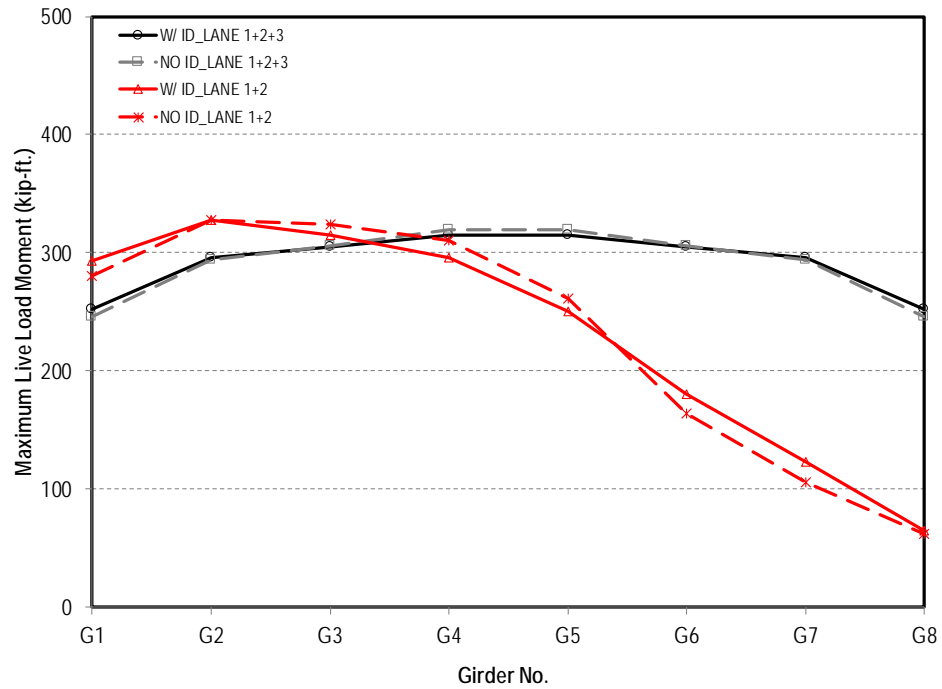


Figure 8-13: Quad beam bridge – 5 ft. spacing and 40 ft. span

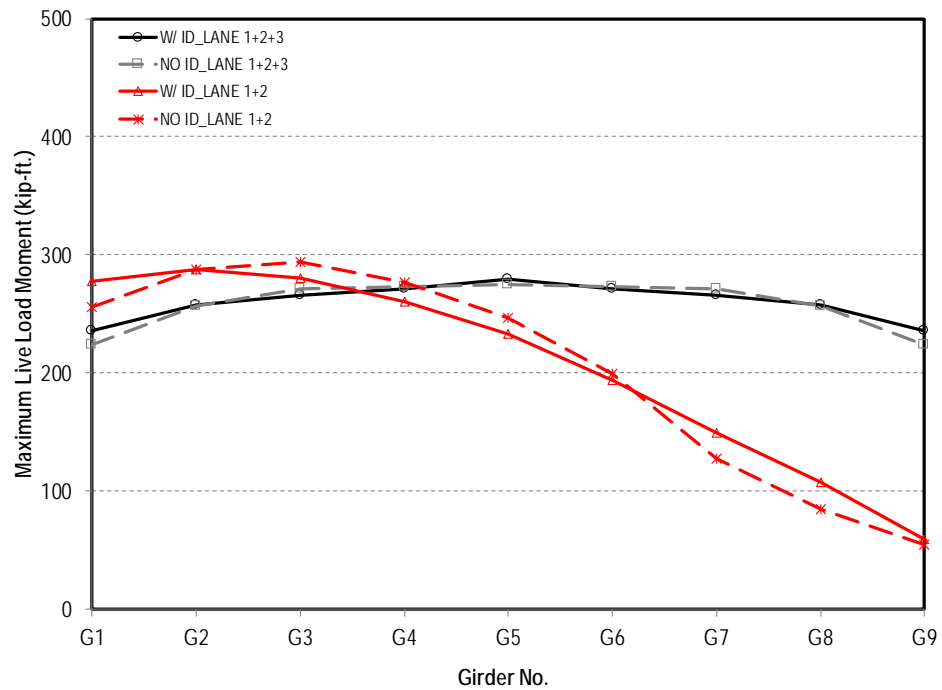


Figure 8-14: Quad beam bridge – 4.4 ft. spacing and 40 ft. span

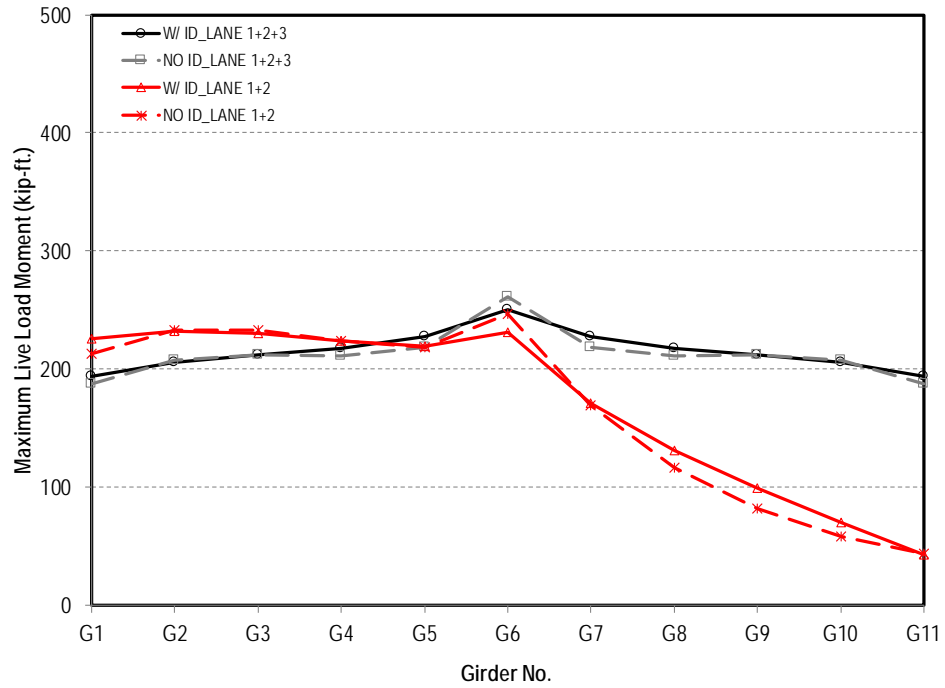


Figure 8-15: Quad beam bridge – 3.5 ft. spacing and 40 ft. span

8.2.2—Effect of Span Length

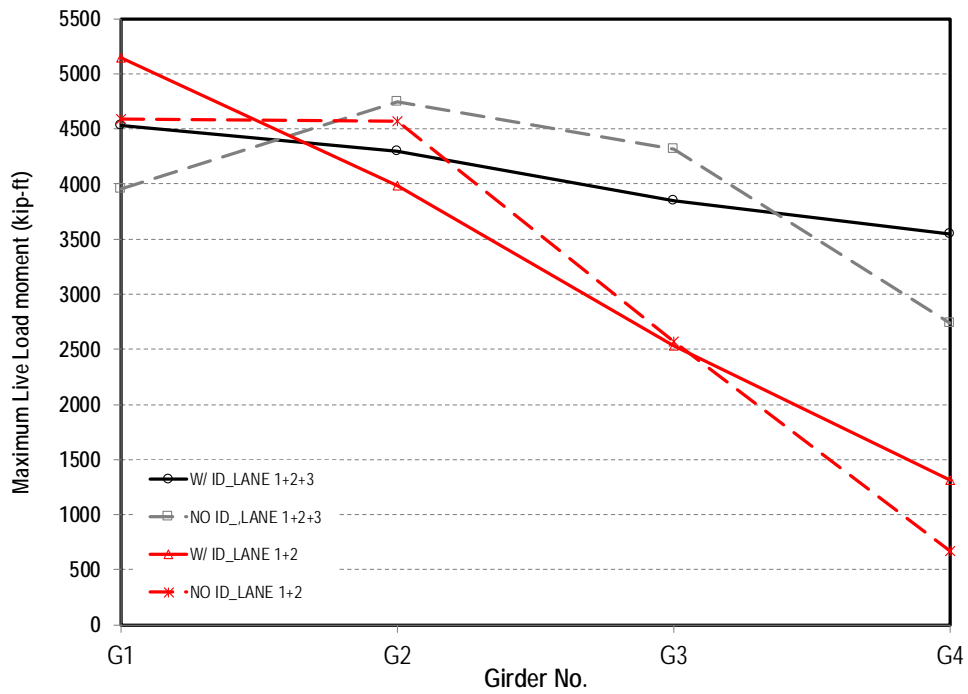


Figure 8-16: BT-78 girder bridge – 12 ft. girder spacing and 145 ft. span length

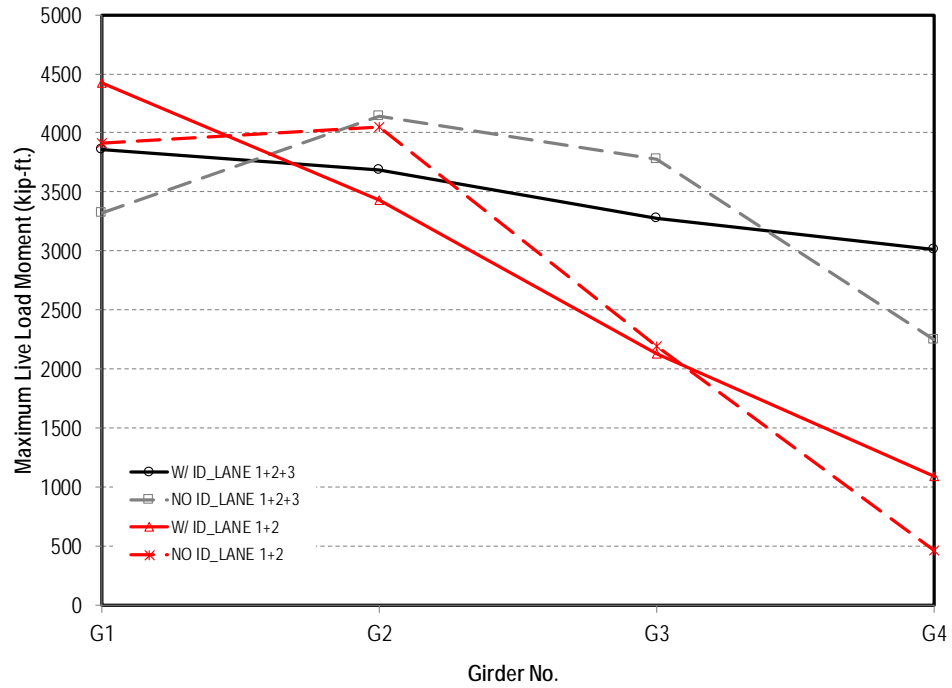


Figure 8-17: BT-78 girder bridge – 12 ft. girder spacing and 130 ft. span length

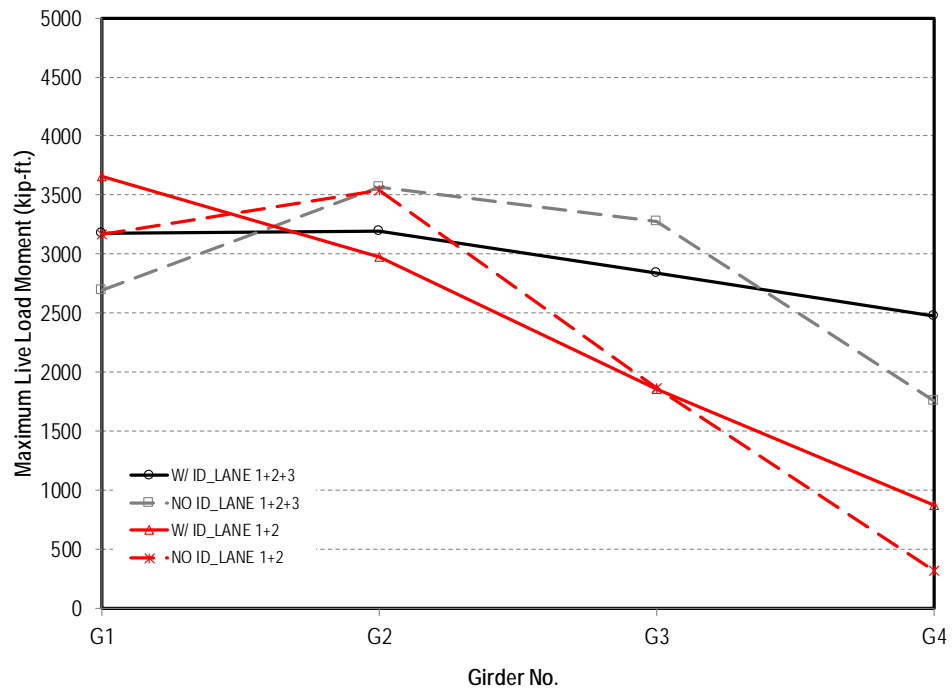


Figure 8-18: BT-78 girder bridge – 12 ft. girder spacing and 115 ft. span length

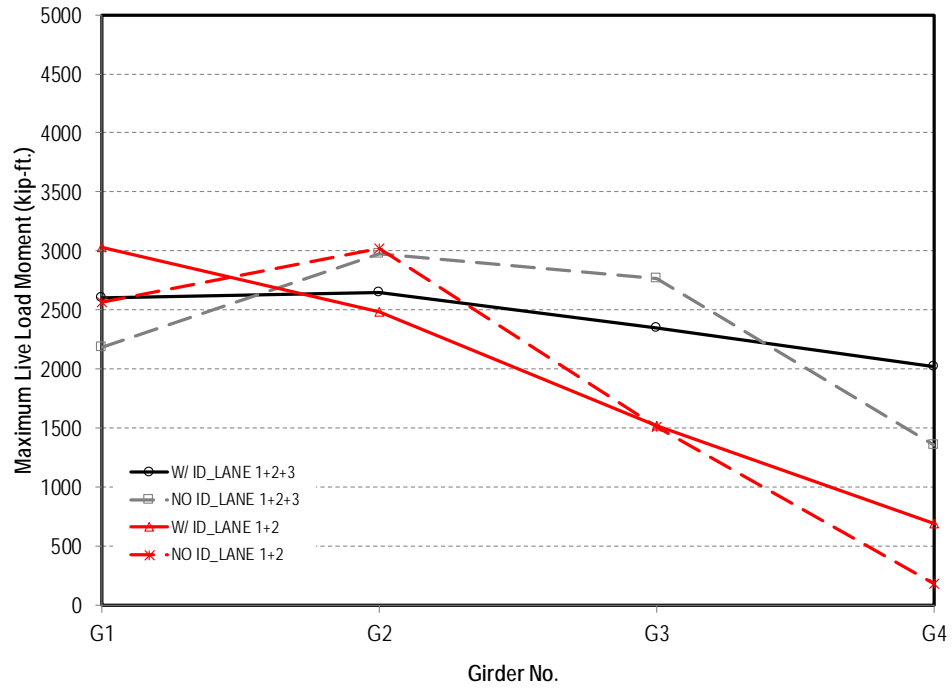


Figure 8-19: BT-78 girder bridge – 12 ft. girder spacing and 100 ft. span length

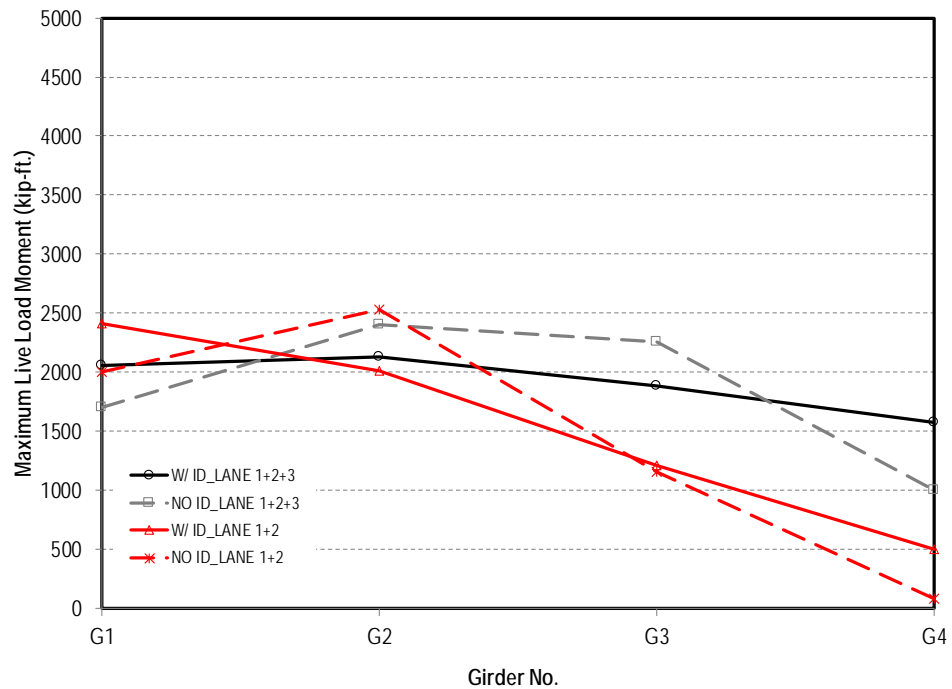


Figure 8-20: BT-78 girder bridge – 12 ft. girder spacing and 85 ft. span length

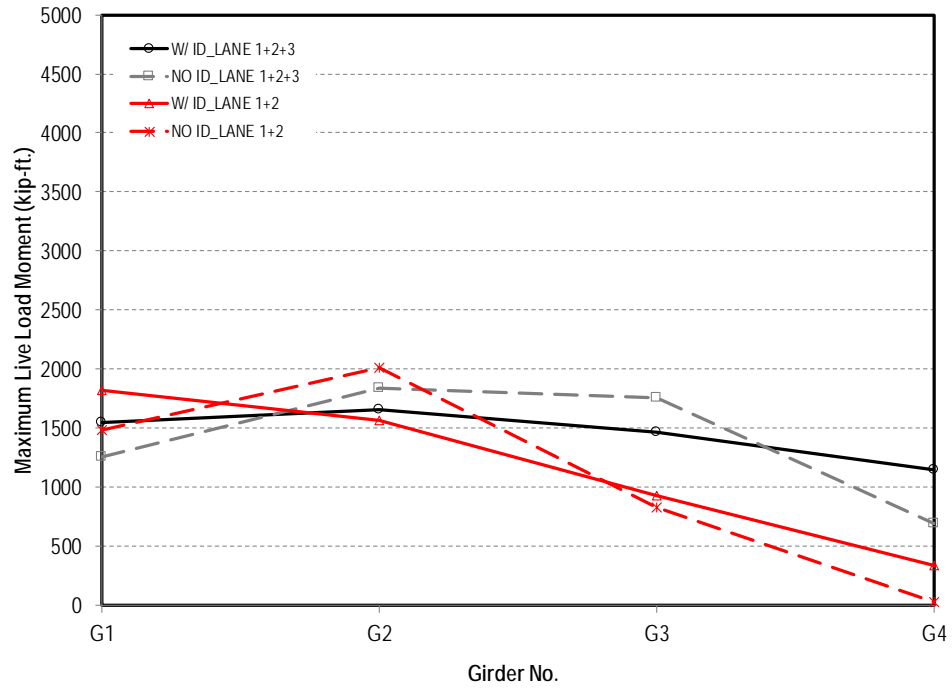


Figure 8-21: BT-78 girder bridge – 12 ft. girder spacing and 70 ft. span length

8.2.3—Effect of Girder Spacing

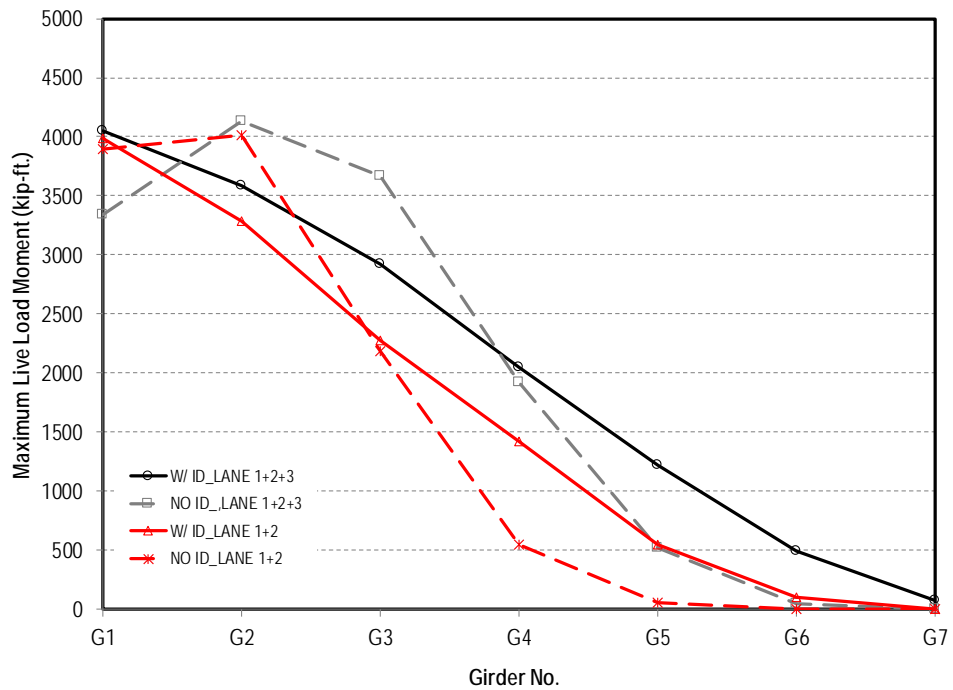


Figure 8-22: BT-78 girder bridge – 12 ft. girder spacing and 130 ft. span length

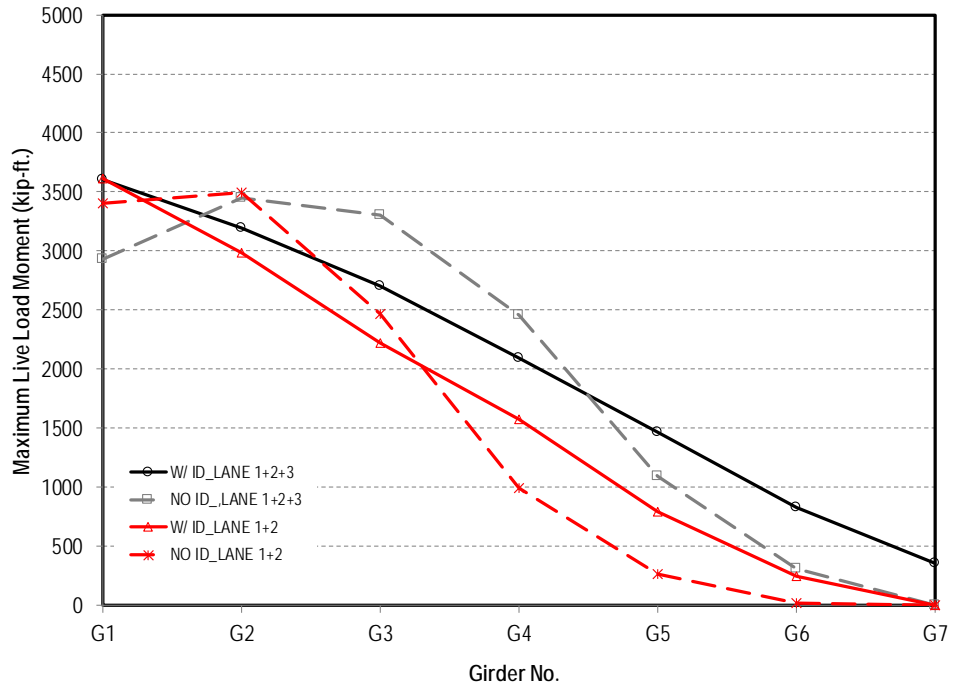


Figure 8-23: BT-78 girder bridge – 10 ft. girder spacing and 130 ft. span length

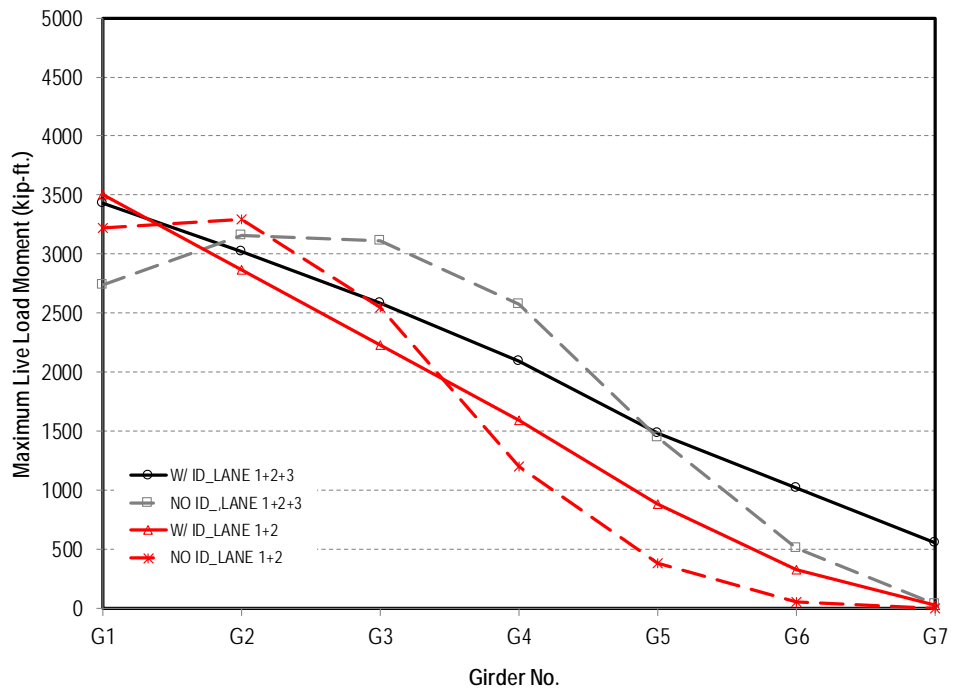


Figure 8-24: BT-78 girder bridge – 9 ft. girder spacing and 130 ft. span length

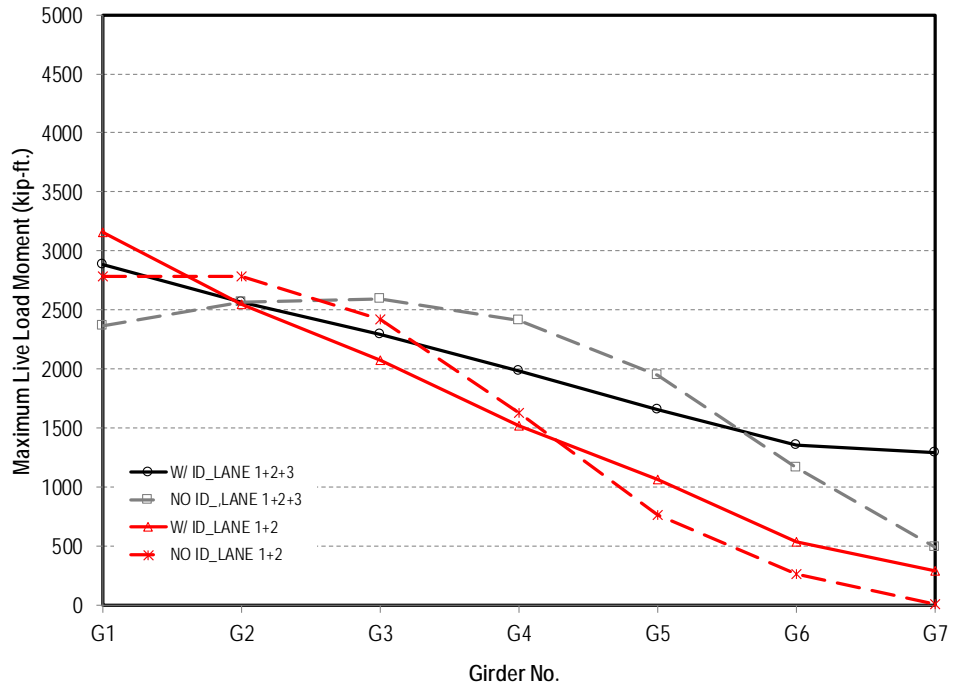


Figure 8-25: BT-78 girder bridge – 7.2 ft. girder spacing and 130 ft. span length

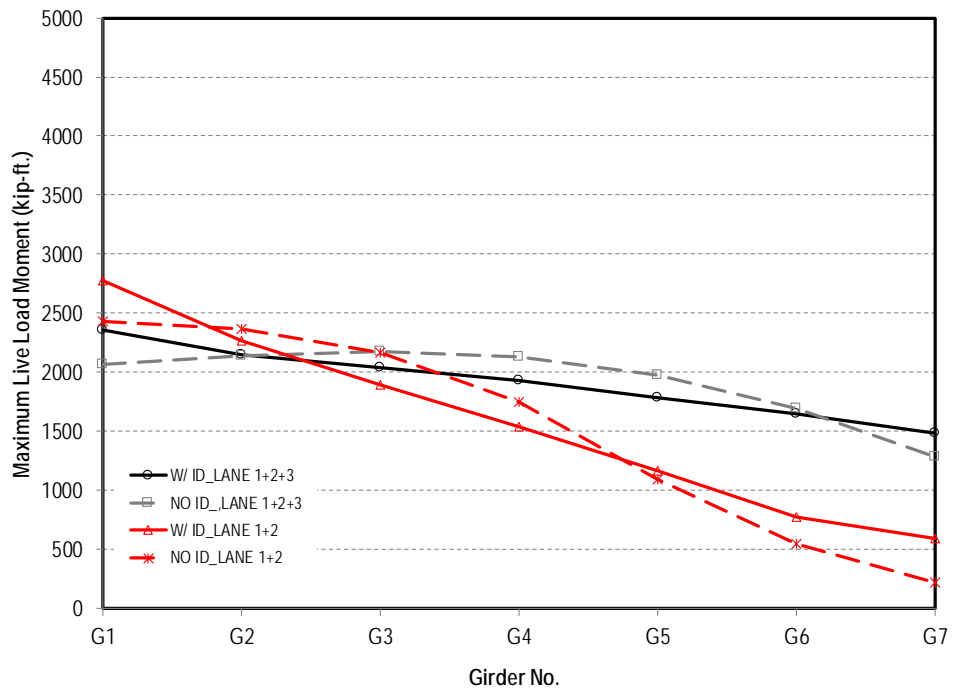


Figure 8-26: BT-78 girder bridge – 6 ft. girder spacing and 130 ft. span length

8.3—Effect of Skew Angle

8.3.1—BT-78 Girder Bridges

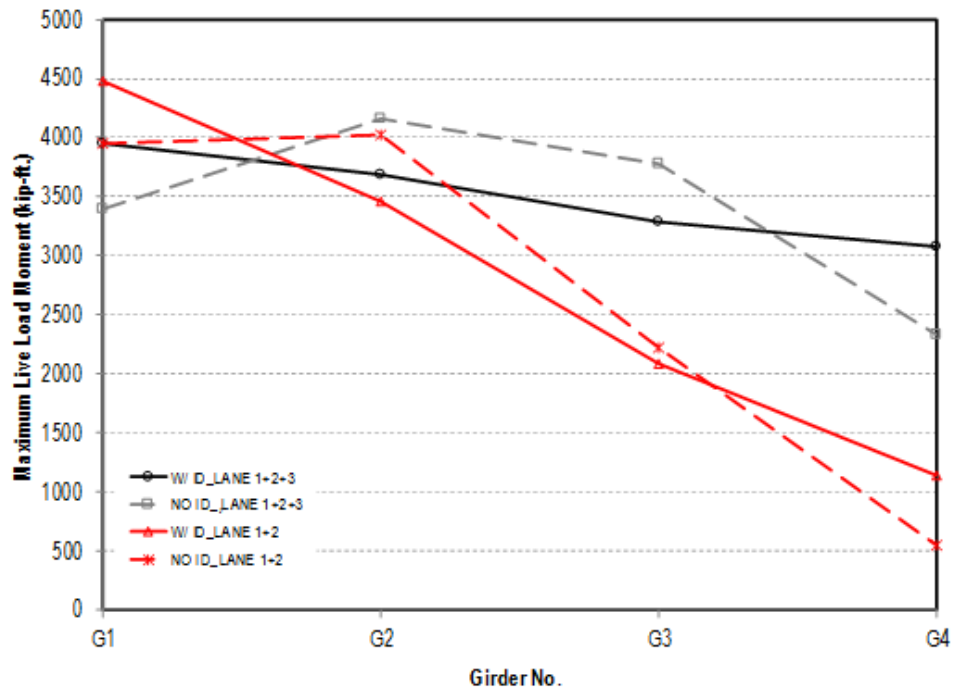


Figure 8-27: BT-78 girder bridge — 08 skew angle

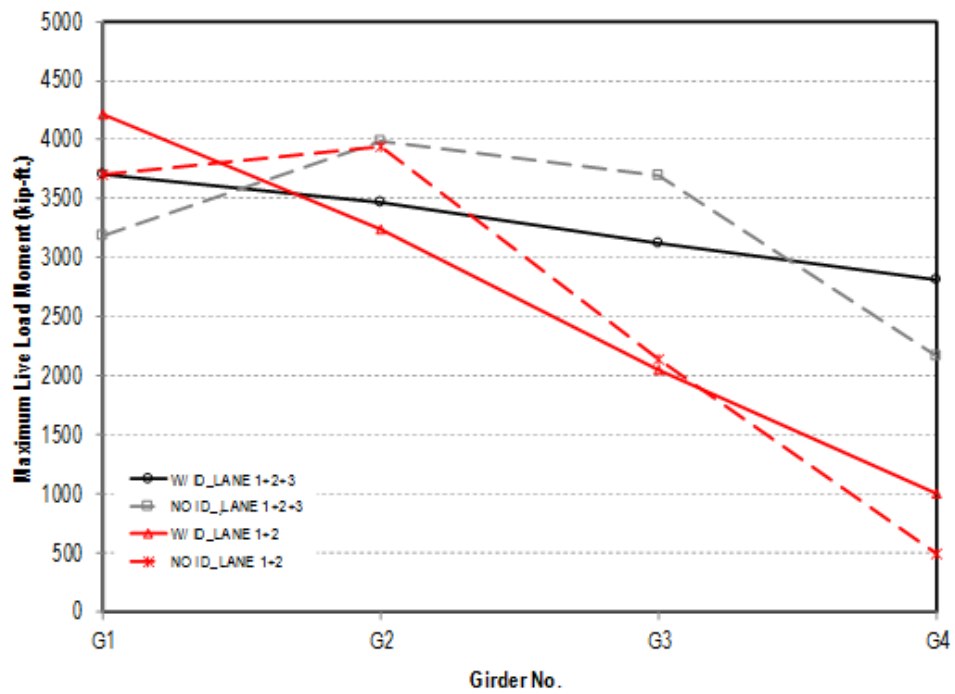


Figure 8-28: BT-78 girder bridge — 308 skew angle

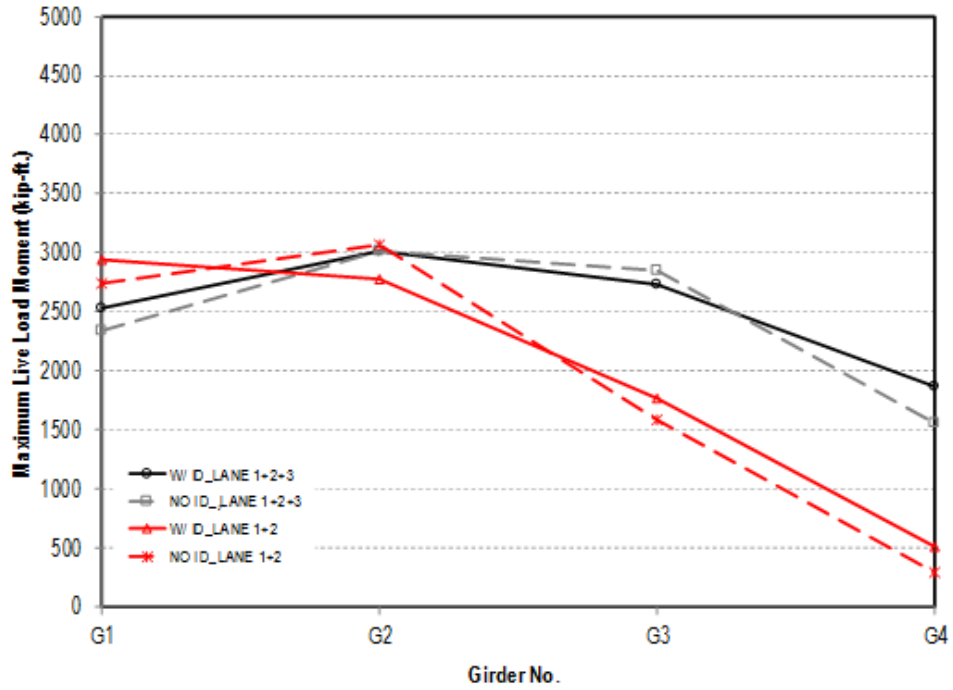


Figure 8-29: BT-78 girder bridge – 608 skew angle

8.3.2—LG-25 Girder Bridges

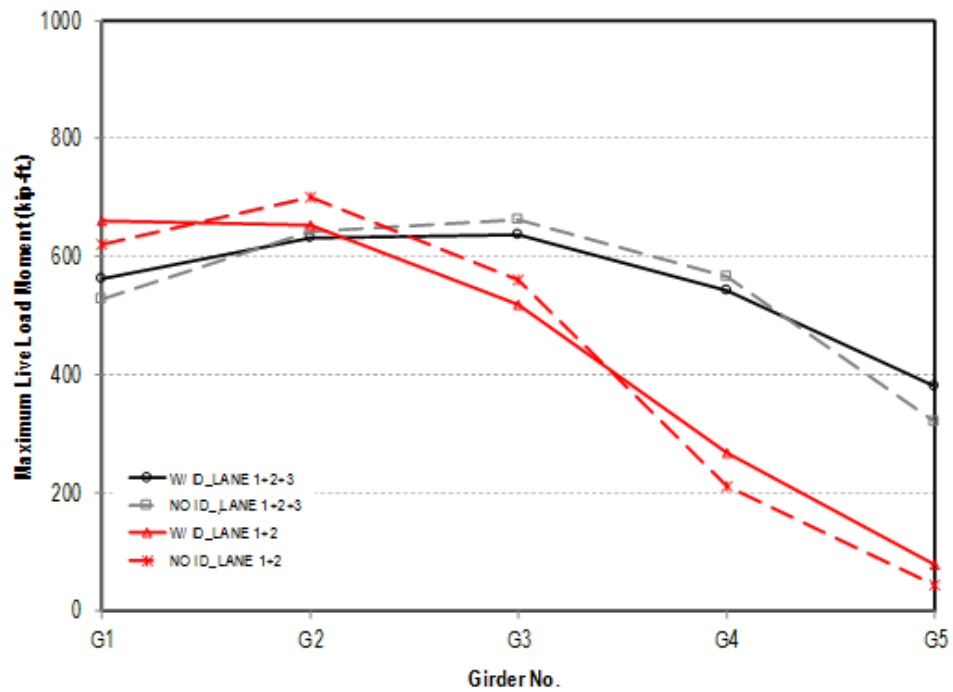


Figure 8-30: LG-25 girder bridge – 08 skew angle

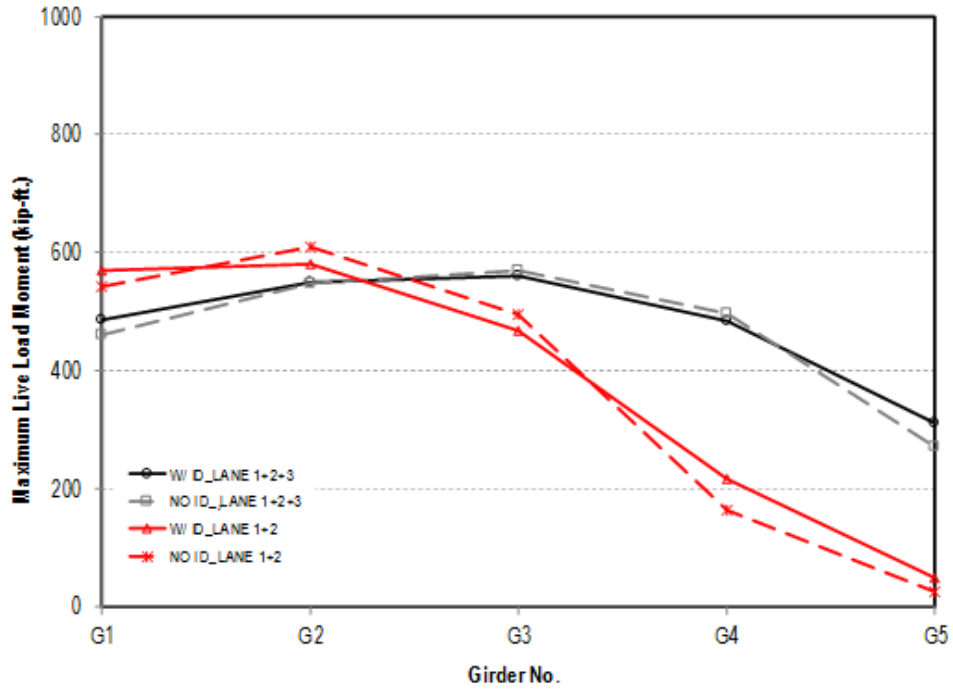


Figure 8-31: LG-25 girder bridge – 308 skew angle

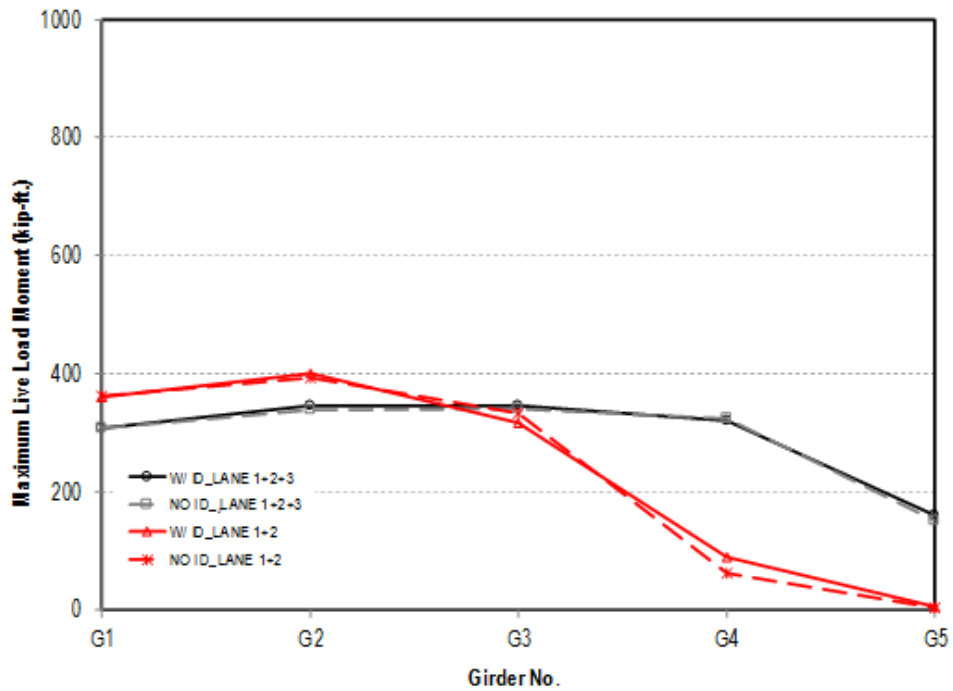


Figure 8-32: LG-25 girder bridge – 608 skew angle

8.3.3—Quad Beam Bridges

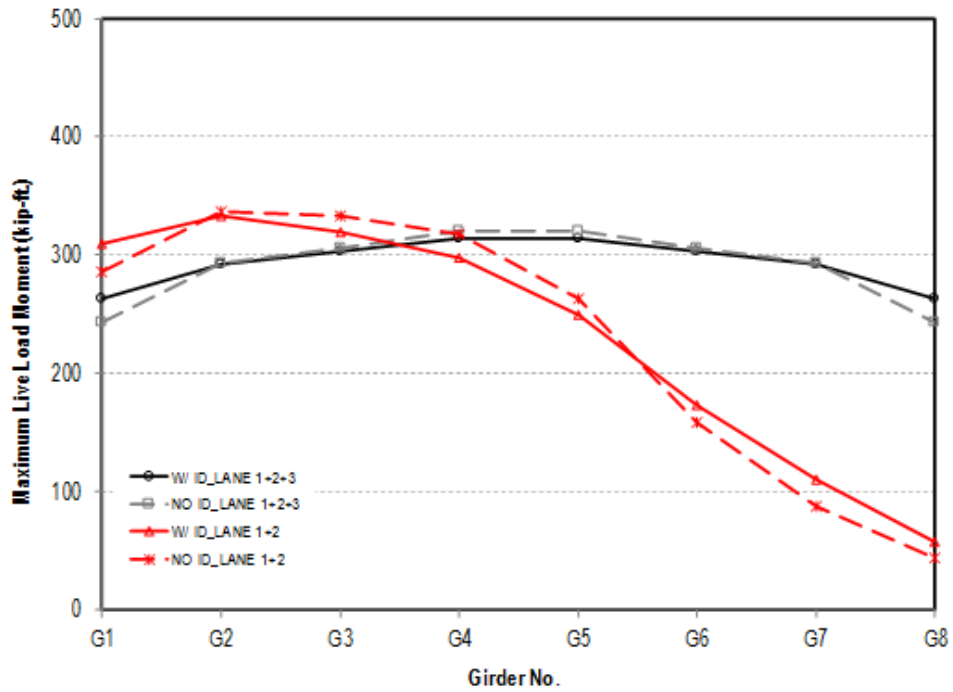


Figure 8-33: Quad beam bridge — 08 skew angle

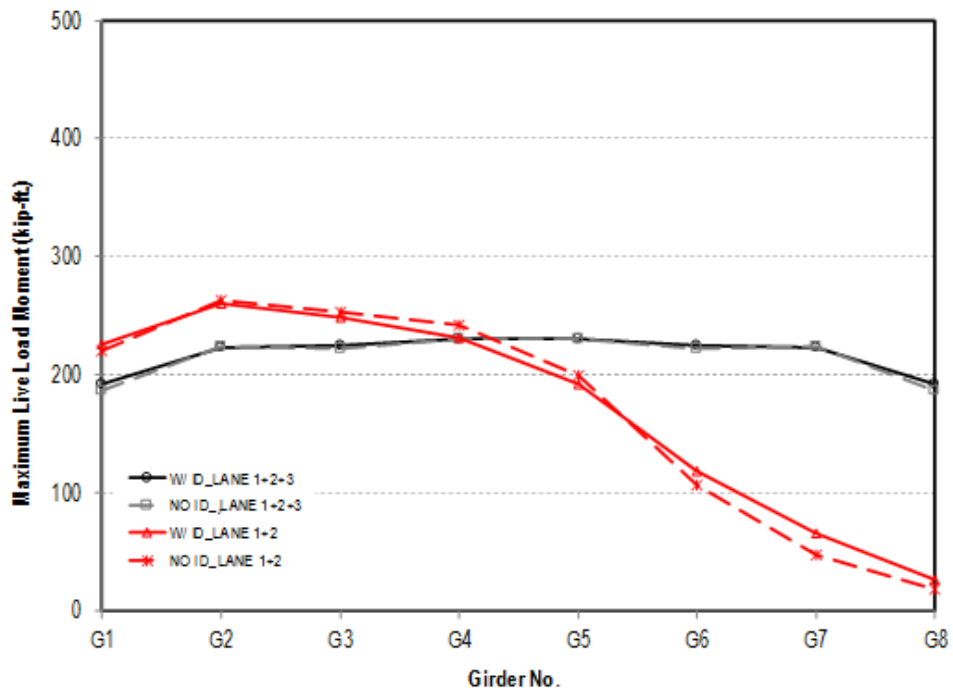


Figure 8-34: Quad beam bridge — 308 skew angle

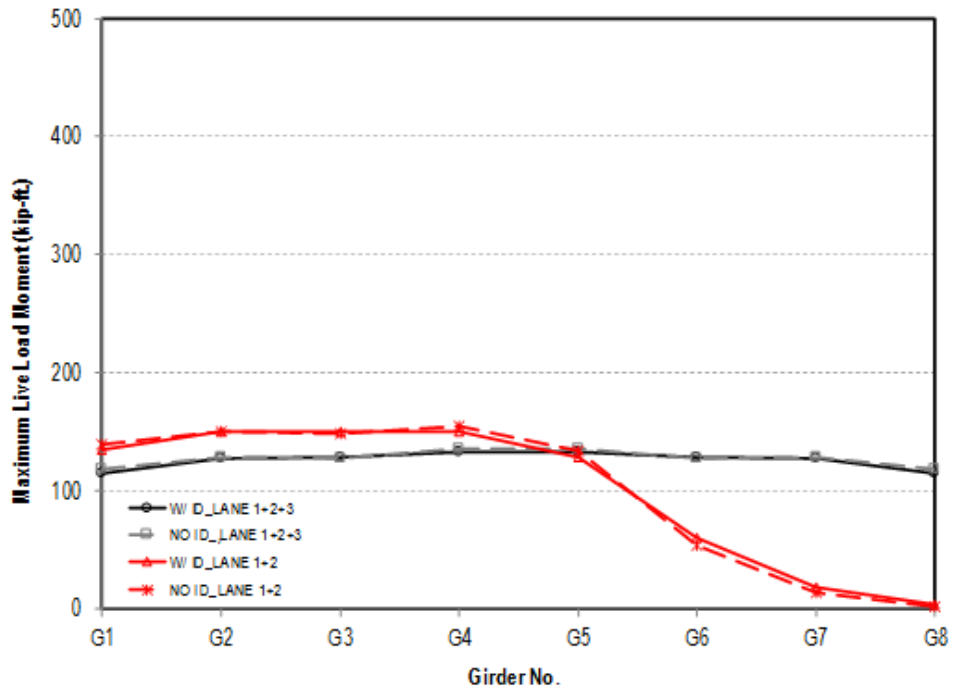


Figure 8-35: Quad beam bridge — 608 skew angle

8.4—Effect of Curvature and Cross Slope

8.4.1—BT-78 Girder Bridges

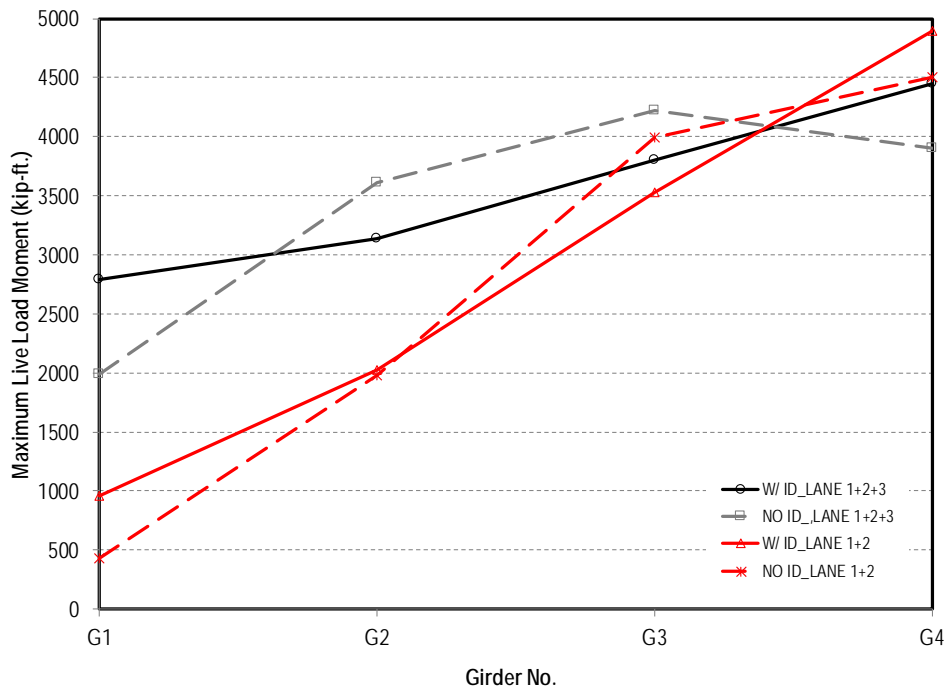


Figure 8-36: BT-78 girder bridge — 1200 ft. radius of curvature and 8% cross slope

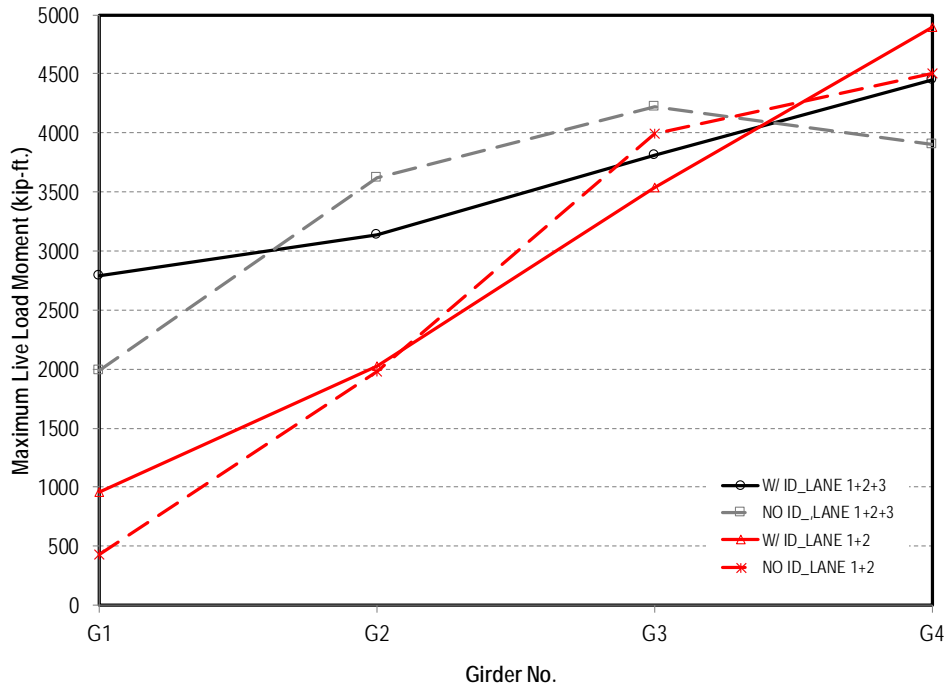


Figure 8-37: BT-78 girder bridge – 1200 ft. radius of curvature and 10% cross slope

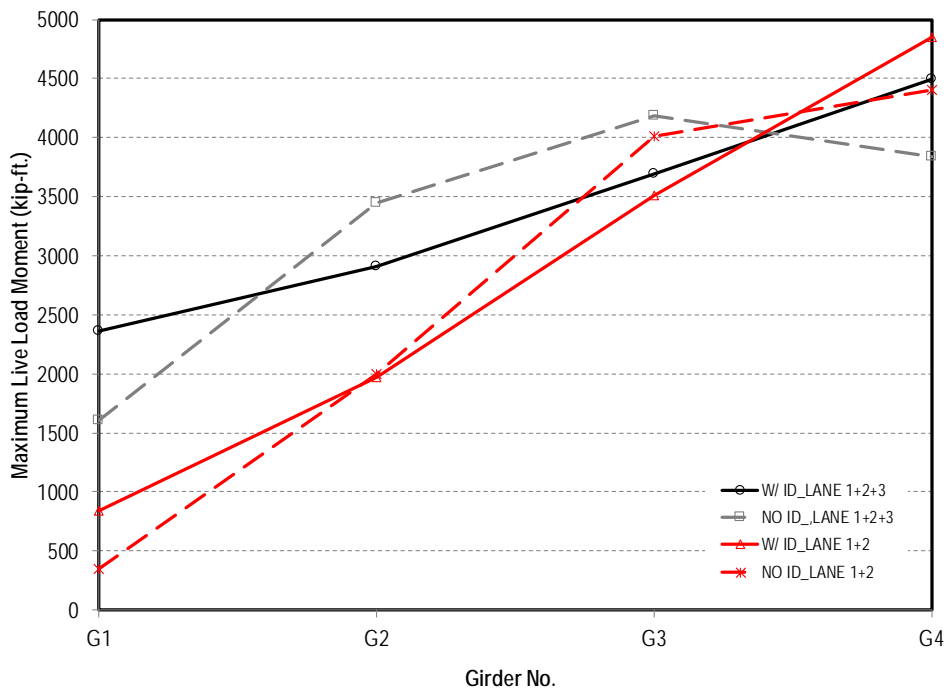


Figure 8-38: BT-78 girder bridge – 1400 ft. radius of curvature and 8% cross slope

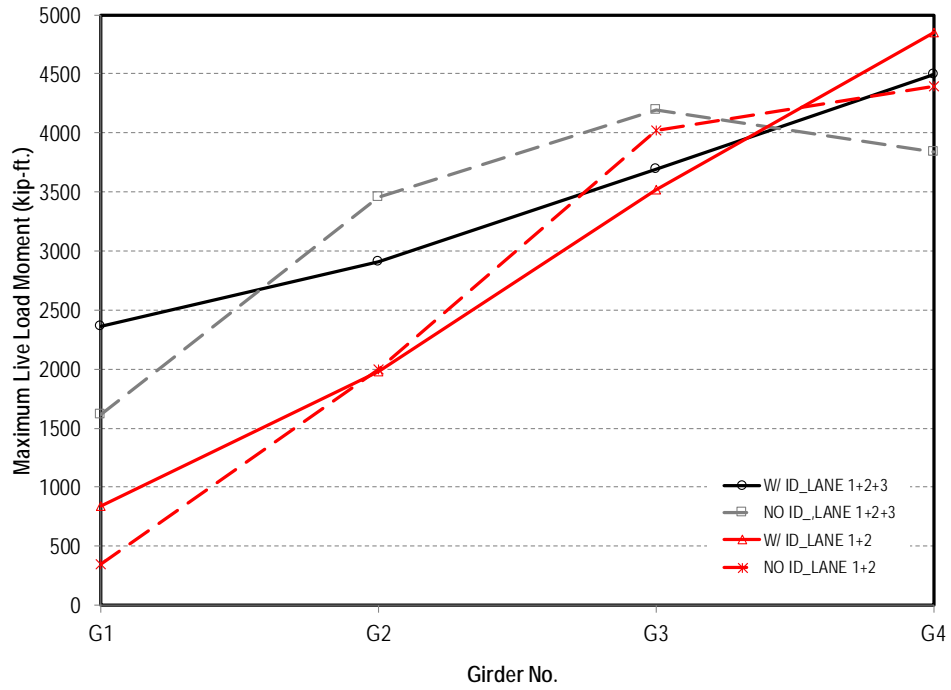


Figure 8-39: BT-78 girder bridge — 1400 ft. radius of curvature and 10% cross slope

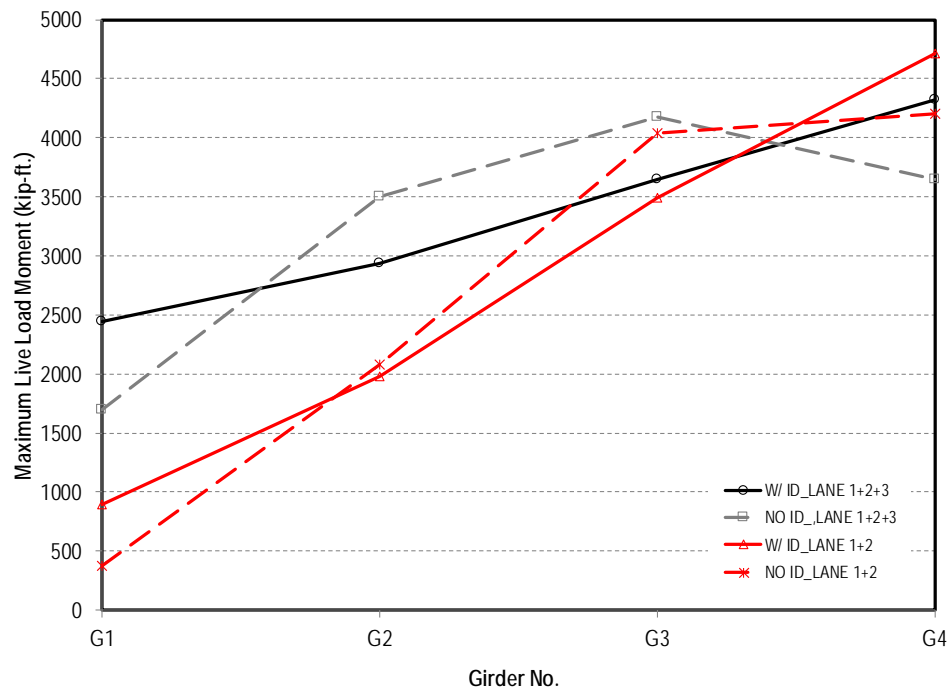


Figure 8-40: BT-78 girder bridge — 2100 ft. radius of curvature and 8% cross slope

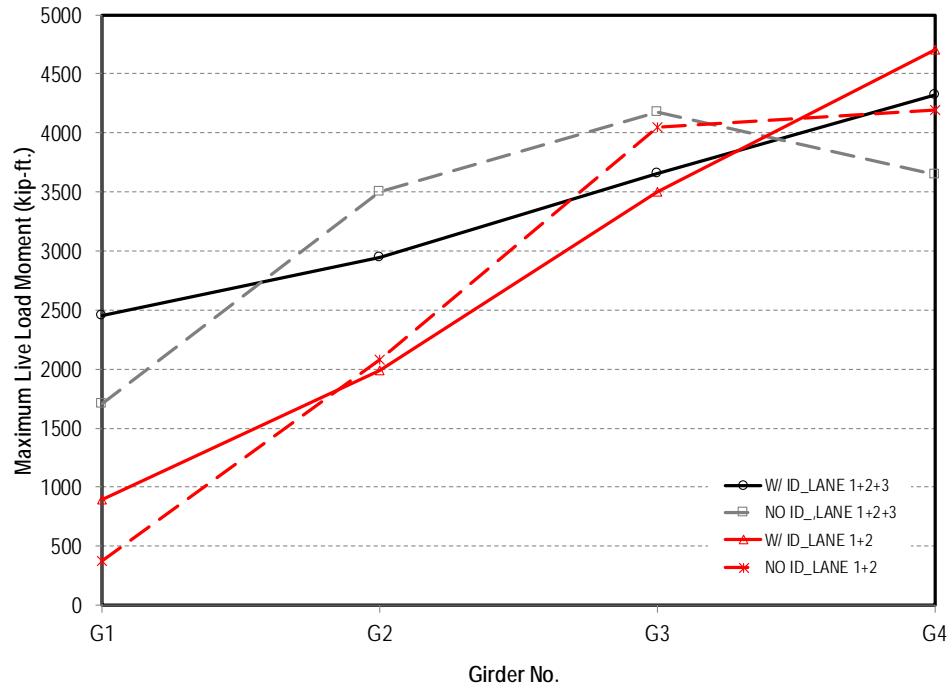


Figure 8-41: BT-78 girder bridge – 2100 ft. radius of curvature and 10% cross slope

8.4.2—LG-25 Girder Bridges

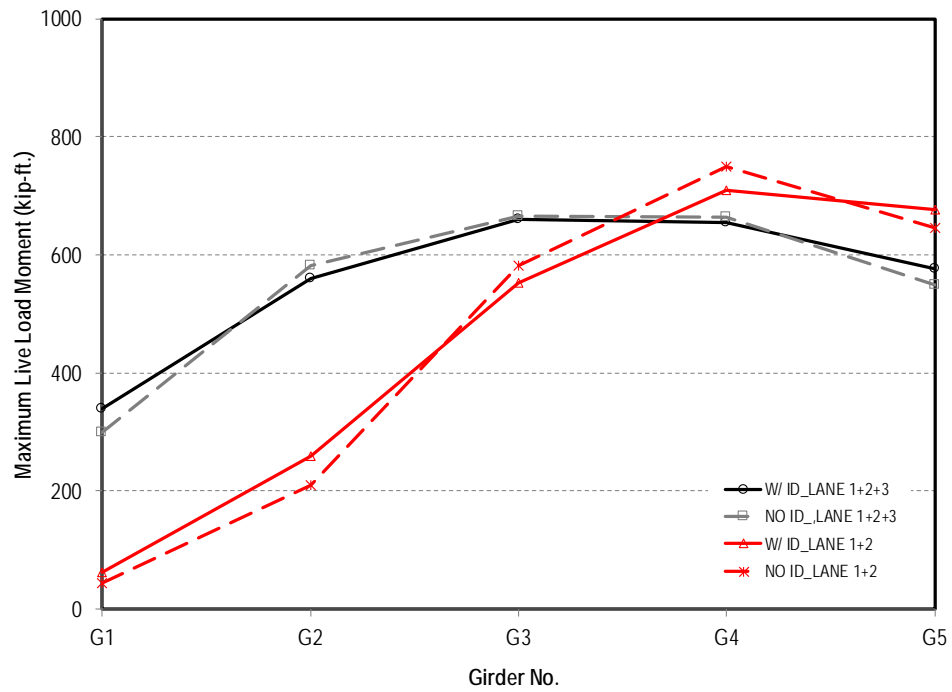


Figure 8-42: LG-25 girder bridge – 500 ft. radius of curvature and 8% cross slope

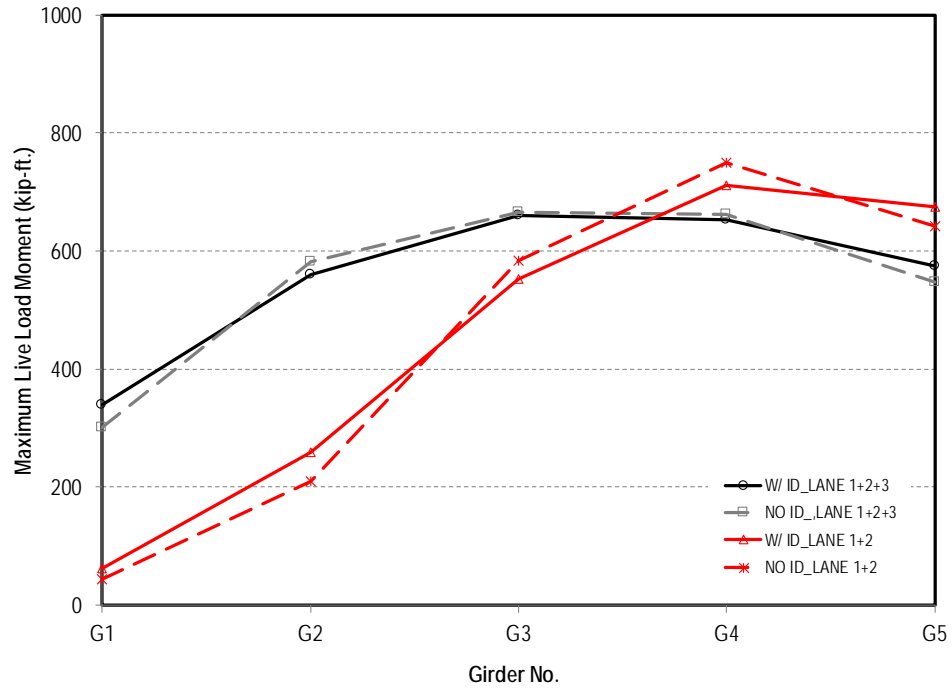


Figure 8-43: LG-25 girder bridge – 500 ft. radius of curvature and 10% cross slope

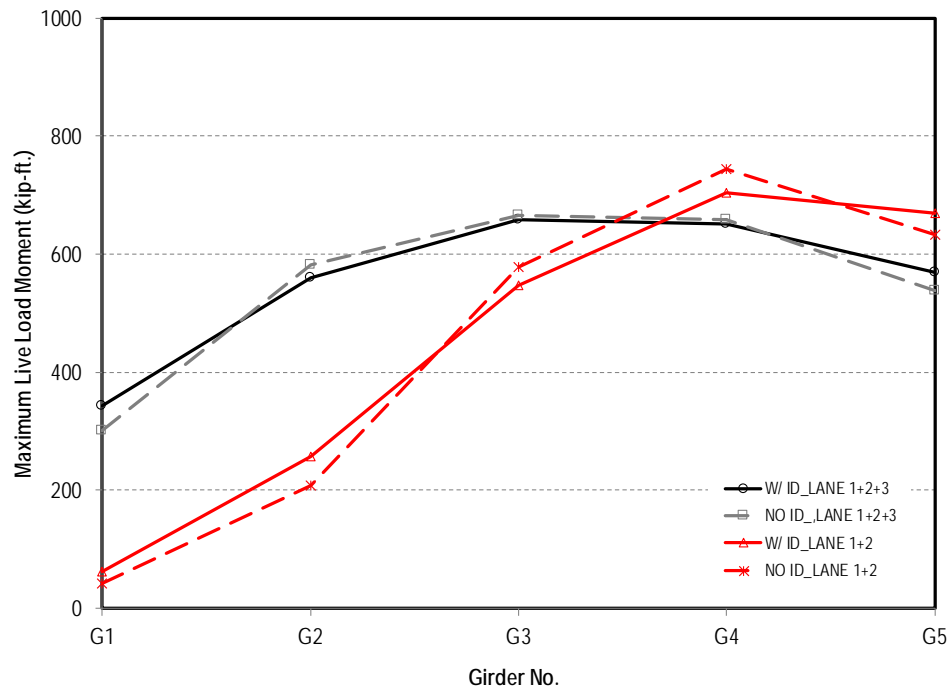


Figure 8-44: LG-25 girder bridge – 800 ft. radius of curvature and 8% cross slope

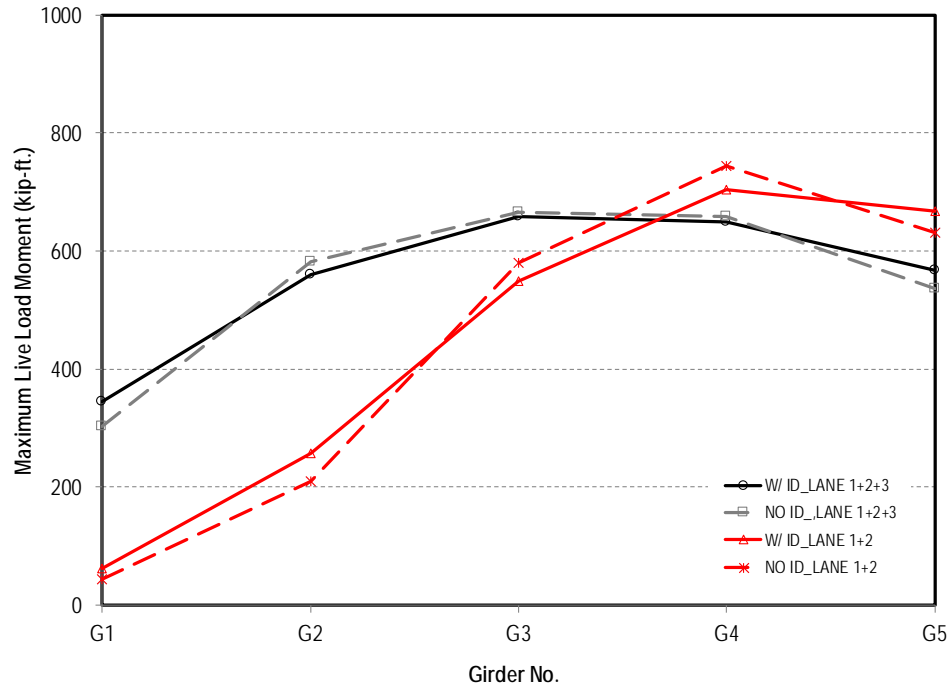


Figure 8-45: LG-25 girder bridge — 800 ft. radius of curvature and 10% cross slope

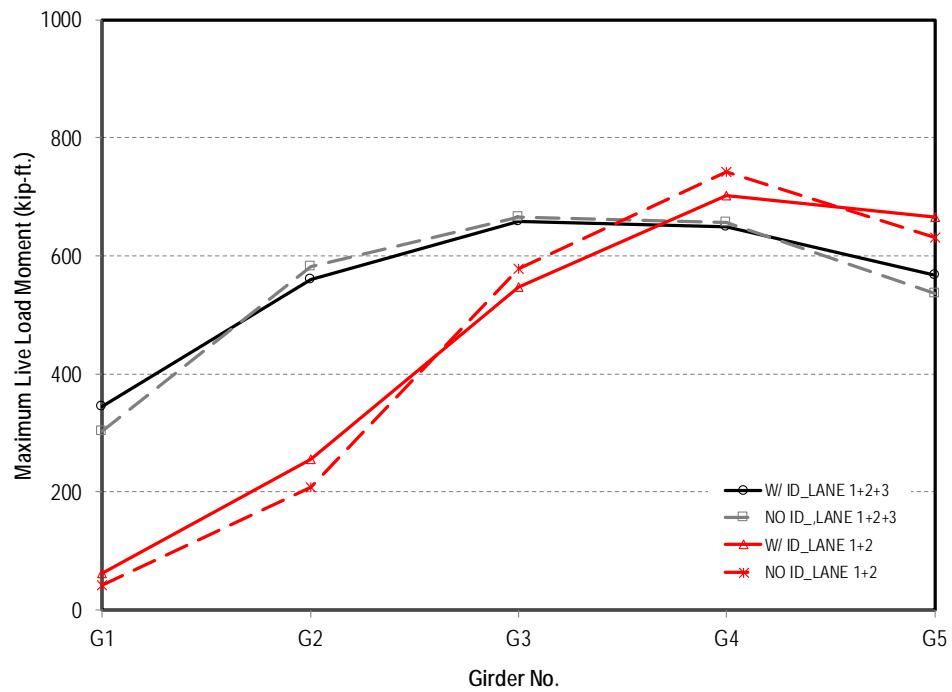


Figure 8-46: LG-25 girder bridge — 1000 ft. radius of curvature and 8% cross slope

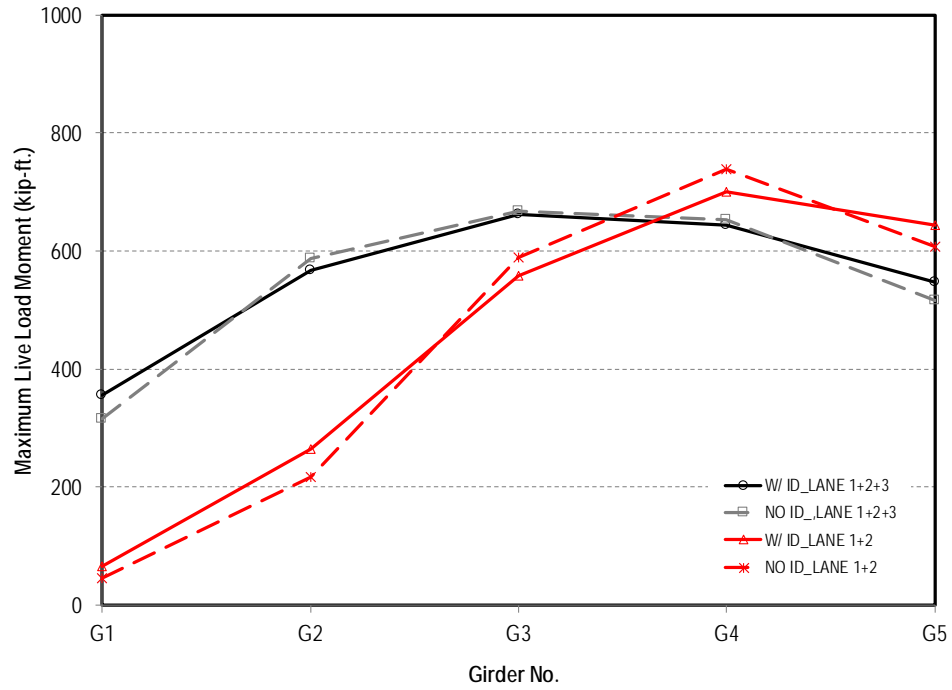


Figure 8-47: LG-25 girder bridge – 1000 ft. radius of curvature and 10% cross slope

8.4.3—Quad Beam Bridges

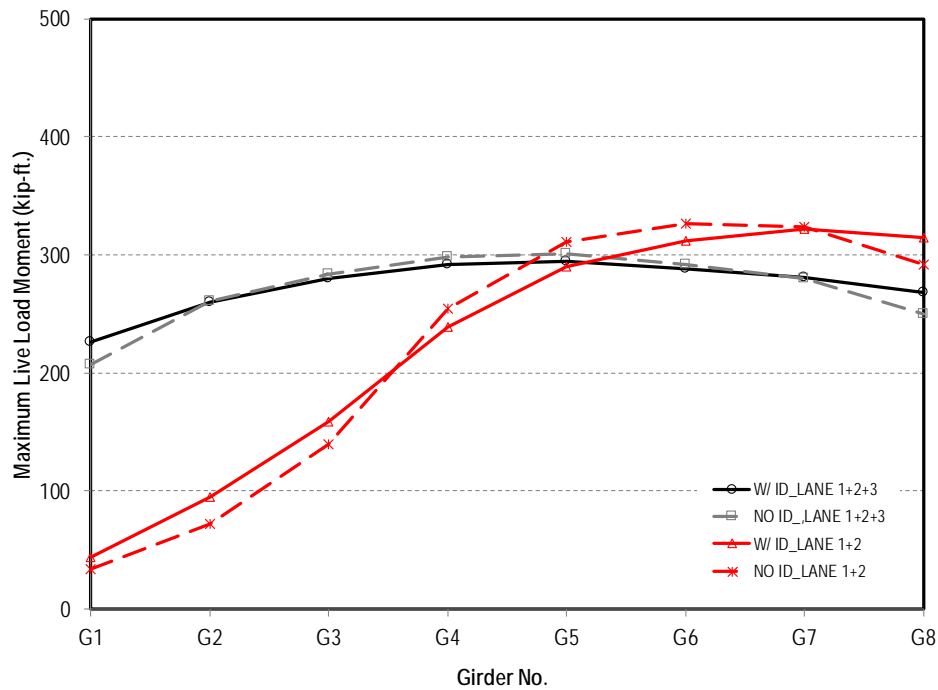


Figure 8-48: Quad beam bridge – 500 ft. radius of curvature and 8% cross slope

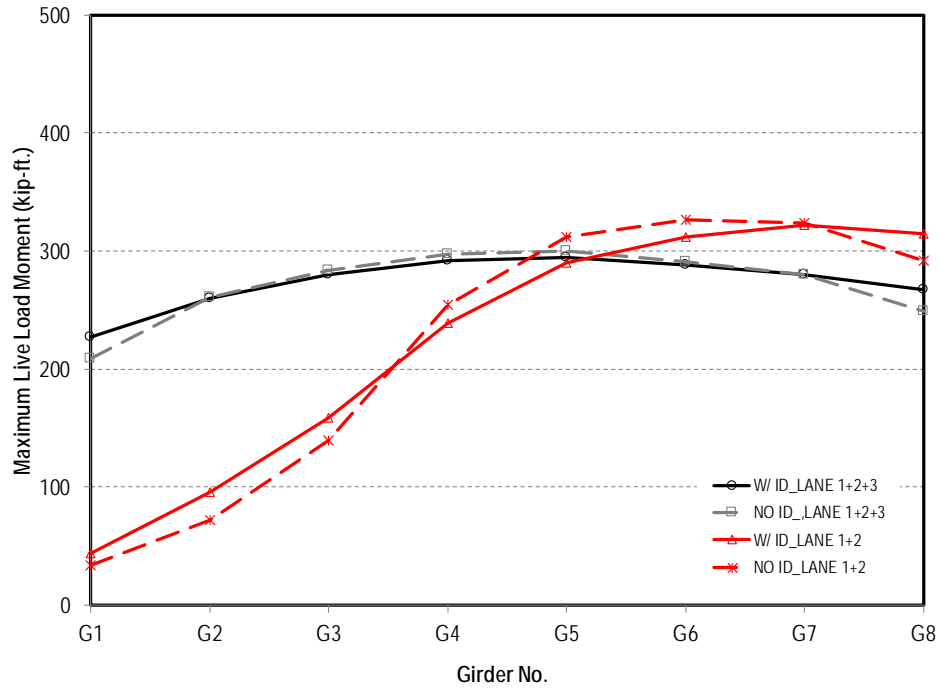


Figure 8-49: Quad beam bridge – 500 ft. radius of curvature and 10% cross slope

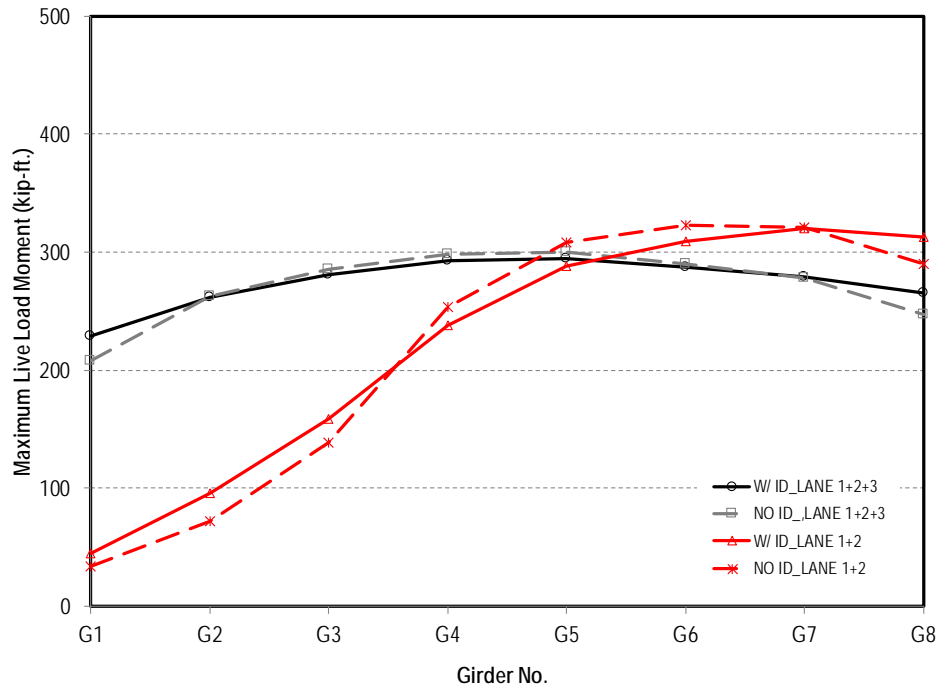


Figure 8-50: Quad beam bridge – 800 ft. radius of curvature and 8% cross slope

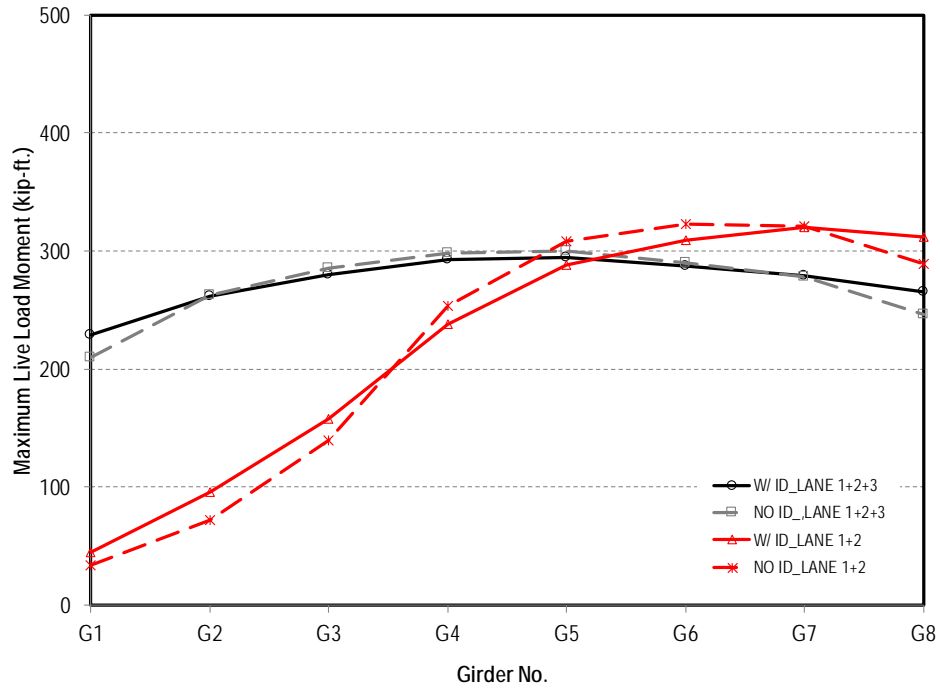


Figure 8-51: Quad beam bridge – 800 ft. radius of curvature and 10% cross slope

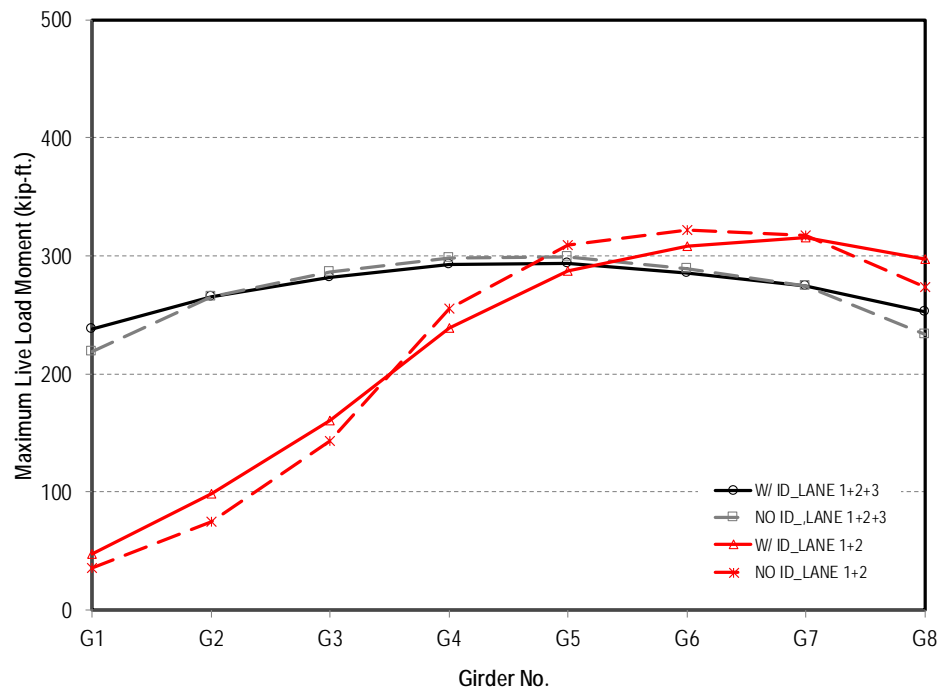


Figure 8-52: Quad beam bridge – 1000 ft. radius of curvature and 8% cross slope

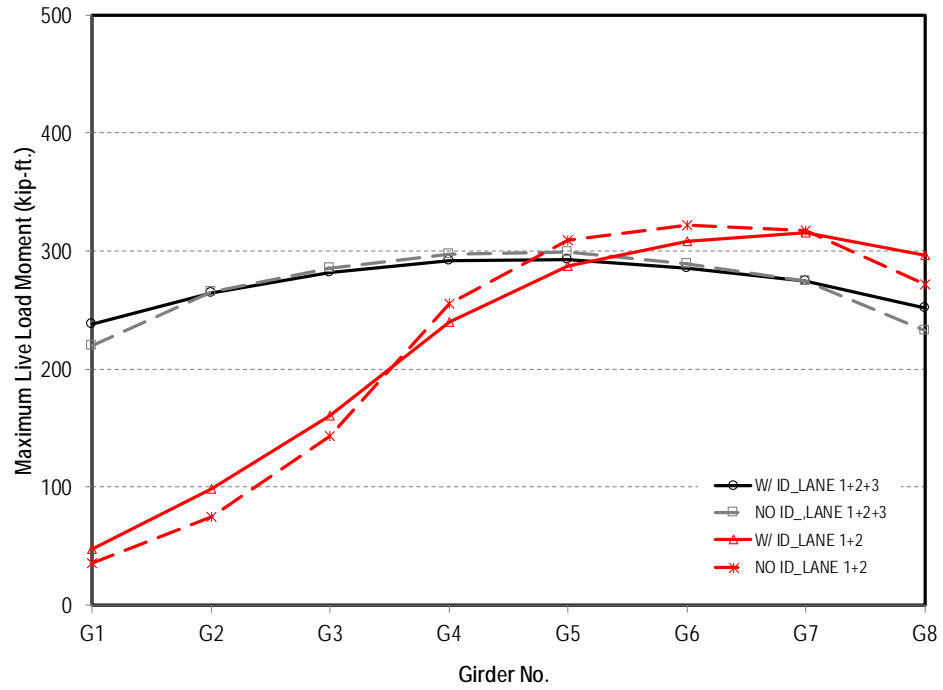


Figure 8-53: Quad beam bridge – 1000 ft. radius of curvature and 10% cross slope